Population Genetics and Growth of the Rabbitfishes *Siganus luridus* and *Siganus rivulatus*: Investigating Factors Structuring Successful Invasion of the Mediterranean Sea

Stephanie Heyworth, BSc Hons

School of Life Sciences, The University of Nottingham

Student Number: 4310032

Thesis submitted for the degree of Masters by Research in Ecology

Under the Supervision of Dr David Feary and Dr Chris Wade

2017/2018 Academic Year

Word count: 35,000

Abstract

Understanding the factors allowing for or, constraining the successful invasion of a new environment will be vital in predicting and monitoring the future success of invasive species. This is especially true in the context of the Mediterranean Sea where hundreds of species have invaded through the Suez Canal from the Red Sea over the last 140 years. *Siganus luridus* and *Siganus rivulatus*, two Lessepsian rabbitfish species, are among the most successful invaders established in the Mediterranean Sea to date, with abundant populations in the eastern, central and western Mediterranean. This project aimed to quantify the effectiveness of two factors for predicting invasion success; population genetic diversity and growth by examining populations of both species across 12 sites, from the eastern to the western Mediterranean basin. Samples from the Red Sea were also included in the phylogenetic analyses to allow for possible identification of founder effects within the introduced range. However, the small Red Sea sample size precluded their use from other analyses and made it impossible to investigate whether there had been an initial genetic bottleneck.

To determine population diversity, sequences for two mitochondrial markers (cytochrome oxidase C subunit I (COI) and the control region (CR)) were obtained from 108 individuals of *S. luridus* and 109 individuals of *S. rivulatus*. Sequences were used to generate and examine maximum likelihood (ML) trees, haplotype network analyses and comparison of haplotype (*h*) and genetic diversity (nucleotide diversity (π) and pairwise distance) between species and populations found along a latitudinal gradient, with increasing distance from Suez Canal. The ML tree and haplotype networks did not demonstrate evidence of geographic segregation of genetic types, but instead indicated high genetic similarity between populations throughout the Mediterranean Sea. The numbers of shared and unique haplotypes demonstrated that movement of invasion is from east to west; however, with increasing distance from the Suez Canal no notable decreases in haplotype or genetic diversity were found. Haplotype diversity was high in both species but lower than previous estimates from the Red Sea, potentially indicating a reduction in haplotype diversity with invasion.

Such estimates of reduction were lower than have been found in other invasive populations (e.g., *Fistularia commersonii*).

Nucleotide diversity levels (π), pairwise distances and F-statistic values revealed close relationships between populations of both species. However, significant levels of moderate to high genetic differentiation between populations of *S. luridus* were apparent. The results of the neutrality tests (Tajima's D, Fu's F and the mismatch distribution) had variable results in both species, though there was evidence to suggest demographic change in Trachila, the Peloponnese for *S. rivulatus* and sites from Turkey, the Peloponnese and the Pelagie Islands for *S. luridus*. The haplotype networks indicate this demographic change is population expansion. It can be argued that *S. luridus* is potentially a more successful invader due to its increased distribution throughout the Mediterranean Sea, higher haplotype diversity and higher genetic structure among populations than *S. rivulatus.* The higher genetic structure indicates greater invasion success as the greater the diversity within the species gene pool, the more capable the species will be at surviving environmental changes and coping with stressors. These factors indicate that genetic diversity may be a successful indicator of invasion success.

To determine whether life history characteristics differed between *S. luridus* and *S. rivulatus* across the Mediterranean Sea, using otolith microchemistry the age and growth rate (using width of annuli as a proxy for annual otolith growth) of 32 individuals of *S. luridus* and 27 of *S. rivulatus* were determined. When inferring growth rates from otolith growth bands *S. rivulatus* showed significantly greater growth than *S. luridus* throughout all sites. Although *S. rivulatus* populations within the eastern Mediterranean Sea demonstrated greater-age-at-length than populations in the central Mediterranean Sea, this pattern was not apparent for populations of *S. luridus*. For this species, sites in the western Mediterranean held the largest individuals for their ages. A linear model was conducted to investigate if annulus, site, species or any of the relationships between these factors had a significant impact on the amount of

growth observed (interpreted from otolith annulus widths). Site did not have a significant effect, indicating differences in environmental factors (SST, salinity and chlorophyll-a) associated with increasing distance from the Suez Canal were not a substantial factor in determining growth. The first year of growth was significantly greater than subsequent years for both species. Certain sites however, demonstrated significantly higher levels of growth for some annuli over others. Overall, the lack of a significant reduction in growth between sites indicates that growth is not a good predictor of invasion success, as the environmental factors expected to impact growth do not.

Acknowledgements

I would sincerely like to thank my incredible supervisors, Dr David Feary and Dr Chris Wade for the support, enthusiasm, expertise and tireless assistance they provided along this journey.

I would also like to thank all the international collaborators that made this project possible; specifically Dr Ernesto Azzurro from the Institute for Environmental Protection and Research, Italy (ISPRA), Mariolina Corsini-Foka and her team from the Hellenic Centre for Marine Research (HCMR) and Institute of Oceanography-Hydrobiological Station of Rhodes, Jane Dimock and Dimitri G. Exarhouleas from Dive Code, in Stoupa, Greece and Daniele D'Agostino (University of Nottingham) for their invaluable assistance in samples collection and kind hospitality, this work would not have been possible without them.

I also owe thanks to Ahmed Saadi (The University of Nottingham) for his advice and guidance throughout this project.

Finally, I would like to thank my parents, Ulrike and Stephen for their endless support and encouragement throughout this year. I would also like to thank the rest of my family and my friends for the reassurance and patience they have provided.

Contents

Chapter 1: A General Introduction 1

1.1 The Elected Study Area: The Mediterranean Basin 1

1.2 Lessepsian Invasion of the Mediterranean Sea 2

1.3 *Siganus luridus* and *Siganus rivulatus* 4

Chapter 2: Population Genetics of Invasive Populations of *Siganus* Species in the Mediterranean Sea 8

2.1 Introduction 8

2.1.1 The Importance of Understanding Genetic Diversity in terms of Invasion 8

2.1.2 Use of Molecular Markers to Evaluate Genetic Diversity and Evolutionary Relationships Between Populations 10

2.1.3 Genetic Diversity and Adaptation to Novel Environments 11

2.1.4 The Current Understanding of the Genetics of Invasion 12

2.1.5 The Genetics of Lessepsian Invasion 13

2.1.6 The Current Understanding of the Genetic diversity of Rabbitfish within the Mediterranean Sea 16

2.1.7 Research Aims and Objectives 17

2.2 Materials and Methods 18

2.2.1 Sample Collection 18

2.2.2 DNA Extraction 22

2.2.3 Polymerase Chain Reaction (PCR) 22

2.2.4 Gel Electrophoresis of PCR Products 24

2.2.5 Purification of PCR Products 25

2.2.6 Sequencing 25

2.2.7 Checking and Editing Sequence Quality 25

2.2.8 Sequence Alignment 25

2.2.9 Generation of a Phylogenetic Tree 26

2.2.10 Generation of Haplotype Networks 27

2.2.11 Measuring Population Diversity Across the Mediterranean Sea 28

2.2.12 Investigation demographic changes 28

2.3 Results 30

2.3.1 Maximum Likelihood Analysis and Pairwise Distance 33

2.3.2 Investigating Genetic Structure within the *Siganus* species 36

2.3.3 Haplotype Network Analysis 39

2.3.4 Population Diversity Indices 46

2.3.5 F-statistics: Analysis of population differentiation 56

2.3.6 Analysis of Evidence of Demographic Changes in *Siganus* species across the Mediterranean Sea 60
2.4 Discussion 65
2.4.1 Evidence for the Presence of Two *Siganus* Species in the Mediterranean Sea 65
2.4.2 Genetic Structure of *S. luridus* and *S. rivulatus* Populations within the Mediterranean Sea 65
2.4.3 Haplotype Diversity of *Siganus* Species within the Mediterranean Sea 67
2.4.4 The History of Mediterranean Siganus Populations 69
2.4.5 The Direction of Invasion 70
2.4.6 Population Genetics 71
2.4.7 Demography of Mediterranean *Siganus* populations 74
Chapter 3: Growth Rate Across the Mediterranean 77
3.1 Introduction 77
3.1.1 Movement from a Tropical, High Productivity, Coral Dominated Sea to a Temperature Sea Characterised by Rocky-Reefs and Algal Barrens 77
3.1.2 How do Environmental Factors Affect Growth Rate? 78
3.1.3 The Importance of Understanding Growth Rate of Lessepsians 81
3.1.4 Aims and objectives 81
3.1.5 Predictions of Ecological Impacts due to Environmental Conditions in the Mediterranean Sea 82
3.2 Materials and Methods 83
3.2.1 Otolith Collection 83
3.2.2 Initial Otolith Preparation 85
3.2.3 Imaging 87
3.2.4 Improving Otolith Quality 87
3.2.5 Calculating Fish Age and Measuring Annuli 90
3.2.6 Analysis of Age-Length Relationships Throughout the Mediterranean Sea 92
3.2.7 Does Otolith Growth Effectively Represent Somatic Growth? 92
3.2.8 Comparing Growth Increments between Sites and Species 92
3.2.9 Environmental Correlates to Life History Parameters 92
3.2.10 Investigating the Impact of Environmental Variables on Growth 93
3.3 Results 94
3.3.1 Age-length Relationships of *S. luridus* and *S. rivulatus* Within the Mediterranean Sea 94
3.3.2 The Relationship Between Otolith Growth and Somatic Growth 97
3.3.3 Investigating Factors that Affect Otolith Growth 99

3.3.4 The Otolith Growth of *S. luridus* and *S rivulatus* Populations within the Mediterranean Sea 100
3.3.5 Environmental Factors that may affect growth within the Mediterranean Sea 106
3.4 Discussion 110
3.4.1 Is Otolith Growth Representative of Somatic Growth? 110
3.4.2 Growth Along a Latitudinal Gradient 110
Chapter 4: Conclusion 116
References 119
Appendices 138
Appendix 1: R Code used to Generate Mediterranean Sites Map 138
Appendix 2: Assigning Traits (sites) to Haplotypes 140
Appendix 3: Age and Length data 141

Chapter 1: A General Introduction

1.1 The Elected Study Area: The Mediterranean Basin

The Mediterranean Sea (Figure 1) is a relatively small, semi-enclosed sea covering approximately 2.51 million km^2 with connections to the Atlantic Ocean and Black Sea through the Strait of Gibraltar and the Bosphorus Strait, respectively (Wuertz 2010). It consists of two distinct basins, the east and west, representing only 0.82% of the world's sea surface area and 0.32% of the world's oceans volume (Wuertz 2010, Papanicolopulu 2015). Despite its relatively small area and enclosed nature, the Mediterranean is known as a biodiversity hotspot with over 17,000 different marine species documented within its waters (Coll *et al.* 2010). This biodiversity is partially the result of the historical rapid environmental change that occurred throughout its geological history (Wuertz 2010). This led to a variety of climatic and hydrological scenarios within the waters that make the Mediterranean Sea suitable for both temperate and subtropical species to live successfully (Wuertz 2010).

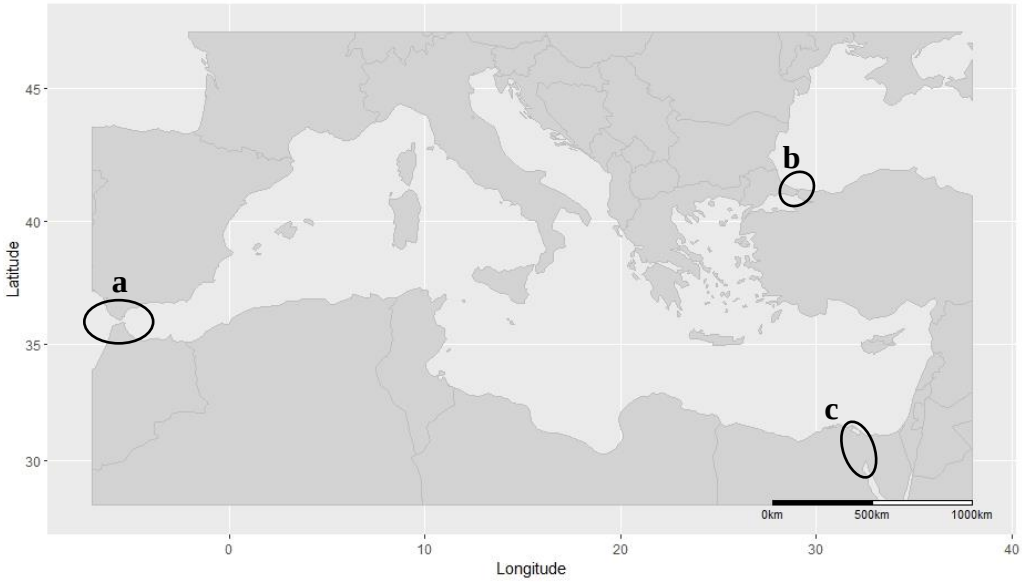

Figure 1: Map of the Mediterranean Sea demonstrating the connections to other bodies of water. Annotation (a) highlights the location of the Strait of Gibraltar, (b) highlights the location of the Bosphorus Strait and (c) highlights the location of the Suez Canal. Map was generated on R version 3.5.1 (R Core

Team 2018) using packages ggplot2 (Wickham 2016) and ggmaps (Kahle and Wickham 2013).

The geographic distribution of species diversity within the Mediterranean Sea is relatively heterogeneous, with multiple studies revealing a decreasing gradient of species richness from north-west to south-east (Emig and Geistdoerfer 2004, Coll *et al.* 2010, Almeida *et al.* 2017). For example, the abundance of species of crustaceans declines from west to east (Almeida *et al.* 2017). Such gradients in biodiversity may be associated with strong gradients in water temperature and salinity, with mean surface temperatures in the west ranging from 15 °C to 25°C and the east ranging from 17 °C to 28 °C between winter and summer respectively (CEAM *et al.* 2018). The salinity gradient ranges from 36 % in the western basin to 39 % salinity in the eastern basin (Wuertz 2010). Interestingly, there is also a trophic gradient with oligotrophy increasing towards the eastern side resulting in lower levels of primary productivity (Danovaro *et al.* 1999).

In 1869, the Mediterranean Sea became connected to the Red Sea by the means of the Suez Canal, a man-made channel constructed to reduce the sailing distance between Europe and Asia. Evolutionarily speaking (within the last five million years), many of the more recent marine species present within the Mediterranean have ancestors originating from the Atlantic Ocean due to the connection formed (the Strait of Gibraltar) following the Pliocene era (Bianchi and Morri (2000). Despite this, the majority of the most recent species recorded (since 1869) are the result of direct migration from the Red Sea through the Suez Canal.

1.2 Lessepsian Invasion of the Mediterranean Sea

With the development of the Suez Canal in 1869, a body of water connecting the Red and Mediterranean Seas, came a warning from Louis Vaillant, a French naturalist, implicating that a migration of species was likely and that the impending results would have both ecological and evolutionary effects (Por 1971). A “Lessepsian” species, a term coined by Por (1971) after Ferdinand de

Lesseps, the developer of the Suez Canal, is one that has invaded from the Red Sea through the Suez Canal, and into the Mediterranean Sea. This migration of species, termed "Lessepsian Invasion" by Por (1978), is known to have dramatically increased biodiversity within the Mediterranean Sea following the introduction of over 96 different fish species (Fricke *et al.* 2015). It is estimated that a minimum of 309 species have invaded since the opening of the Suez Canal (Golani 2010). These species range from small invertebrates like molluscs and crabs to larger fish species (Çeviker and Albayrak 2006, Sará *et al.* 2008, Bariche and Bernardi 2009, Jackson *et al.* 2015).

The increase in the number of introductions of species from the Red Sea into the Mediterranean Sea in recent years is thought to be associated with the continued enlargement of the Suez Canal (Galil *et al.* 2017). Many ecological studies have also associated changing environmental conditions, such as increasing sea surface temperatures (SSTs) with the increasing number of invasive species entering and dispersing throughout the Mediterranean Sea (Lasram and Mouillot 2009, Mavruk *et al.* 2017).

Although there are at least 309 documented Lessepsian species present within the Mediterranean Sea, not all species are equally successful (Golani 2010). Some species have become established throughout the entire Mediterranean sea, for example, the blue-spotted cornetfish (*Fistularia commersonii*), perhaps the most successful Lessepsian species to date (Azzurro *et al.* 2013). Other Lessepsian species for example the half-smooth golden puffer-fish (*Lagocephalus spadiceus*) are less successful in terms of their distribution being restricted largely to the eastern basin, with few sightings within the central Mediterranean (Kiparissis *et al.* 2018). Other species are thought to be successful in terms of the relative abundance they reach within the regions they invade; the white-head fish (*Etrumeus teres*) is becoming highly abundant in Greece with predictions it is likely to become an important fishery resource following a haul of 2500 kg from Chiana Bay by purse-seine (Kasapidis *et al.* 2007). What

determines the invasion success of a species is unclear and is a factor this project aims to investigate.

1.3 *Siganus luridus* and *Siganus rivulatus*

The dusky spinefoot (*Siganus luridus*) and the marbled spinefoot (*Siganus rivulatus*) rabbitfish both belong to the family Siganidae which falls within the order Perciformes (Greenwood *et al.* 1966, Kuriiwa *et al.* 2007). The family Siganidae is composed of only one genus, *Siganus*, which is made up of at least 28 species (Woodland 1990, Randall and Kulbicki 2005). However, there is still some argument regarding whether all these species are distinct as hybridisation has been identified between both closely and distantly related species; meaning it is uncertain whether they are hybrids or distinct species with hybrid origin (Kuriiwa *et al.* 2007).

S. luridus and *S. rivulatus* populations within the Mediterranean all evolved from ancestors within the Red Sea (Farag Abziew and Ali 2016). However, both invasive Lessepsian species are now found and known to have been present within the Mediterranean Sea for over 60 years (Steinitz 1927, Ben-Tuvia 1964). Both species entered the Mediterranean Sea through the Suez Canal but in at least two separate invasions; *S. rivulatus* was one of the earliest invaders documented and was first recorded in 1927 (Steinitz 1927). Comparatively, *S. luridus* was identified in the Mediterranean almost 30 years later in 1956 (Ben-Tuvia 1964).

Despite their long-term presence in the Mediterranean *S. luridus* and *S. rivulatus* are noted to have different distributions throughout the Mediterranean Sea (Figure 2). Individuals of *S. luridus* have been identified across the entire Mediterranean, from large established populations in Lebanon, Turkey, Cyprus, Greece, Malta and the Sicily Strait to small groups of individuals recorded in unexpected locations such as France (Azzurro and Andaloro 2004, Boris *et al.* 2009, Sala *et al.* 2011, Schembri *et al.* 2012). Interestingly, *S. rivulatus* does not

have established populations as far west as *S. luridus*. Some of the most westerly recorded populations of *S. rivulatus* are those in the South Adriatic Sea of Croatia and those on the coast of Tunisia (Golani 2002, Dulĉić and Pallaoro 2004). It was recently confirmed that the 'sightings' of *S. rivulatus* in Malta were in fact misidentifications of *S. luridus*, revealing that the *S. rivulatus* is not established in Malta and has a much reduced dispersal capability than *S. luridus* (Schembri *et al.* 2012).

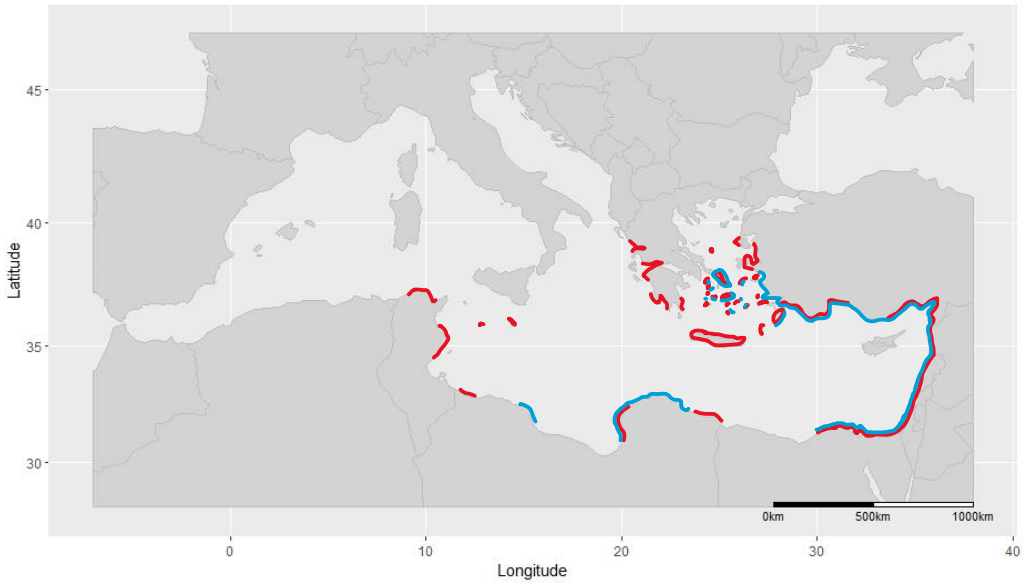

Figure 2: A map of the Mediterranean Sea showing the distributions of the two invasive rabbitfish species. Red areas signify presence of established populations of *Siganus luridus* and blue areas demonstrate the records of established populations of *Siganus rivulatus*. Figure adapted from Azzurro et al. (2016) and Galil (2008). The map was generated on R version 3.5.1 (R Core Team 2018) using packages ggplot2 (Wickham 2016) and ggmaps (Kahle and Wickham 2013). Coloured annotations were added manually.

The differences in the geographic distribution of populations between *S. luridus* and *S. rivulatus* throughout the Mediterranean are surprising given the overlapping ecological niches of the two species as mainly shallow water dwelling, herbivorous schooling fish (Bardamaskos *et al.* 2009). However, it is

thought that this overlap leads to out-competing of one species over another, allowing only one to become established depending on the ecosystem (Bardamaskos *et al.* 2009). The overlap in Cyprus is surprising because of reduced primary productivity in the area compared with the rest of the Mediterranean Sea meaning it is the most oligotrophic region (Danovaro *et al.* 1999). Despite this, it is likely there is less competition within the eastern Mediterranean because conditions are most similar to the those in the species' ancestral environment.

Irrespective of the discrepancies in the species' distribution throughout the Mediterranean Sea, both *S. luridus* and *S. rivulatus* are considered highly effective invaders (Bariche *et al.* 2009). For example, while investigating the depleted algal biomass of the eastern Mediterranean Sea's rocky-reef ecosystems, an important ecosystem within the Mediterranean basins, Sala *et al.* (2011) showed that in regions in Turkey *Siganus* species can together account for up to between 83 % and 95 % of herbivore abundance, with the native species *Sparisoma cretense* making up the remaining 17 % to 5 %. In the same study the other major native herbivorous fish *Sarpa salpa* was not documented in the study areas (Sala *et al.* 2011). In addition, observations by Azzurro *et al*. (2017) indicate that populations of *S. luridus* are still increasing in abundance. Within Linosa (one of the Pelagie Islands in the Strait of Sicily) the relative abundance of *S. luridus* increased from 0.17 individuals per 250 m^2 in 2005 to 0.36 individuals per 250 m^2 in 2015, resulting in *S. luridus* schools containing over 100 individuals. (Azzurro *et al.* 2017).

It is their wide distributions and high abundances that demonstrates the success of these species, making *S. luridus* and *S. rivulatus* particularly interesting for ecological studies, as both species pose great threats to their novel environment of the Mediterranean Sea. For example, both species have been documented feeding on algal forests resulting in the development of barren plains characterised by only bare rock and a few encrusting algal species (Sala *et al.* (2011). In the colder months both species of rabbitfish feed non-selectively,

consuming the native species food resources (Bariche 2006). Not only does deforestation by rabbitfish result in depletion of native species food resources it also reduces the complexity of the environment, removing canopies of large macroalgae, such as *Cytoseria* and *Sargassum* species (Vergés *et al.* 2014). Loss of algal canopy may also affect a range of species which utilise algal forests for protection or food use, with continued loss of forests potentially resulting in the decreased abundance of various species of *Blenniidae*, *Gobiidae* and *Tripterygiidae* within Mediterranean coastal habitats (Cheminée *et al.* 2013).

Lessepsian invasion has proven to be beneficial to the fishery industry within the Mediterranean. For example, both *Siganus* species are becoming an important commercial resource throughout the Mediterranean, with high commercial use in areas from Lebanon to Greece (Carpentieri *et al.* 2009, Corsini-Foka *et al.* 2017). This is likely the result of their increasing abundance and their expanding inhabited depths (Schembri *et al.* 2012). The use of the species in fisheries is thought to be important for regulation of population numbers, reducing abundance of adult individuals and enabling restoration of algal forests from bare-rock barrens (Sala *et al.* 2011).

Chapter 2: Population Genetics of Invasive Populations of *Siganus* Species in the Mediterranean Sea

2.1 Introduction

2.1.1 The Importance of Understanding Genetic Diversity in terms of Invasion

To critically understand and therefore determine the factors that may have enhanced or impeded settlement of invasive species, the genetic diversity of both the ancestral and derivative populations are vital to consider (Azzurro *et al.* 2006). The term 'genetic diversity' refers to the extent that the genome or certain genes differ between individuals within a population. High genetic diversity represents high variation in the genome or certain genes, while low genetic diversity represents a lack of variation (Nei 1987).

Genetic diversity within populations can be measured by quantifying haplotype diversity (i.e., the likelihood that two alleles (alternate versions of genes) when randomly sampled will be different, *h*) or nucleotide diversity (i.e., calculation of the mean number of differences per site when a pair-wise comparison of the sequences is conducted, π). These both describe the diversity in a population (Nei 1987).

Comparing the genetic diversity and specific genotypes of the novel environment (in this case the Mediterranean Sea) to those of the ancestral environment it is possible to gain an understanding of the history of invasion. The history of an invasive population can be traced through the means of phylogenetic and network analysis using genetic data from the newly invaded and ancestral populations. For example, if an invasion is sequential, with sites being invaded sequentially by a subset of individuals present within the previous site's population, a genetic signature from the original population will remain in the population of each sequentially invaded site. As time continues mutations (i.e., changes in the DNA sequence) will accumulate in the original and new

populations, so newer, derivative populations will have the same initial haplotypes in addition to several new changes distinct from those of the natal population. This theory relies on minimal genetic mixing between these distinct populations. If invasion is not sequential, but instead all sites are invaded simultaneously, there will be an equal amount of variation throughout the entire Mediterranean basin with the same haplotypes found in all locations with little to no variation.

Following the invasion of and dispersal across a novel environment, a distinct genetic signature will remain within the invasive population based on the number of initial genotypes present within the original invading group(s), this allows for identification of the mechanism of invasion used (Golani *et al.* 2007, Bariche and Bernardi 2009). A genetic bottleneck, also known as a founder effect, results when an invasion initiates from an initial, small group of invading individuals out of a larger population (Azzurro *et al.* 2006). As a result, the invasive population will have a reduced number of the ancestral population's haplotypes within it. For example, the Lessepsian invasive bluespotted cornetfish (*F. commersonii*) showed a decreased number of haplotypes with a reduction from 49 haplotypes within Red Sea natal populations to just two haplotypes within the Mediterranean Sea (haplotype diversity decreased accordingly from $h = 0.997$ to $h = 0.009$) (Golani *et al.* 2007). The opposite of a genetic bottleneck is termed 'continuous invasion', wherein the invasive population has high genetic diversity, similar to the level of the original population (Bernardi *et al.* 2010). Continuous invasion has been demonstrated in the Mediterranean Sea by a number of Lessepsian invasive species, including the blue-barred parrotfish, *Scarus ghobban* and the silver-cheeked toadfish *Lagocephalus sceleratus* (Bariche and Bernardi 2009, Coro *et al.* 2018).

In the case of the Lessepsian invasion, invasive species are unlikely to have been present within the Mediterranean Sea for long enough to develop mutations in their mitochondrial DNA sequences that are unique to their subsequent populations. Thus, any variation observed within the species is expected to have been present since the initial invasion (Davies *et al.* 1999, Bonhomme *et al.*

2003, Azzurro *et al.* 2006). It is plausible that a reduction in genetic diversity may be identified within the hypervariable mitochondrial region when comparing between Red Sea and Mediterranean populations as a result of a genetic bottleneck. Subsequently, small reductions in genetic diversity between individual populations in the Mediterranean would not be unexpected if the invasion was to have occurred sequentially, in a 'stepping-stone' fashion.

2.1.2 Use of Molecular Markers to Evaluate Genetic Diversity and Evolutionary Relationships Between Populations

Two sources of genetic variation between individuals can be used to investigate the genetic diversity of a population. These are the variation within the nuclear genome and the variation within the mitochondrial genome; obtained through collection of nuclear microsatellite data and collection of mitochondrial haplotype data respectively (Zhang and Hewitt 2003). Microsatellites are short, conserved sequences on chromosomes which vary in the number of sequence repetitions present, making them ideal for genetic finger-printing, and thus genetic diversity comparisons between individuals and individuals of different populations (Vieira *et al.* 2016). Mitochondrial haplotype data is easily and cost-effectively obtained through means of PCR amplification and sequencing to identify base changes within a nucleotide sequence of a mitochondrial gene. To determine evolutionary relationships between both individuals and populations within ecological studies mitochondrial DNA is the preferred data source (mtDNA) (Wilson *et al.* 1985, Moritz *et al.* 1987, Zhang and Hewitt 2003, Galtier *et al.* 2009).

It is the number of base changes that determines the genetic diversity of the population in question. Following amplification, mitochondrial sequences are used for generation of phylogenetic trees and haplotype networks (to allow identification of relationships between individuals) in addition to comparison of nucleotide diversity (π) and identification of haplotype diversity (h) (Nei 1987). Mitochondrial data was elected above nuclear data to study in this project as it evolves approximately ten times faster than the nuclear genome, providing the

best basis to study population level variation within the elected species (Brown *et al.* 1979). Cytochrome oxidase C subunit I (COI), a mtDNA fragment, is considered a standard tool for taxonomical and phylogenetic studies in this respect and is the most frequently used as it is taxonomically verified to cover more taxa than any other (Ratnasingham and Hebert 2007, Deagle *et al.* 2014). Although COI is useful due to the large range of species it can amplify, it is limited by the lack of conservation within the primer binding sites (Deagle *et al.* 2014). Other mitochondrial genes used for phylogenetic and diversity studies include the control region (i.e., CR, the D-loop), Cytochrome b, 12s and 16s (Sanna *et al.* 2011). Of these, the CR allows for sequencing of the most variable part of the mitochondrial genome as it contains a region known as the hyper-variable region (Murakami *et al.* 2001). Because the CR is the mitochondrial region evolving most rapidly and thus is the most variable at the intra-specific level, it allows for resolution of recent divergences of closely related populations, such as those that have recently invaded the Mediterranean Sea (Lee *et al.* 1995).

2.1.3 Genetic Diversity and Adaptation to Novel Environments

High levels of genetic diversity within invasive species ancestral populations are thought to facilitate the adaptation of invasive populations to a new environment (Roman and Darling 2007). This is due to a greater variety of possible phenotypes encoded into the genome, some of which hypothetically allow for greater suitability to a new environment than others, and thus a greater likelihood that an important biological role can still be fulfilled by the phenotype in question (Bock 1980). Essentially, genetic diversity can act as a potential predictor of how capable a species may be to adapt or respond to selection events occurring within a new environment with different physiological constraints (Lee 2002, Azzurro *et al.* 2006). A high genetic diversity indicates a greater chance of adaptation to the novel environment, and thus, survival. For this study, it was hypothesised that a greater genetic diversity within the invasive population might equate to a higher level of 'invasion success' as determined by the extent of the species' geographic distribution within the novel environment.

Measures of haplotype and genetic diversity such as *h* and π are important when trying to understand the events that led to the new populations settling, because the mechanism of invasion can restrict the number of haplotypes entering the novel environment (Bernardi *et al.* 2010). If the number of haplotypes is reduced in the Mediterranean Sea compared to the Red Sea, then theoretically the likelihood of invasion success should be reduced (Roman and Darling 2007). However, with Lessepsian invasion, this is seemingly not always the case, as reviewed by (Bernardi *et al.* 2010). For example, the invasion of *F. commersonii* into the Mediterranean was the result of a small number of initial, highly successful individuals that were capable of rapid dispersal across the Mediterranean (Golani *et al.* 2007, Azzurro *et al.* 2013, Jackson *et al.* 2015). The case study of *F. commersonii* is important to consider as a 96 % reduction in haplotype number would be expected to reduce fitness, despite this, *F. commersonii* is perhaps the most successful Lessepsian species to date (Golani *et al.* 2007). This indicates that genetic diversity of the ancestral and invasive populations are perhaps not the only predictor of invasion success.

2.1.4 The Current Understanding of the Genetics of Invasion

The question of how the genetic diversity of the resultant invasive population is affected following the invasion of a novel environment is still under fierce debate with results from studies on a range of both marine and terrestrial faunal and floral species showing variable outcomes; from a high level of haplotype or nuclear diversity in the invasive population, consistent with the ancestral population to a drastically reduced level of diversity in the resultant invasive population.

Two separate studies utilising various microsatellite loci have investigated the genetic variation within and between the invasive and ancestral populations of the slipper limpet (*Crepidula fornicata*), a species of marine gastropod. Both studies documented that following invasion of European bays and estuaries the species retained high genetic diversity in the resultant, invasive populations with levels similar to those of the populations within the species' native range

(Dupont and Viard 2003, Viard *et al.* 2006). Studies such as these are important because they support the hypothesis that Roman and Darling (2007) presented, that invasion, and thus adaptation to a new environment is facilitated by high levels of genetic diversity. The hypothesis is supported by multiple other studies including that by Lejeusne *et al.* (2014) where researchers demonstrated the oriental shrimp (*Palaemon macrodactylus*), a species now resident in temperate estuaries worldwide, demonstrates high genetic diversity across the globe with no evidence of a founder effect.

Conversely, studies on other marine organisms have documented a drastic reduction in genetic diversity between ancestral and their resultant invasive populations. The Japanese skeleton shrimp (*Caprella mutica*) originates from South-East Asia but within the last 50 years has been introduced into both the coasts of North America and the North Atlantic waters of Europe (Ashton *et al.* 2007). Using the mitochondrial marker Cytochrome Oxidase I (COI) Ashton *et al.* (2008) found that the number of haplotypes and the levels of genetic diversity present in the invasive range was drastically reduced from that of the species' native range; the number of haplotypes of the COI region dropped from 31 haplotypes in the ancestral population to only 7 haplotypes within the invasive populations and nucleotide diversity dropped from a maximum of 0.14 to as low as 0.00. This is important to consider as it supports the theory that a reduced genetic diversity can result from invasion of a novel environment, as proposed by Azzurro *et al.* (2006). This evidence disagrees with the Roman and Darling (2007) hypothesis that high genetic diversity (initially) will allow for successful invasion.

2.1.5 The Genetics of Lessepsian Invasion

The majority of studies investigating the genetic diversity within and between Lessepsian populations and their ancestral counterparts have been centred within the Eastern Mediterranean basin; this is likely the result of the greater abundance of Lessepsian species in the eastern basin as a result of the proximity to the Suez Canal (Bernardi *et al.* 2010, Turan 2010). This research has unexpectedly, and

almost unanimously, revealed a similarity in levels of genetic diversity between the invasive Mediterranean and ancestral Red Sea populations of a large number of different marine species, from fish and invertebrates to angiosperms (Bernardi *et al.* 2010). For example, the blue-barred parrotfish (*S. ghobban*) demonstrates an insignificant change in the levels of both haplotype and genetic diversity between the invasive and ancestral populations (Bariche and Bernardi 2009). Using the mitochondrial control region and the nuclear ribosomal S7 protein fragment, Bariche and Bernardi (2009) demonstrated that the sequences from the Mediterranean populations, which were highly variable, were not significantly different from, and clustered closely with those of ancestral populations from the Indian Ocean. The lack of reduced haplotype and nucleotide diversity once again agrees with the Roman and Darling (2007) hypothesis that high diversity allows for successful invasion. However, once again, high diversity within the invasive population was not expected, as a genetic bottleneck was predicted to have occurred, the high diversity and closely clustering sequences indicated a lot of movement of individuals across from the Red Sea into the Mediterranean signifying a lack of a barrier to colonisation.

The goldband goatfish (*Upeneus moluccensis*) is another example of a Lessepsian species demonstrating an insignificant level of genetic diversity between eastern Mediterranean populations and ancestral populations, as the genetic distance between populations remained relatively consistent following invasion of the Mediterranean sea (Golani and Ritte 1999). Golani and Ritte (1999) used 21 genetic loci from liver and muscle enzymes to analyse the genetic similarity between the invasive Mediterranean and Red Sea populations. Their results showed that the genetic distance between the Mediterranean and Red Sea populations was distance = 0.004, calculated as per the Nei (1978) index. This is a very low value showing minimal change between the genetic sequences of the Mediterranean and Red Sea populations. If only some genetic types were capable of invading through the Suez Canal, the genetic diversity (distance) would be expected to increase between populations. This is not the case suggesting high connectivity between the Mediterranean Sea and the Red Sea, characteristic of a continuous invasion and continued movement of haplotypes.

Similar genetic studies conducted on populations of Lessepsian species within the central Mediterranean have also found that there is a lack of genetic diversity between individual populations throughout the Mediterranean Sea in addition to the ancestral populations within the Red Sea. For example, a study conducted by Terranova *et al.* (2006) investigating the genetic diversity between invasive Mediterranean populations of the invertebrate *Brachidontes pharaonis* (a species of mussel native to the Red Sea and Indian Ocean) failed to demonstrate a significant difference in haplotype or nuclear diversity between the oldest (Israeli) and most recently established population (Sicilian) within the Mediterranean Sea.

The concept of high genetic connectivity between populations has led to the formation of the hypothesis that Lessepsian invasion of species involves continuous gene flow from the Red Sea and a continuous invasion of individuals maintaining genetic connectivity to the Red Sea (Bernardi *et al.* 2010). This is supported by the maintained high genetic diversity both between invasive populations and between invasive and ancestral populations of *S. ghobban*, *U. moluccensis* and *B. pharaonis* (Golani and Ritte 1999, Terranova *et al.* 2006, Bariche and Bernardi 2009). This hypothesis is further supported by evidence provided by Azzurro *et al.* (2006) who were able to demonstrate preservation of Red Sea and eastern Mediterranean population's mitochondrial diversity within the most recently established, western-most population of dusky spinefoot rabbitfish (*S. luridus*), with no founder event or bottleneck history present within the Mediterranean. This suggests that diversity has been present since the start of the invasion, but connectivity to the Red Sea is maintained (Bernardi *et al.* 2010).

The bluespotted cornetfish, (*F. commersonii*) is a seemingly rare exception to the observation of a maintained level of genetic diversity between the invasive Mediterranean and ancestral Red Sea populations (Golani *et al*., 2007; Jackson *et al*., 2015; Sanna *et al*., 2011). Thus, it also disagrees with the concept of

continuous invasion. A study by Golani *et al*. (2007) revealed a drastic drop in the haplotype diversity between ancestral and invasive populations from 46 haplotypes present in the native range to only two in the Mediterranean; a shift in diversity from $h = 0.997$ to $h = 0.009$ respectively. This distinct bottleneck has not, however, impacted the species' ability to disperse and become established within the novel environment of the Mediterranean Sea; termed a "Lessepsian sprinter" by Tenggardjaja *et al.* (2013) it is understood that *F. commersonii* is one of the most rapid Lessepsian colonisers of the Mediterranean Sea to date. In only seven years *F. commersonii* had successfully become established throughout the entire Mediterranean Sea (Jackson *et al.* 2015). The species is predicted to have spread across the two basins within the Mediterranean at rates of over 1000 km per year (Azzurro *et al.* 2013). The expansive distribution of *F. commersonii* in the novel environment accompanied with the species' rapid dispersal rate makes it one of the most successful Lessepsian invaders to date. This is especially true considering that there are very few extensively distributed Lessepsian species present within the Mediterranean Sea (Jackson *et al.* 2015). *F. commersonii*'s extreme success demonstrates that an extreme bottleneck of genetic diversity during invasion is not necessarily a limiting factor, and does not necessarily constrain the ability of a species to successfully invade a novel environment.

2.1.6 The Current Understanding of the Genetic diversity of Rabbitfish within the Mediterranean Sea

As expected, based on findings for the majority of Lessepsian species, within the eastern Mediterranean Sea neither a genetic bottleneck nor founder effect was detected during genetic studies focusing on *S. luridus* or *S. rivulatus* (Bonhomme *et al.* 2003, Hassan *et al.* 2003). Using both mitochondrial and nuclear markers Hassan *et al*. (2003) demonstrated that Syrian populations (collected from Lattakia) of both *S. rivulatus* and *S. luridus* included similar levels of genetic diversity to the ancestral populations within the Red Sea, confirming the initial rejection of the idea that a genetic bottleneck had reduced genetic diversity within the Mediterranean populations of both these species. This trend of a high level of genetic diversity and common Red Sea haplotype presence within

Mediterranean populations is however seemingly not maintained throughout the Mediterranean Sea. Research investigating the western-most recorded populations of *S. luridus*, found on the shores of Linosa, in the Strait of Sicily, indicate a decrease in genetic diversity when compared to populations within the Red Sea. Using the mitochondrial CR marker, Azzurro *et al*. (2006) recorded a decreased haplotype diversity in the western Mediterranean population of 0.879 and a similarly decreased nucleotide diversity of 0.592 compared to the Red Sea population's haplotype and nucleotide diversity of 0.978 and 0.958 respectively.

2.1.7 Research Aims and Objectives

The main aim of this genetic study is to further the understanding of genetic diversity of the invasive rabbitfish species, *S. luridus* and *S. rivulatus* within the Mediterranean Sea.

The project aims to increase the pool of genetic data available by adding additional sample sites (throughout the eastern, central and western Mediterranean Sea) and increasing the genetic sequence data available for the mitochondrial control region. Additionally, another marker (COI) will be used to sample individuals from the same sites within the eastern, central and western Mediterranean Sea. Incorporation of the central and western sites will allow more detailed investigation into the presence of a genetic bottleneck and any demographic changes within *Siganus* populations of the Mediterranean Sea. Following submission of this thesis these sequences will be uploaded to GenBank and added to a genetic barcoding library being developed by Ernesto Azzurro.

Further investigation into the now 12-year old "newly" settled population of *S. luridus* documented by Azzurro *et al*. (2006) will be conducted to investigate if the presence of a reduced genetic and haplotype diversity remain in comparison to the Red Sea and the rest of the Mediterranean Sea. If so, these factors could indicate a genetic bottleneck occurred from a secondary, sequential invasion from a different Mediterranean site.

2.2 Materials and Methods

Unless otherwise states all images of *S. luridus* and *S. rivulatus* were taken by Randall (1997), obtained from FishBase (Froese and Pauly 2018) and are freely available for non-commercial use.

2.2.1 Sample Collection

Tissue samples from individuals of the two invasive species of rabbitfish present within the Mediterranean Sea, *S. luridus* and *S. rivulatus*, were collected from fish markets, sourced through spearfishing and collected by local fisherman from five study area locations around the Mediterranean basin between the years 2016 to 2018; Linosa, the Peloponnese, Turkey, Rhodes and Cyprus. (Figure 3). Following communication with local fisherman and fish markets it became clear that in the Eastern Mediterranean, including Turkey, Cyprus and Rhodes the two species are commonly used as a food resource, however this was seemingly not the case in the more central and western locations of the Peloponnese and Linosa. An unsuccessful attempt was made to collect samples from Malta. Unfortunately, in early March it seems the species aren't highly abundant, and when caught the fishermen simply return them to the water as they are of no commercial value. Efforts were made to ensure that any fish sourced from fish markets were caught locally to the study area.

Fish were collected from four sites in Cyprus (Figure 4a), one site in Rhodes (Figure 4b), one site in Turkey (Figure 4c), one site on the island of Linosa (Figure 4d) and five sites in the Greek Peloponnese (Figure 4e).

Following collection, samples were photographed alongside a label showing the sample ID to enable future clarification of species identification. Photos were taken for all populations where whole individuals were collected directly. Some individuals are missing photo IDs as a small tissue sample was provided by an external source. Samples were then stored on ice to prevent degradation of the DNA within fin and muscle tissue. Within 24 hours a fin-clip or dorsal muscle

sample was taken and stored in 99% ethanol at -20 ^{o}C until further processing was conducted.

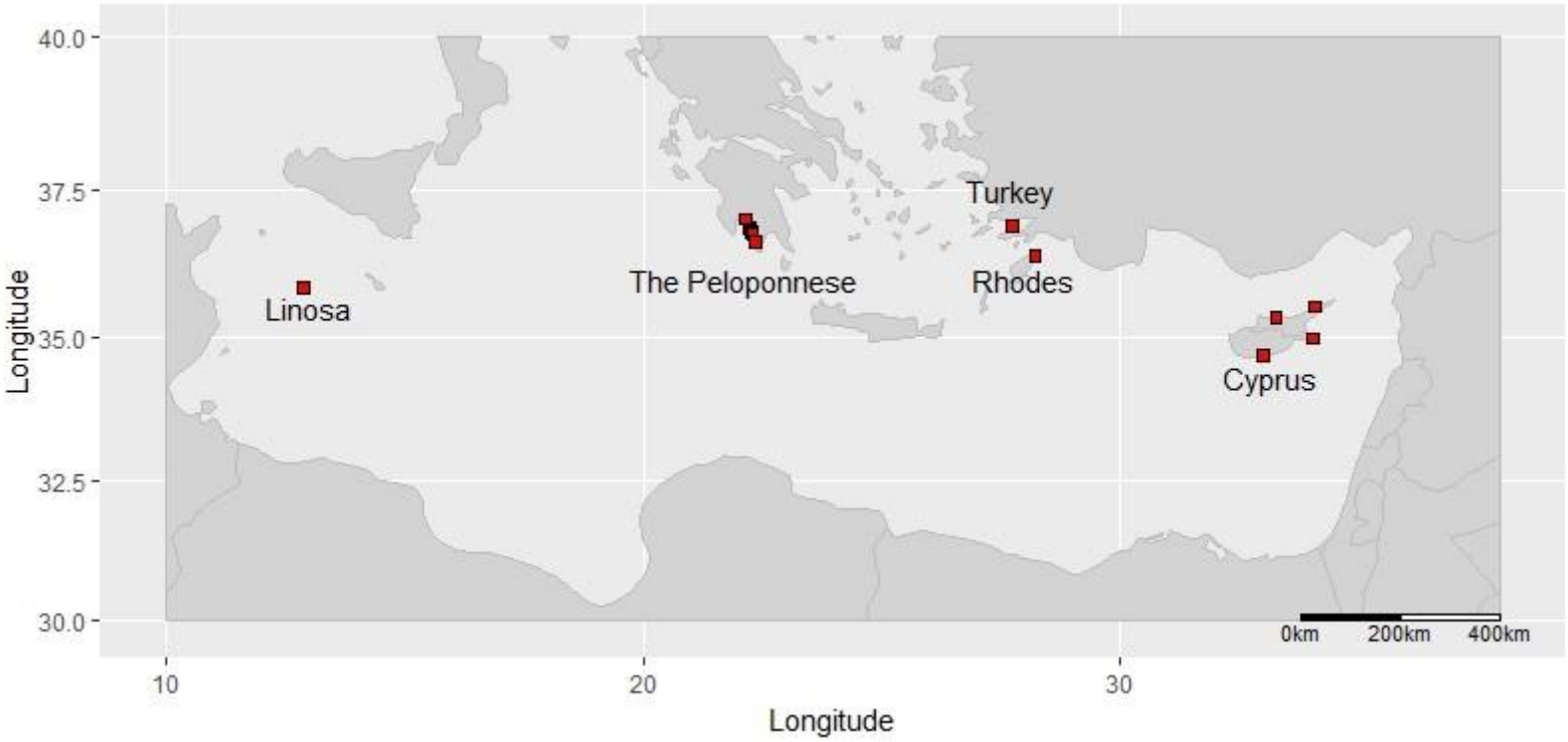

Figure 3: **Study areas throughout the Mediterranean basin.** Study sites are indicated by red squares. The x-axis represents the longitude and the y-axis represents the latitude. Maps were generated on R (R Core Team 2018) using decimal coordinate data and the packages ggplot2 (Wickham 2016), rgdal (Bivand *et al.* 2018) and ggmap (Kahle and Wickham 2013). See Appendix 1 for the code used.

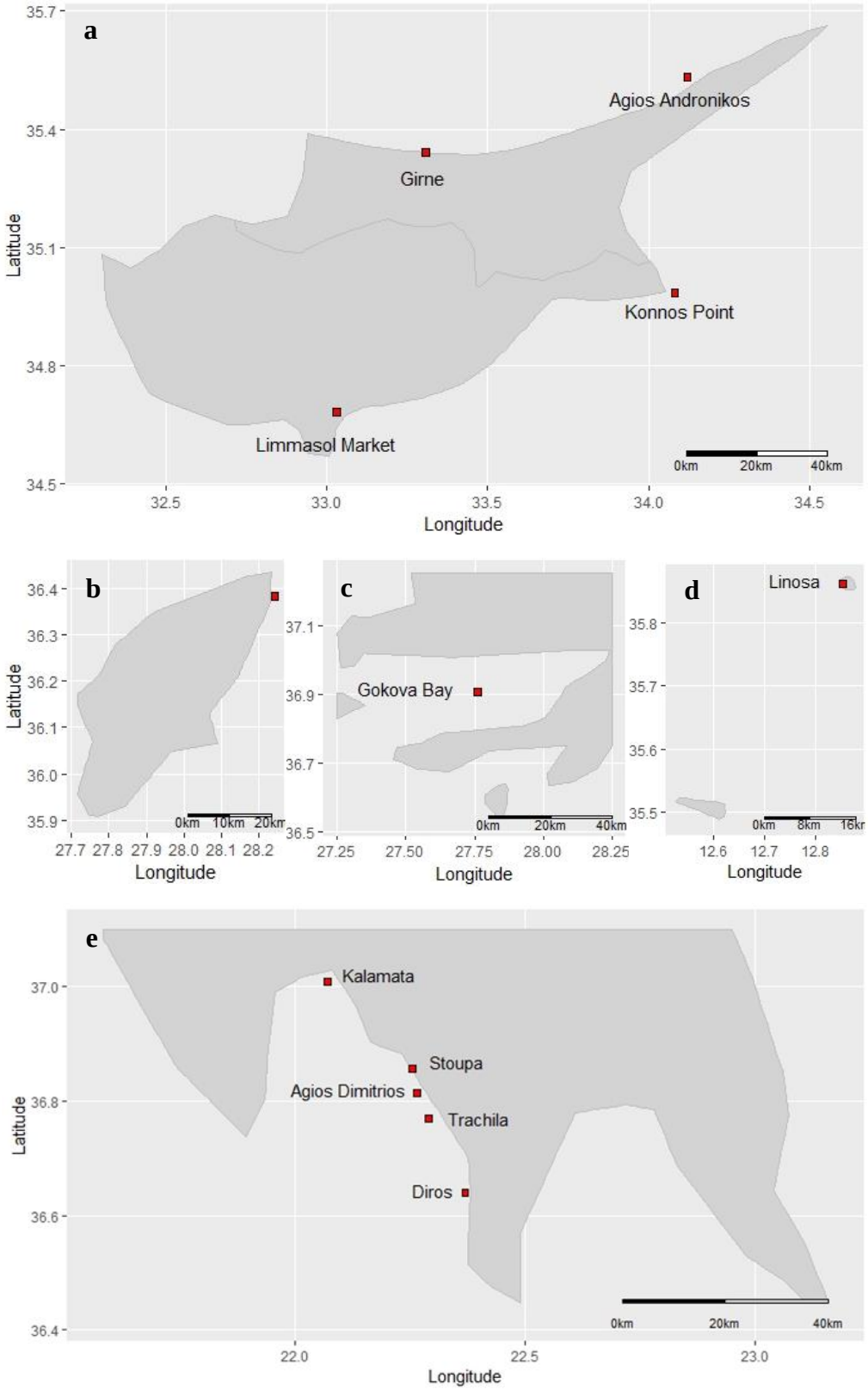

Figure 4: Sampling sites within the study areas of (a) Cyprus, (b) Rhodes, (c) Turkey, (d) the Pelagie Islands and (e) the Peloponnese. Red squares indicate the study areas. The x and y axes refer to the longitude and latitude

respectively. Maps were generated on R (R Core Team 2018) using decimal coordinate data and the packages ggplot2 (Wickham 2016), rgdal (Bivand *et al.* 2018) and ggmap (Kahle and Wickham 2013).

2.2.2 DNA Extraction

DNA was extracted from fin or dorsal muscle tissue. A modified version of the Goodacre and Wade (2001) protocol using 2% CTAB was selected due to its high efficacy in DNA extraction (Xin and Chen 2012). 2 mm^3 samples of tissue were taken and ground using Sigma Aldrich acid-washed beads (G8772). A 2% solution of CTAB was added (100 mM Tris HCL, 20 mM EDTA, 1.4M NaCl and 2% CTAB) followed by 0.2% β-mercaptoethanol and 10 mg/ml (10 µL) proteinase K solution. Samples were incubated at 55 ^oC for a minimum of three hours, until the tissue was completely digested. A chloroform: isoamyl alcohol (24:1) mix was used to separate the aqueous and organic phases through mixing for 1 minute and centrifugation for 5 minutes at 13,000 g using a Thermo Electron Corporation, IEC MicroCL 17 centrifuge. The aqueous phase containing the DNA was taken and the entire chloroform: isoamyl alcohol process repeated for further purification. 2.5 times the volume of ice-cold ethanol (99%) and $1/10^{th}$ the total volume sodium acetate (NaAc) 3 M were added and the aqueous phase stored overnight at -80 ^oC. The frozen samples were centrifuged at 13,000 g for 15 minutes in order to pellet the DNA and the ethanol was removed. To remove further impurities the pellet was then washed with 70% ethanol by centrifuging the pellet with the ethanol at 13,000 g for 5 minutes. The ethanol was then removed and the pellet air dried at 45 ^oC for 15 minutes. The DNA was then resuspended in 200 µl TRIS HCl (pH 8.0).

2.2.3 Polymerase Chain Reaction (PCR)

Two mitochondrial markers, Cytochrome Oxidase C Sub-unit I (COI) and the control region (CR), alternatively known as the d-loop, were amplified using PCR. For CO1, primers FishF2 and FishR2, (Table 1), designed by Ivanova *et al*. (2007) were used to amplify a sub-section of the gene. Where amplification proved unsuccessful the alternative primers FishF1 and FishR1 (Ward *et al.*

2005) were utilised. For the control region, primers Cr-e and Cr-a (Lee *et al.* 1995) were used.

Table 1: PCR primers used for the amplification of the Cytochrome Oxidase I and the control region. Genetic loci (genes) primer names and their associated sequences (5'-3').

Gene	Primer	Sequence
Cytochrome Oxidase 1	FishF2	TCGACTAATCATAAAGATATCGGCA
	FishR2	ACTTCAGGGTGACCGAAGAATCAGAA
Cytochrome Oxidase 1	FishF1	TCAACCAACCACAAAGACATTGGCAC
	FishR1	TAGACTTCTGGGTGGCCAAAGAATCA
Control Region	Cr-e	CCTGAAGTAGGAACCAGATG
	Cr-a	TTCCACCTCTAACTCCCAAAGCTAG

From all the individuals collected from each site DNA was extracted and the COI and the CR markers were sequenced. The aim was to sequence between eight and 20 samples per site where numbers permitted.

All PCRs were conducted following the Bioline BIOTAQ™ protocol (BIO-21060). The PCR reaction mix for the CO1 gene contained 1x NH_4 reaction buffer, 1.5 mM $MgCl_2$ solution, 0.2 mM dNTP solution (containing dATP, dCTP, dGTP and dTTP), 0.2 µM of both the forward and reverse primers, 0.5 u TAQ, 1 µL of the DNA solution and sterile, deionised water to make up the total volume to 25 µL. For the CR, the same reaction mix was used with the exception of the $MgCl_2$ concentration which was increased to 2.5 mM. The amplification was performed in an MJ Research, Inc PTC-100 (Programmable Thermal Controller) thermal-cycler. Thermocycling conditions can be seen in Table 2.

Table 2: PCR Cycling conditions used for amplification of fragments from the mitochondrial cytochrome oxidase I and control region markers.

Stage	Temperature (ºC)	Duration (Seconds)	Cycles
Initial Denaturation	95	120	1
Denaturation	94	30	35
Annealing	56	30	
Extension	72	60	
Final elongation	72	600	1

A negative control was also used in each round of PCRs. This contained all the components except the DNA template. If this showed a positive result for amplification the products would be discarded due to suspected contamination.

2.2.4 Gel Electrophoresis of PCR Products

Gel electrophoresis was conducted on a 1.5% agarose gel containing 0.05 µg/mL ethidium bromide at 100 V for 1 hour and 30 minutes. Resultant bands on the gels formed by PCR products present within the gels were imaged using UV light through the use of a NuGenius Gel Documentation System. A 100 bp BIOLINE ladder (Hyperladder) (BIO-33056) was run alongside PCR products to ensure products were of the expected fragment size, indicating successful amplification of the target loci. For COI, the amplified fragment was expected to be approximately 655 base pairs (bp) in length. (Bingpeng *et al.* 2018). For CR, the fragment was expected to be approximately 390 bp in length (Lee *et al.* 1995).

2.2.5 Purification of PCR Products

The products were purified in preparation for sequencing using the Sigma-Aldrich GenElute™ PCR Clean-Up Kit (NA1020) following the supplied protocol.

2.2.6 Sequencing

Purified PCR products at a concentration of 10 ng/µL were sent to Source Bioscience in Nottingham, or GeneWiz in Essex for Sanger sequencing of single strands. Both companies used 3730xl DNA analysers. For COI the forward primers FishF2 or FishF1 were used for sequencing. For the CR the reverse primer CR-e was used.

2.2.7 Checking and Editing Sequence Quality

Sequences were returned from Source Bioscience and GeneWiz in .seq and .ab1 trace formats. To ensure sequences were of high quality, the traces were analysed in 'Trev', part of the Staden Package allowing visualisation of chromatograms and editing of the associate sequences (Bonfield *et al.* 2002). The reverse complement sequences of the PCR primers were removed from the 3' end of the sequence and sequences were cropped at the 5' end to remove poor quality sequence at the start of the read. Any errors in sequences (missing bases/miscalled bases) were rectified in Trev (Bonfield *et al.* 2002).

2.2.8 Sequence Alignment

Sequences were aligned using the program Genetic Data Environment (GDE) (Smith *et al.* 1994) by manually inserting gaps into regions where some sequences were missing bases in respect to other sequences and where appropriate with respect to the encoded amino acid sequences. The only sites used for the analyses were those that unambiguously aligned across all sequences.

2.2.9 Generation of a Phylogenetic Tree

Maximum likelihood (ML) phylogenetic trees were produced in PhyML version 3.1 (Guindon *et al.* 2010). In total 3 ML trees were constructed. One tree for each genetic marker individually (COI and CR) containing sequences from both species and one tree of concatenated gene sequences (containing sequences of both COI and CR concatenated from the same individuals) was generated. For all trees, a sequence from the corresponding marker of *Siganus vulpinus*, a closely related teleost fish, were downloaded from GenBank and used as the outgroups. The accession numbers for the sequences taken from GenBank are KP194712 and AY057327 for COI and CR, respectively. The data was exported from GDE in phylip format (.phy) and imported into PhyML version 3.1 (Guindon *et al.* 2010).

Maximum likelihood trees were constructed using a general time reversible model of evolution incorporating a gamma correction (GTR+G) (see Table 3 for settings). 1,000 bootstrap replicates were used. The output of these analyses were viewed in the program FigTree version 1.4.3 (Rambaut 2016). Because it was not possible to amplify and sequence both the COI and the CR markers from all individuals, 38 individuals were excluded from the concatenated analysis. A sequence of the species *Siganus vulpinus* a closely related teleost fish as determined by Borsa *et al*. (2007) was chosen as the outgroup for the analysis, as consistent with a previous genetic study conducted by Azzurro *et al.* (2006).

Table 3 – Settings used within PhyML in order to produce a phylogenetic tree.

Setting	Selected Option
Data type (DNA/AA/Generic)	DNA
Input sequences interleaved (or sequential)	interleaved
Analyze multiple data sets	no
Run ID	none
Model of nucleotide substitution	GTR
Optimise equilibrium frequencies	yes
Proportion of invariable sites (fixed/estimated)	fixed (p-invar = 0.00)
One category of substitution rate (yes/no)	no
Number of substitution rate categories	16
Gamma distributed rates across sites	yes
Gamma distribution parameter (fixed/estimated)	estimated
Optimise tree topoLOGy	yes
Starting tree (BioNJ/parsimony/user tree)	BioNJ
Tree topoLOGy search operations	NNI moves (fast, approximate)
Non parametric bootstrap analysis	yes (1000 replicates)
Approximate likelihood ratio test	no

2.2.10 Generation of Haplotype Networks

In order to make haplotype networks, the same alignments were used as in the phylogenetic tree analysis. This was exported as a FASTA (.fas) file and imported into the program DNA Sequence Polymorphism version 6.11.01 (DnaSP6) (Rozas *et al.* 2017). A new haplotype data file was generated and saved as a NEXUS file (.nex) with gaps not considered and invariable sites set to be removed. The resulting text document was edited to add a section identifying the traits (the site from which the individuals were collected) and

assigning the number of individuals from each site to each haplotype (an example of this text can be found in Appendix 2). Population Analysis with Reticulate Trees (POPART) (Leigh and Bryant 2015) was used to open the modified .nex file and generate a median-joining network (Bandelt *et al.* 1999).

2.2.11 Measuring Population Diversity Across the Mediterranean Sea

To gain an understanding of the degree of variation within each marker and between populations, multiple indices of genetic difference were calculated. DnaSP6 was used to measure haplotype diversity (*h*) through generation of a haplotype NEXUS file and nucleotide diversity (π) (Rozas *et al.* 2017). The mean pairwise distances between populations and all individuals within the Mediterranean Sea were calculated using distance matrices generated in PAUP* version 4.0 (Phylogenetic analysis using parsimony) (Swofford 2002). Pairwise distances were calculated between all sequences using the GTR+G model of evolution; from these the required mean distances were calculated.

F_{ST} (F-statistics) were calculated between individual populations of the species separately using Arlequin version 3.5 (Excoffier and Lischer 2010). Values were interpreted based on guidelines that $F_{ST} = 0.00$ demonstrates panmixia (high levels of mixing) and $F_{ST} = 1.00$ represents great population structure (little to no mixing); values >0.00 but ≤0.05 were taken to signify minimal genetic differentiation, values >0.05 but ≤0.15 are thought to represent moderate differentiation within the markers used and values >0.15 but ≤0.25 are thought to show high levels of genetic diversity within the population. Finally, levels >0.25 represent extremely high levels of genetic differentiation.

2.2.12 Investigation demographic changes

To investigate the presence of changes in population size, three tests of neutrality were conducted; Tajima's D (Tajima 1989), Fu's F (Fu 1997) and a mismatch distribution test. These tests rely on identifying if populations are evolving in accordance with the Wright-Fisher neutral model of evolution and that all

mutations are selectively neutral (Fu 1997). The neutral theory of evolution states that variation is produced by mutation, which leads to genetic diversity. It also states that this variation is removed by the effects of genetic drift (Hedrick 2011). Arlequin was used to conducted Tajima's D and Fu's F tests with 10,000 permutations (Excoffier and Lischer 2010).

Tajiima's D tests investigate the relationship between two DNA-level forms of genetic variation; the number of segregating sites present and the mean number of nucleotide differences (Tajima 1989). Essentially, the equilibrium between mutation and drift is tested by calculating the frequency of mutations and the number of events that lead to differences at the variable sites. A value of zero will result when mutation and drift are at equilibrium; positive values signify a reduced frequency of rare alleles than expected and a negative value indicates a higher than expected frequency of rare alleles. These indicate balancing selection or population contraction and positive selection or population expansion following a genetic bottleneck respectively.

Fu's F is a similar but more powerful test that takes the number of haplotypes in a population into account to identify the relationship between mutation and drift and thus expansion or selection within a population (Fu 1997, Ramírez-Soriano *et al.* 2008). A negative value for Fu's F also represents an excess of rare alleles thought to be due to a high number of recent mutations.

DnaSP6 (Rozas *et al.* 2017) was used to conduct a mismatch distribution test. This tested the presence of observed pairwise differences in the nucleotide sequence against the expected values for a growing population. Another test that can indicate population expansion. The expected result identifying presence of a population that fits the neutral model is an uneven multimodal distribution, while a population with recent, sudden expansion will demonstrate a unimodal distribution with larger values for the mismatch occurring over time (Rogers and Harpending 1992, Grant 2015).

2.3 Results

In total 108 samples of *S. luridus* and 109 samples *S. rivulatus* were collected from 12 sites with increasing distances from the Mediterranean Sea (Table 4). PCR was used to amplify two mitochondrial markers (COI and the CR) were sequenced from each of these individuals to allow for sequencing. Once primers and ambiguous sites were removed, the COI and CR alignments had lengths of 548 and 346 nucleotides respectively. The concatenated alignment comprised of 895 nucleotide sites.

Complications were encountered when amplifying both genes from a few individuals, so the final number of each species from each site used for the concatenated analysis is displayed in Table 5.

Table 4: The number of individuals from each site, with increasing distances from the Suez Canal, successfully amplified for the two mitochondrial markers (cytochrome oxidase C sub-unit I (COI) and the control Region (CR) used for analysis of diversity within the Mediterranean Sea.

Site	Distance from the Suez Canal (km)	Number of *S. luridus*		Number of *S. rivulatus*	
		COI	CR	COI	CR
Limmasol	384	7	7	10	10
Konnos Point	442	0	0	4	4
Girne	465	0	0	20	23
Agios Andronikos	507	0	0	12	13
Kallithea	681	20	20	7	17
Gokova Bay	750	20	19	12	10
Diros	1097	19	18	7	13
Trachila	1107	0	0	10	12
Agios Dimitrios	1110	15	14	0	0
Stoupa	1117	11	11	0	0
Kalamata	1124	0	0	6	7
Linosa	1873	16	17	0	0
Total	n/a	108	106	88	109

Table 5: The number of individuals from each site, with increasing distances from the Suez Canal, used for concatenated sequence analysis of diversity within the Mediterranean Sea.

Site	Distance from the Suez Canal (km)	Number of individuals	
		Siganus luridus	***Siganus rivulatus***
Limmasol	384	7	10
Konnos Point	442	0	4
Girne	465	0	20
Agios Andronikos	507	0	10
Kallithea	681	19	6
Gokova Bay	750	20	12
Diros	1097	18	6
Trachila	1107	0	10
Agios Dimitrios	1110	14	0
Stoupa	1117	11	0
Kalamata	1124	0	6
Linosa	1873	17	0
Total	n/a	106	86

2.3.1 Maximum Likelihood Analysis and Pairwise Distance

The ML tree built from concatenated sequences of the COI and CR markers confirmed that there are two genetically distinct *Siganus* groups present within the Mediterranean Sea (Figure 5). The first group consists solely of *S. luridus* individuals and is supported in 99.6 % of bootstrap replicates. The second group is made up only of *S. rivulatus* individuals and is supported in 96.8 % of bootstraps. The structure of the concatenated tree concurs with the two unrooted ML trees generated for the COI and the CR data individually which also resolve two clear groups; one for *S. luridus* and one for *S. rivulatus* (Figures 6a and 6b).

Pairwise distances calculated using PAUP (Phylogenetic Analysis Using Parsimony) version 4.0 (Swofford 2002) clearly support the two distinct species groupings. When individuals within each species were compared, the mean pairwise intra-species distances were 0.025 (2.5 %) for *S. luridus* and 0.004 (0.4 %) for *S. rivulatus*. These are very low values and are not unexpected when comparing distance between individuals of the same species. These values are over 10-fold lower than the inter-species mean pairwise distance value obtained when comparing between *S. luridus* and *S. rivulatus*; 0.27 (27%).

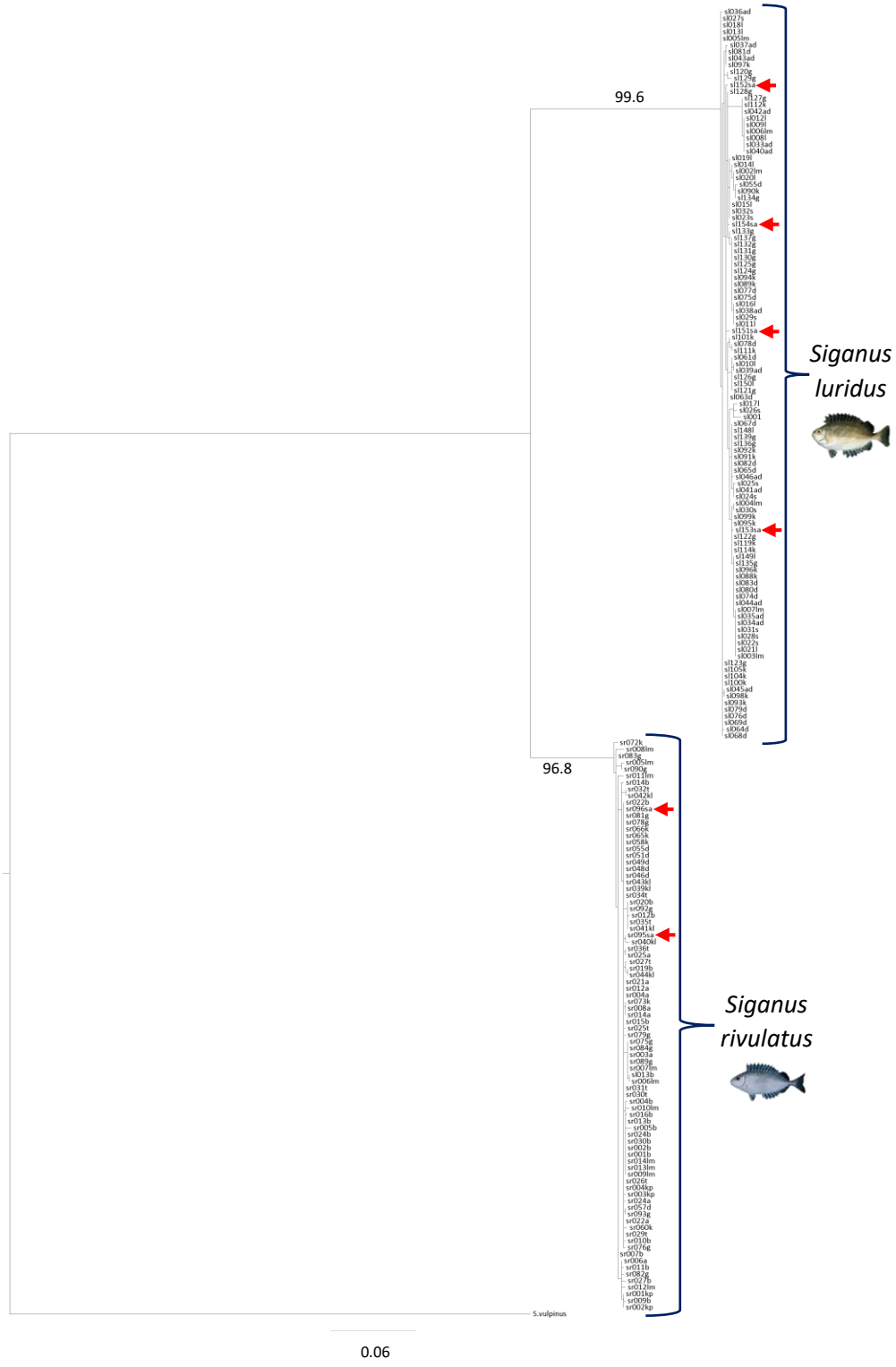

Figure 5: Maximum likelihood phylogenetic tree constructed from concatenated sequences of the mitochondrial cytochrome oxidase C sub-unit I and the control region from individuals of *S. luridus* and *S. rivulatus* collected throughout the Mediterranean Sea. Six individuals from the Red Sea, highlighted by red arrows with ID labels finishing letters with the letters

'sa', were included to add context from the ancestral environment. The tree is rooted using the closely related species, *Siganus vulpinus* as an outgroup as determined by (Borsa *et al.* 2007) and utilised as the outgroup in a similar study conducted by Azzurro et al. (2006). Bootstrap values (%) are displayed for the branches separating the species into two distinct groups. The tree was constructed in PhyML version 3.1 (Guindon *et al.* 2010) and visualised using FigTree version 1.4.3 (Rambaut 2016). The scale bar shows the genetic distance.

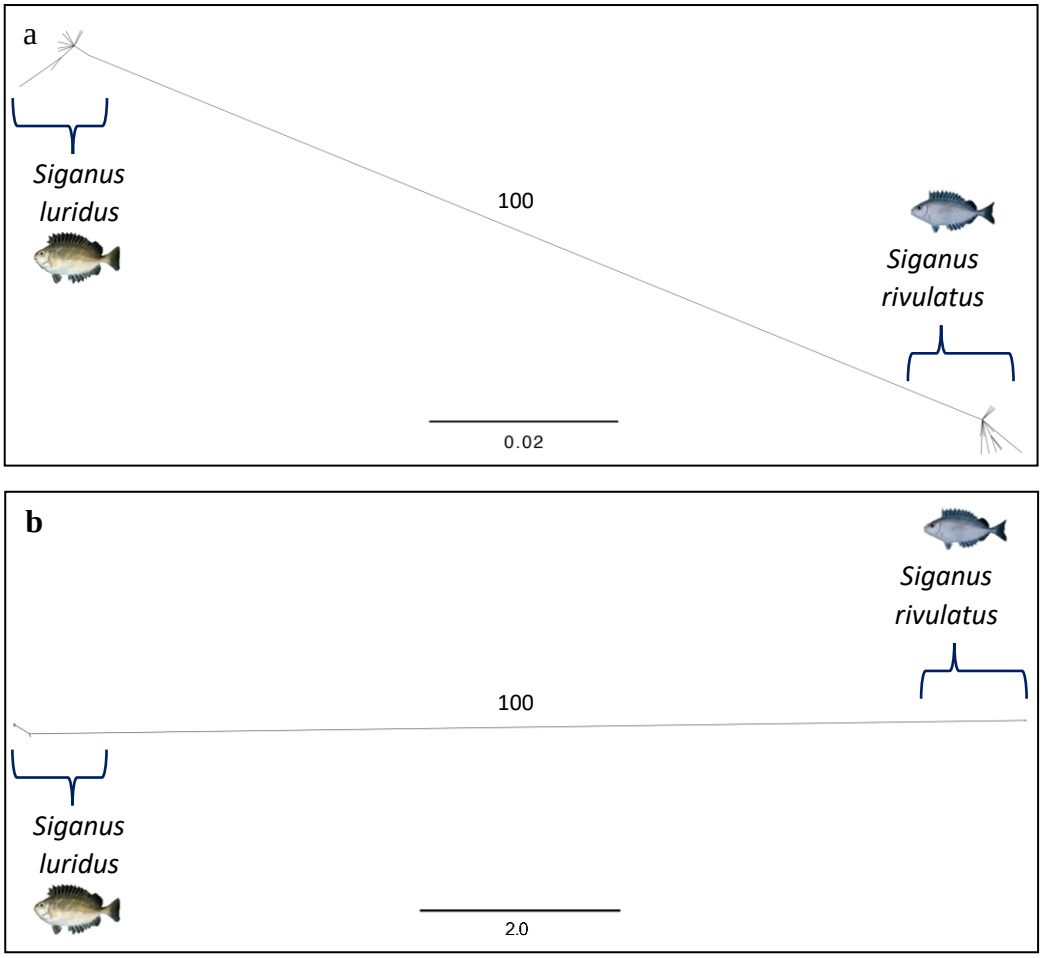

Figure 6: Unrooted maximum likelihood trees constructed from sequences of the mitochondrial markers (a) cytochrome oxidase C sub-unit I and (b) the control region obtained from individuals of *Siganus luridus* and *Siganus rivulatus* collected from within multiple locations within the Mediterranean Sea. Both trees a and b show two distinct species groups, one for *S. luridus* and one for *S. rivulatus*, separated by 100 % of bootstraps on both trees. Trees were constructed using PhyML version 3.1 (Guindon *et al.* 2010) and visualised using

FigTree version 1.4.3 (Rambaut 2016); tip labels have been removed to show the structures of the trees. The scale bars show the genetic distances.

In summary, the results of the maximum likelihood trees and the pairwise distance analysis agree that there are two genetically distinct groups of *Siganus* present within the Mediterranean Sea. Incidentally, these two groups are consistent with the species classifications.

2.3.2 Investigating Genetic Structure within the *Siganus* species

Phylogenetic analyses were undertaken to investigate the inter-relationships within the *S. luridus* and *S. rivulatus* populations in order to determine if there is any genetic structure present within or between the populations studied and to try and identify possible haplogroups (Figure 7).

Within the *S. luridus* group, there was minimal bootstrap support for the groupings within this part of the tree (Figure 7a). Only one branch was supported by a bootstrap value greater than 70 %; this branch was highly supported with 92 % bootstrap support and consists of individuals collected from Limmasol (Cyprus), Kallithea (Rhodes), Gokova Bay (Turkey), Agios Dimitrios (the Peloponnese) and Linosa (the Pelagie Islands), regions within the eastern, central and western Mediterranean Sea. The rest of tree shows weak bootstrap support with the majority of branches supported in less than 50 % of bootstrap replicates. Eight branches, however, did demonstrate bootstraps of between 50 % and 70 %. The *S. rivulatus* group (Figure 7b) showed similar results with only two of the internal branches displaying bootstraps over 70 %; the first branch with a bootstrap value of 82 % led to only two individuals, the first from Limmasol (Cyprus) and the second from Gokova Bay (Turkey), both sites within the Eastern Mediterranean. The second branch with >70 % bootstrap support consisted of two individuals form the central Mediterranean basin, one from Trachila (the Peloponnese) and the second from Kalamata (the Peloponnese). This branch was supported by 87 % of bootstraps. Similar to the *S. luridus* group,

the majority of the internal branches within the *S. rivulatus* were supported by less than 50 % of bootstraps. Once again, seven, a small number of branches, were supported by 50 % to 70 % of bootstraps.

In support of the lack of genetic structure, the short branch lengths on the tree identifiable by the scale bar shown in (Figure 5) demonstrate that there is minimal genetic differentiation within each of the species clades as many individuals are separated from others into groups with very short branch lengths. The only notable branch length is that separating the two species; it is very long showing a high level of differentiation (a great genetic distance) between the two species.

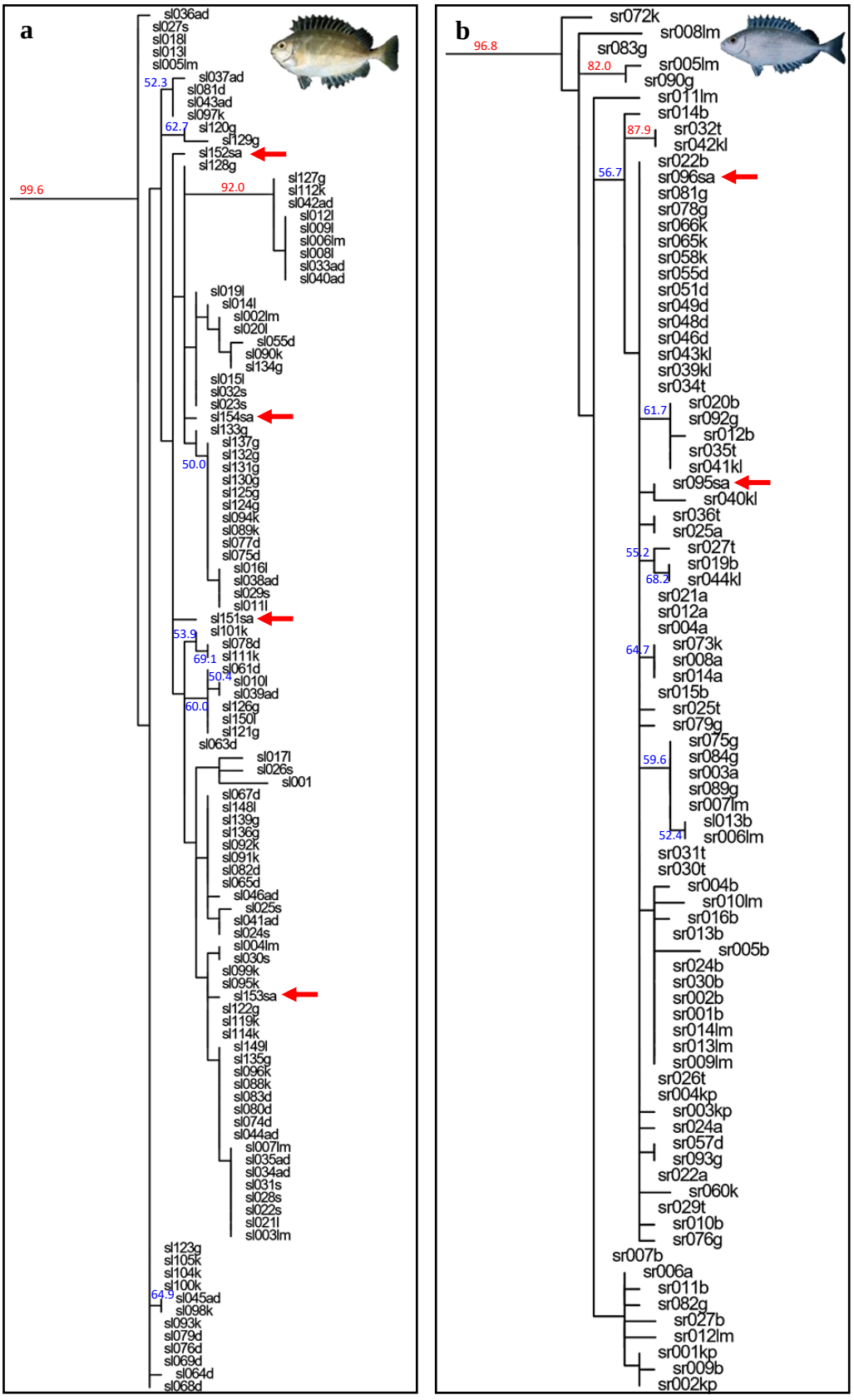

Figure 7: More detailed images of the (a) *Siganus luridus* and (b) *Siganus rivulatus* species branches from the concatenated tree (Figure 5). Bootstrap

values based on 1000 bootstrap replicates are shown on the trees; only bootstrap values over 50% are shown. Branches with bootstrap support of ≥70. 0 % are demonstrated by the values in red. 'Sl' and 'sr' at the start of the IDs refer to individuals of the species *S. luridus* and *S. rivulatus* respectively. The letters at the end of the IDs refer to the site from which the individuals were collected; sa = Saudi Arabia (highlighted by red arrows), kp = Konnos Point, lm = Limmasol, a = Agios Andronikos, b = Girne, k = Kallithea, g = Gokova Bay, d = Diros, t = Trachila, ad = Agios Dimitrios, s = Stoupa, kl = Kalamata, and l = Linosa. The tree was generated in PhyML version 3.1 (Guindon *et al.* 2010), and visualised using FigTree version 1.4.3 (Rambaut 2016).

2.3.3 Haplotype Network Analysis

Analyses of the concatenated sequences showed that there were 36 different haplotypes present within the *S. luridus* populations of the Mediterranean Sea with a haplotype diversity (*h*) of 0.959; this means that there is a 95.9 % probability that when randomly sampled, the sequences from two individuals in this group will be different. The diversity within the *S. rivulatus* populations within the Mediterranean Sea is estimated to be slightly lower at 0.906, however the number of haplotypes present was greater 39.

The *S. luridus* network (Figure 8a) generated from concatenated sequences shows a high number of haplotypes many of which belong to one or a very small number of individuals. The most common haplotype is haplotype 28; this is shared by 10 individuals (9.4% of the total *S. luridus* individuals incorporated in this analysis) and is found within three different sites (Kallithea in Rhodes, Gokova in Turkey and Diros in the Peloponnese). No haplotypes are shared between every site and the most sites a haplotype is found in is four. Additionally, there is no clear genetic structure demonstrated within the haplotype network as most haplotypes have multiple connections to other haplotypes. This means the haplotypes reticulate, often reconnecting with evolutionary lines from which they parted initially. More dominant haplotypes often branch out in bifurcations; for example, haplotype 27 bifurcates into

haplotypes 24 and 20. Interestingly, haplotype 27 is found in Kallithea (Rhodes), Gokova Bay (Turkey) and Diros (the Peloponnese) and the subsequent, related haplotype 24 is found in Diros and haplotype 20 is found in found in both Kallithea and Gokova Bay. The network also shows that 41 % (15 out of 36) of the documented haplotypes belong to only one individual each in this study (n = 106).

The network constructed based on the concatenated sequences of *S. rivulatus* (Figure 8b) demonstrated a more distinct genetic structure. The most common haplotype was haplotype 5; this was shared by 45 individuals (37.8% of the total number of *S. rivulatus* inidividuals studied), across eight different sites (Konnos Point (Cyprus), Girne (Cyprus), Agios Andronikos (Cyprus), Kallithea (Rhodes), Gokova Bay (Turkey), Diros (the Peloponnese), Trachila (the Peloponnese) and Kalamata (the Peloponnese)). Interestingly, 72 % (28 out of 39) of the haplotypes found within the *S. rivulatus* group are unique to one individual each in this study, despite the smaller sample size (n = 86) than that of the *S. luridus* group studied. Haplotypes belonging to only one individual are referred to as 'unique haplotypes' within this study. There is a clear star-shape present within the centre of the haplotype network; a number of the unique haplotypes and a few haplotypes shared by a small number of individuals radiate out from haplotype 5, the predominant haplotype, with tick-marks showing a very low number of changes between the predominant and the radiating haplotypes. There is a multifurcate chain of haplotypes in the network branching out from haplotype 25, which are distantly connected to haplotypes 5, 21, 4 and 30. The haplotypes in this chain differ from the previous by only one or two changes in the nucleotide sequence.

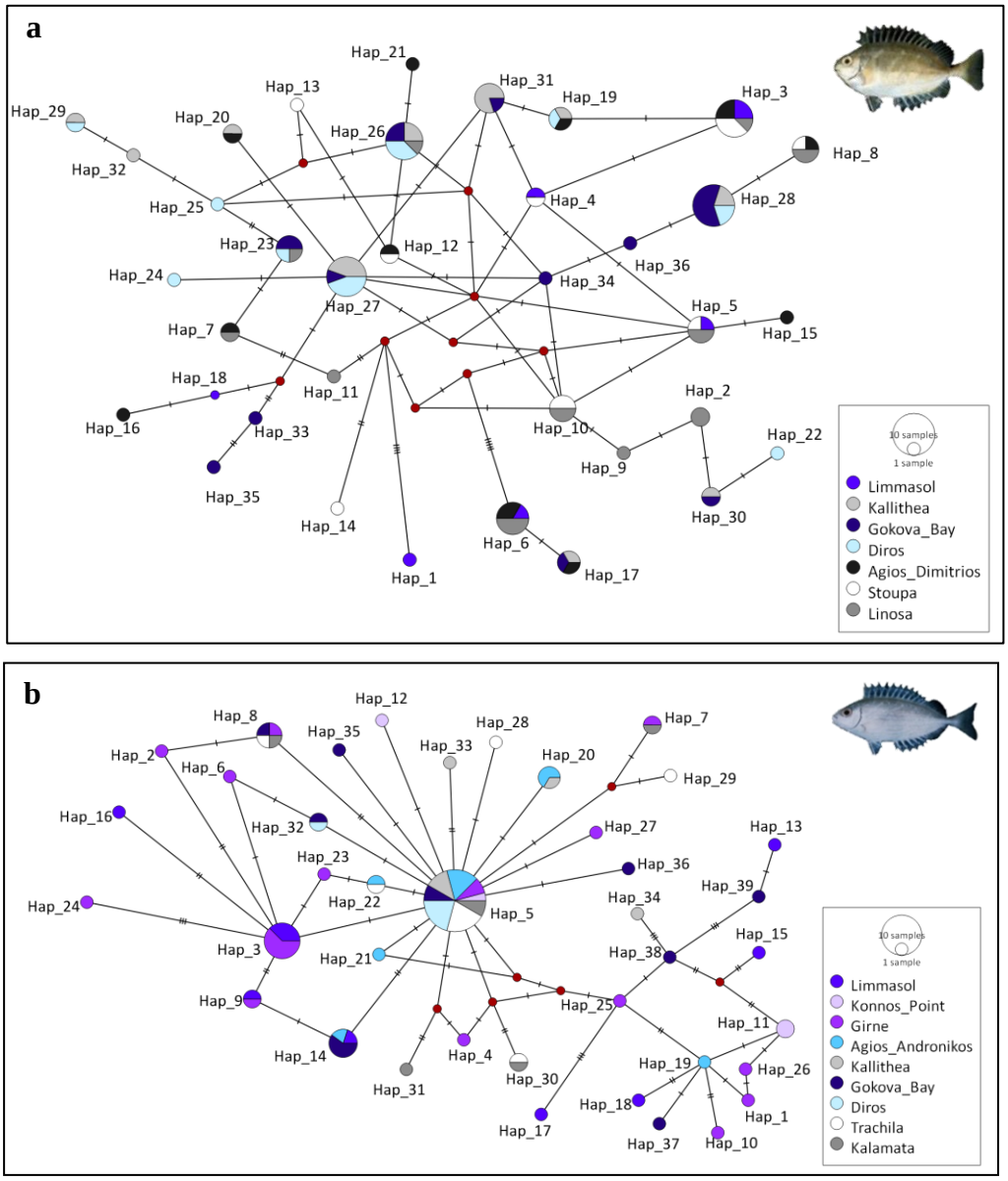

Figure 8: Median-joining haplotype networks for the concatenated sequences of (a) *S. luridus* and (b) *S. rivulatus* individuals. Networks were generated in POPART version 1.7 (Leigh and Bryant 2015) using haplotype data generated from FASTA files of sequences in DnaSP6 (Rozas *et al.* 2017). The key indicates which colours on the haplotype pie charts within the network refer to which site. Tick marks indicate nucleotide changes. Small red nodes are median vectors attributed to "unsampled" haplotypes hypothesised by the program.

Using the concatenated sequence data the presence of unique haplotypes (belonging to only one individual) compared to shared haplotypes (haplotypes belonging to >1 individual) was analysed between sites. For *S. luridus* (Figure 9a) unique haplotypes are more common in sites within the eastern and central Mediterranean (Gokovay Bay, Turkey and Diros, the Peloponnese). Shared haplotypes are most frequent in Linosa, the western-most site used within the study. For *S. rivulatus* (Figure 9b) unique haplotypes are most common in sites closest to the Suez Canal, Girne (Northern Cyprus), Limmasol (Southern Cyprus) and Gokova Bay (Turkey). The number of shared haplotypes is relatively consistent throughout all sites, as demonstrated in the haplotype network (Figure 8b) where the dominant haplotype is shared by the majority of sites and shared haplotypes vary within which sites they are shared between.

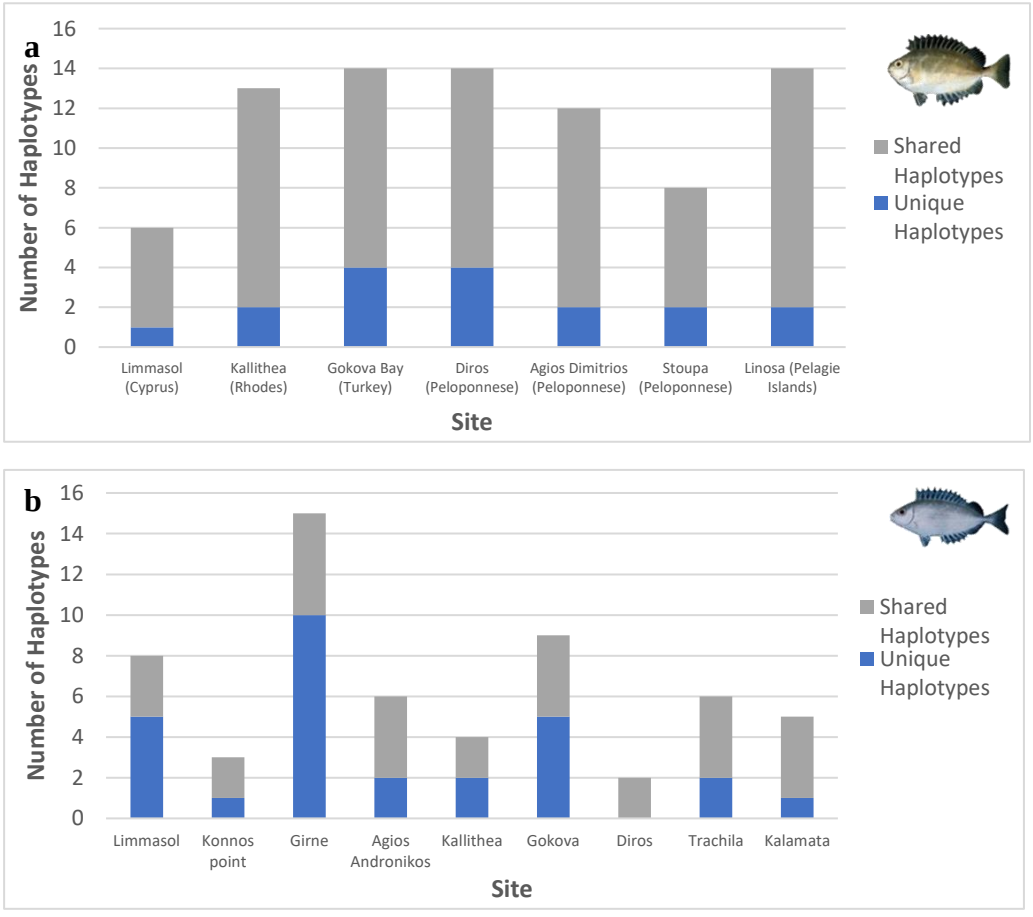

Figure 9: A graphical representation of the number of shared and unique haplotypes present within each site sampled within the Mediterranean Sea for (a) *S. luridus* and (b) *S. rivulatus*. The graph is based on the haplotype data

generated from concatenated mitochondrial sequences of Cytochrome Oxidase C Sub-unit I and the control region in DnaSP6 (Rozas *et al*. 2017).

The haplotype networks for the individual mitochondrial markers were generated to investigate relationships between haplotypes for each marker individually. There were only 11 haplotypes present within the COI network for *S. luridus* (Figure 10a). Unlike the haplotype network generated for the concatenated sequences, the COI sequences show a star-shaped network, with the dominant haplotype (haplotype 3, shared by 51 individuals across all seven sites) radiating out into the other 10 existing haplotypes. This is also the case for *S. rivulatus* COI network (Figure 10b) where haplotype 3 is the dominant haplotype (shared by 44 individuals across all nine sites) and 11 of the 16 remaining haplotypes radiate out from it directly, once again in a star-like pattern. Of these 11 haplotypes one branches into three distinct haplotypes, all shared across multiple sites. Another of the 11 haplotypes branches into a unique haplotype. Only three unique haplotypes are present within the COI network for *S. luridus*, however 7 (almost 50%) of those in the *S. rivulatus* network are unique.

A subtle star-like radiation of haplotypes from haplotype 5 was present in the CR network for *S. luridus* (Figure 11a). Of the 17 haplotypes present, eight of them where shared across four or more sites and five were unique. A more distinct star-like pattern of radiation was present within the network constructed for the CR of *S. rivulatus* collected from various sites across the Mediterranean Sea (Figure 11b). Haplotype 5 (shared across all sites by 45 individuals) was connected directly to 11 of the 32 haplotypes present. Similarly to the concatenated network, the CR network for *S. rivulatus* also demonstrated a multifurcating chain of largely unique haplotypes.

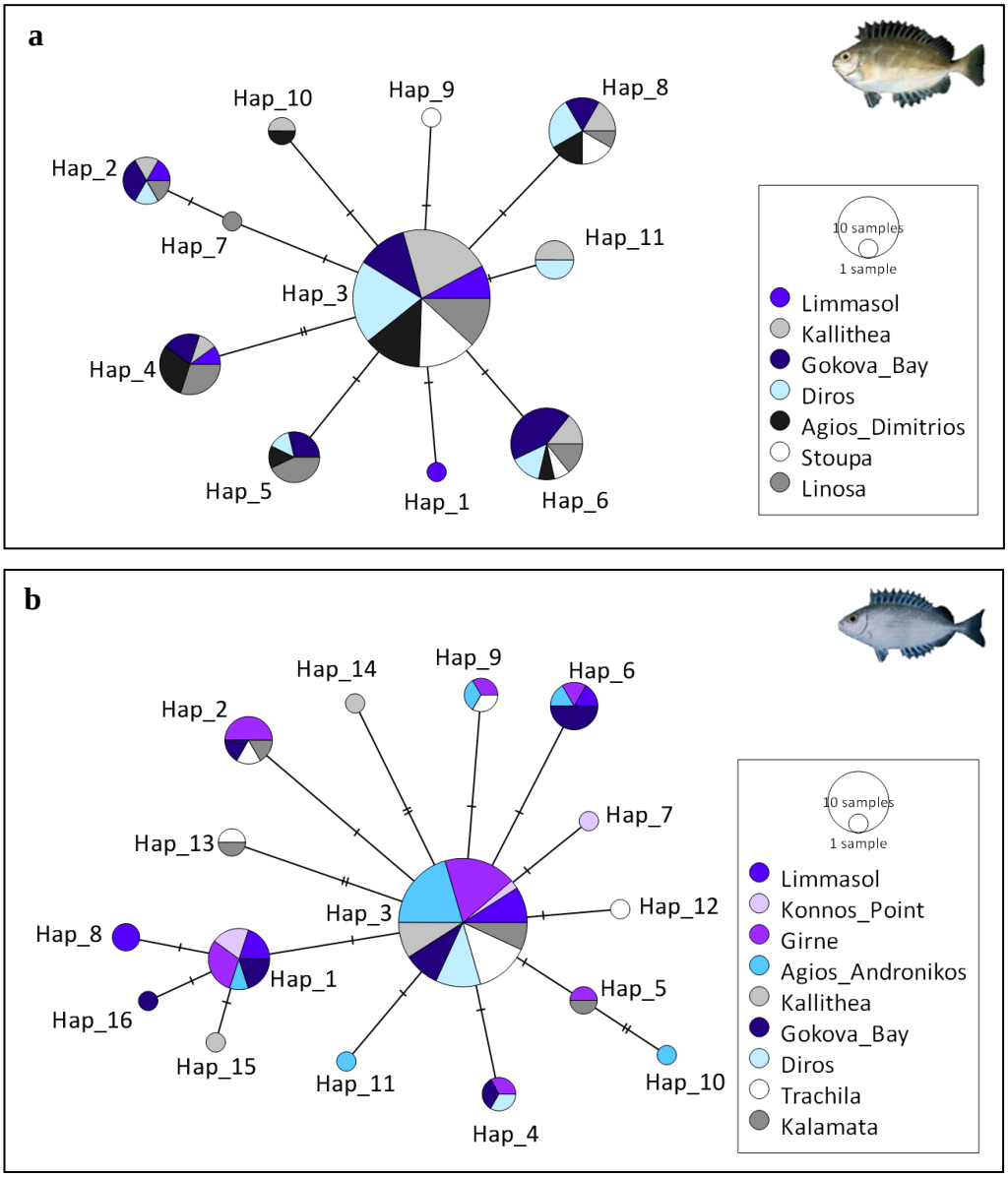

Figure 10: Median-joining haplotype networks constructed for the mitochondrial marker cytochrome oxidase C sub-unit I from sequences of (a) *Siganus luridus* and (b) *Siganus rivulatus* collected at various sites throughout the Mediterranean Sea. Networks were generated in POPART version 1.7 (Leigh and Bryant 2015) using haplotype data generated from FASTA files of sequences generated in DnaSP6 (Rozas *et al.* 2017). The key indicates which colours on the haplotype pie charts within the network refer to which site. Tick marks indicate nucleotide changes. Small red nodes are median vectors attributed to "unsampled" haplotypes hypothesised by the program.

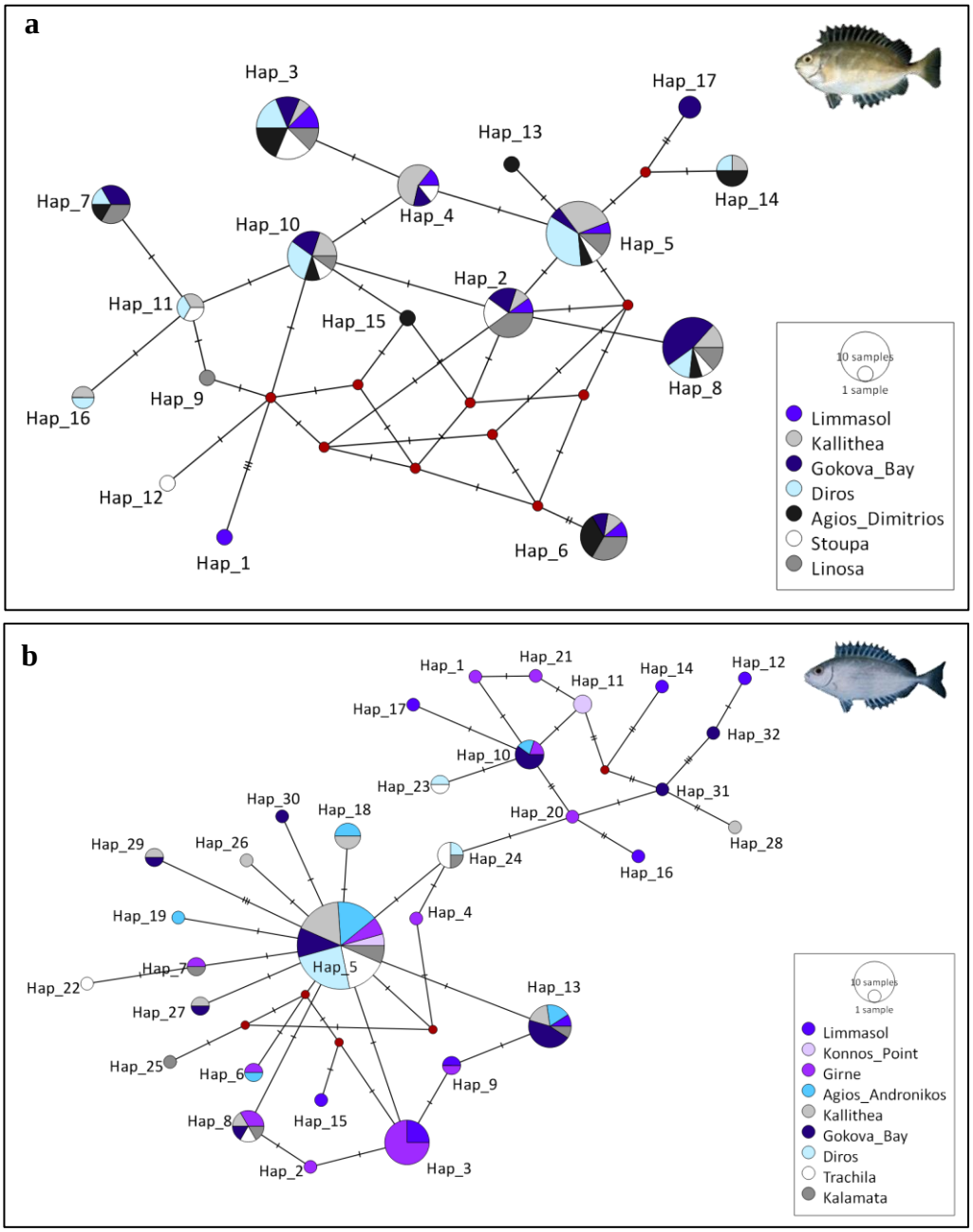

Figure 11: Median-joining haplotype networks constructed for the mitochondrial marker the control region from sequences of (a) *Siganus luridus* and (b) *Siganus rivulatus* collected at various sites throughout the Mediterranean Sea. Networks were generated in POPART version 1.7 (Leigh and Bryant 2015) using haplotype data generated from FASTA files of sequences generated in DnaSP6 (Rozas *et al.* 2017). The key indicates which colours on the haplotype pie charts within the network refer to which site. Tick marks indicate nucleotide changes. Small red nodes are median vectors attributed to "unsampled" haplotypes hypothesised by the program.

2.3.4 Population Diversity Indices

Population-level data for the number of haplotypes, number of variable sites, levels of haplotype diversity (*h*), levels of nucleotide diversity (π) and the mean pairwise distance within all populations were produced using DnaSP6 (Rozas *et al.* 2017), PAUP (Swofford 2002) and the concatenated sequences. For *S. luridus*, all study sites presented high levels of haplotype diversity, with all values greater than $h = 0.90$; ranging from $h = 0.90$ to $h = 0.98$ (Table 6). Despite the lower value for haplotype diversity for *S. rivulatus*, the majority of populations still demonstrated sufficiently high haplotype diversity, with a range from $h = 0.33$ to $h = 0.94$ (Table 7). The individuals collected from the population in Diros showed an exceptionally low haplotype diversity of 0.33 when compared to the rest of the *S. rivulatus* populations, all of which demonstrated levels of haplotype diversity over the value of $h = 0.78$. The standard deviations are low for all calculated values showing low variation around the mean haplotype diversity calculated for each population, of both species.

Although for the concatenated data haplotype diversity is high, overall genetic diversity within both species is low. Nucleotide diversity levels recorded for populations of *S. luridus* within the Mediterranean Sea consistently gave values lower than $\pi = 0.00675$. These low values signify that a very small proportion of the observed nucleotide sites differ within the populations studied. The range within the *S. luridus* populations of the Mediterranean Sea was from $\pi = 0.0031$ (or 0.31 %) in Stoupa to $\pi = 0.0067$ (or 0.67 %) in Agios Dimitrios. Levels of nucleotide diversity were lower within the *S. rivulatus* populations, again reflecting the reduced diversity present. The range within the *S. rivulatus* group studied was from $\pi = 0.0003$ (0.03%) in Diros to $\pi = 0.0064$ (0.64%) in Limmasol. The extremely low nucleotide diversity value of $\pi = 0.0003$ within the *S. rivulatus* population of Diros, indicates very high genetic similarity within the population. The increased similarity, and reduced haplotype diversity of *S. rivulatus* when compared to *S. luridus* are re-emphasised in the overall species

values of nucleotide diversity across the Mediterranean Sea, wherein the value for *S. luridus* is $\pi = 0.00516$ and for *S. rivulatus* is $\pi = 0.00405$.

The mean pairwise distance was calculated as another measure to view the distance between sequences within the populations of *S. luridus* and *S. rivulatus* within the Mediterranean Sea. All values for mean pairwise distance are low and in agreement with the low values of the calculated nucleotide diversity. The mean pairwise distance value for *S. luridus* is over ten-fold greater than for *S. rivulatus* at distance = 0.142 and distance = 0.004 respectively. These values represent the percentage of changes within the nucleotide sequences of each population; *S. luridus* has a mean distance of 14.2 % between the individuals studied, whereas *S. rivulatus* has a mean distance of only 0.4 %. Mean pairwise distances within populations of *S. luridus* were consistently lower than or equal to 0.61 % and always greater than 0.31%, with the exception of Agios Dimitrios (the Peloponnese), which had a high value of 14.8%. The range of pairwise distances within the studied *S. rivulatus* populations of the Mediterranean Sea was 0.03 % in Diros (the Peloponnese), an extremely low value, to 0.67 % in Limmasol (Cyprus). The average inter-species pairwise distance between *S. luridus* and *S. rivulatus* within the Mediterranean was 0.27, or 27 %, a high value, as expected when comparing two distinct species.

Table 6: Genetic diversity indices from concatenated sequence data for populations of *Siganus luridus* sampled from seven sites across the Mediterranean Sea. Standard deviations are given below the values. Number of haplotypes, number of variable sites, haplotype diversity and nucleotide diversity were calculated using DnaSP6 (Rozas *et al.* 2017). Pairwise distance was calculated using PAUP version 4.0 (Swofford 2002).

Sampling Site	Number of Haplotypes	Number of Variable sites	Haplotype Diversity (*h*)	Nucleotide Diversity (π)	Pairwise Distance
Limmasol	6	14	0.9524 ±0.096	0.00589 ±0.00148	0.00610 ±0.00369
Kallithea	11	18	0.9211 ±0.037	0.00376 ±0.00070	0.00384 ±0.00271
Gokova	12	18	0.9006 ±0.059	0.00482 ±0.00079	0.00496 ±0.00319
Diros	10	13	0.9150 ±0.041	0.00362 ±0.00041	0.00368 ±0.00179
Agios Dimitrios	12	18	0.9780 ±0.035	0.00674 ±0.00075	0.14804 ±0.14385
Stoupa	8	9	0.9273 ±0.066	0.00315 ±0.00051	0.00319 ±0.00168
Linosa	12	17	0.9559 ±0.033	0.00587 +0.00078	0.00576 ±0.00365
***S. luridus* total**	36	29	0.9592 ±0.006	0.00516 ±0.00033	0.14199 ±0.14350

Table 7: Genetic diversity indices from concatenated sequence data for populations of *Siganus rivulatus* sampled from nine sites across the Mediterranean Sea. Standard deviations are given below the values. Number of haplotypes, number of variable sites, haplotype diversity and nucleotide diversity were calculated using DnaSP6 (Rozas *et al.* 2017). Pairwise distance was calculated using PAUP version 4.0 (Swofford 2002).

Sampling Site	Number of Haplotypes	Number of Variable sites	Haplotype Diversity (*h*)	Nucleotide Diversity (π)	Pairwise Distance
Limmasol	8	17	0.9333 ±0.077	0.00647 ±0.00108	0.00679 ±0.00354
Konnos Point	3	7	0.8333 ±0.222	0.00506 ±0.00146	0.00529 ±0.00372
Girne	15	19	0.9421 ±0.043	0.00426 ±0.00066	0.00439 ±0.00277
Agios Andron-ikos	6	9	0.8444 ±0.103	0.00240 ±0.00083	0.00245 ±0.00227
Kallithea	4	10	0.8000 ±0.172	0.00375 ±0.00164	0.00390 ±0.00388
Gokova	9	16	0.9394 ±0.058	0.00460 ±0.00090	0.00476 ±0.00302
Diros	2	1	0.3333 ±0.215	0.00038 ±0.00024	0.00038 ±0.00055
Trachila	6	9	0.7778 ±0.137	0.00202 ±0.00061	0.00205 ±0.00161
Kalamata	5	10	0.9333 ±0.122	0.00375 ±0.00088	0.00382 ±0.00190
***S. rivulatus* Total**	39	43	0.9056 ±0.026	0.00405 ±0.00040	0.00418 ±0.00324

Azzurro et al. (2006) published a similar study utilising only the CR marker, for this reason the diversity indices for COI and CR were also analysed separately. High haplotype diversity for both species can be observed for the CR with *S. luridus* (Table 8) demonstrating a higher value of $h = 0.904$ compared to the $h = 0.836$ demonstrated by *S. rivulatus* (Table 9). Values for haplotype diversity of COI are lower at $h = 0.748$ for *S. luridus* (Table 10) and $h = 0.717$ for *S. rivulatus* (Table 11). Higher levels of haplotype diversity are consistently observed in the *S. luridus* species between the two mitochondrial markers. For the CR of *S. luridus* all haplotype diversity values are high and fall between the range of $h = 0.850$ and $h = 0.960$. The range for the haplotype diversity of COI of *S. rivulatus* is much greater ranging from $h = 0.294$ to $h = 0.940$. The lowest haplotype diversity is found within Diros (the Peloponnese) with a value of $h = 0.295$.

The nucleotide diversity for both species is consistently low for both the CR and COI markers. All values for both species and both markers fall below $\pi = 0.0132$. Nucleotide diversity is lower in *S. rivulatus* than *S. luridus* for both the CR and COI markers. *S. luridus* and *S. rivulatus* demonstrated nucleotide diversity values for the CR of $\pi = 0.008$ and $\pi = 0.007$ respectively. These are low values but the nucleotide diversity of COI was even lower at values of $\pi = 0.0022$ and $\pi = 0.0020$ for *S. luridus* and *S. rivulatus* respectively. For *S. luridus* there nucleotide diversity values ranged between $\pi = 0.00619$ and $\pi = 0.01196$ with the lowest and highest values being found in Linosa (the Pelagie Islands) and Agios Dimitrios (the Peloponnese) respectively. *S. rivulatus* populations demonstrated a greater range with values ranging from $\pi = 0.00262$ in Diros (the Peloponnese) to $\pi = 01319$ in Limmasol (Cyprus)

The low nucleotide diversity values within both species and both genetic markers are consistent with the low pairwise distance values representing a very low level of genetic diversity within both markers of both species. Once again, for the CR and COI the genetic distance of *S. luridus* is greater than that of *S. rivulatus* with respective values of distance = 0.00902 and distance = 0.00763 for CR. The

values for COI were lower overall, but *S. luridus* still demonstrated higher levels with a value of distance = 0.00232 compared to the *S. rivulatus* value of distance = 0.00195. For the CR of *S. luridus* the range of pairwise distances was between 0.00657 and 0.01429 with the lowest and highest values being found in Stoupa (the Peloponnese) and Agios Dimitrios (the Peloponnese) respectively. For *S. rivulatus* the range of pairwise distances was between 0.00527 and 0.01641 with the lowest and values being found in Trachila (the Peloponnese) and Limmasol (Cyprus) respectively. For COI the ranges were between distance = 0. 00127 and distance = 0.00306 for *S. luridus* with the lowest value found in Stoupa (the Peloponnese) and the highest value found in Linosa (the Peloponnese). For *S. rivulatus* the range was between distance = 0.00061 and distance = 0.00249 with the lowest value found in Diros (the Peloponnese) and the highest value found in Kallithea (Rhodes).

Table 8: Genetic diversity indices for the control region of populations of *Siganus luridus* sampled from seven sites across the Mediterranean Sea. Standard deviations are given below the values. Number of haplotypes, number of variable sites, haplotype diversity and nucleotide diversity were calculated using DnaSP6 (Rozas *et al.* 2017). Pairwise distance was calculated using PAUP version 4.0 (Swofford 2002).

Sampling Site	Number of Haplotypes	Number of Variable sites	Haplotype Diversity (*h*)	Nucleotide Diversity (π)	Pairwise Distance
Limmasol	6	9	0.9524 ±0.096	0.01117 ±0.00275	0.01315 ±0.00863
Kallithea	10	10	0.9000 ±0.043	0.00665 ±0.00129	0.00738 ±0.00607
Gokova	9	11	0.8538 ±0.068	0.00826 ±0.00154	0.00940 ±0.00735
Diros	8	7	0.8562 ±0.059	0.00636 ±0.00077	0.00684 ±0.00400
Agios Dimitrios	9	11	0.9231 ±0.050	0.01196 ±0.00139	0.01429 ±0.00861
Stoupa	8	9	0.9044 ±0.041	0.00970 ±0.00151	0.00657 ±0.00349
Linosa	6	8	0.9273 ±0.066	0.00619 ±0.00085	0.01118 ±0.00858
***S. luridus* total**	17	17	0.9040 ±0.010	0.00837 ±0.00062	0.00902 ±0.00706

Table 9: Genetic diversity indices for the control region of populations of Siganus rivulatus sampled from nine sites across the Mediterranean Sea. Standard deviations are given below the values. Number of haplotypes, number of variable sites, haplotype diversity and nucleotide diversity were calculated using DnaSP6 (Rozas et al. 2017). Pairwise distance was calculated using PAUP version 4.0 (Swofford 2002).

Sampling Site	Number of Haplotypes	Number of Variable sites	Haplotype Diversity (*h*)	Nucleotide Diversity (π)	Pairwise Distance
Limmasol	8	14	0.9333 ±0.077	0.01319 ±0.00244	0.01641 ±0.00923
Konnos Point	2	5	0.6667 ±0.204	0.00975 ±0.00298	0.01197 ±0.00927
Girne	12	12	0.8419 ±0.070	0.00728 ±0.00137	0.00878 ±0.00723
Agios Andron-ikos	6	8	0.7821 ±0.105	0.00476 ±0.00149	0.00533 ±0.00535
Kallithea	8	13	0.7794 ±0.099	0.00507 ±0.00161	0.00527 ±0.00643
Gokova	9	14	0.8655 ±0.051	0.00841 ±0.00154	0.00996 ±0.00777
Diros	3	5	0.2949 ±0.156	0.00262 ±0.00178	0.00632 ±0.00313
Trachila	5	8	0.6667 ±0.141	0.00461 ±0.00186	0.00527 ±0.00527
Kalamata	6	7	0.8929 ±0.111	0.00512 ±0.00151	0.00626 ±0.00404
***S. rivulatus* Total**	32	30	0.8355 ±0.030	0.00703 ±0.00071	0.00763 ±0.00765

Table 10: Genetic diversity indices for the cytochrome oxidase c subunit I marker of populations of *Siganus luridus* sampled from seven sites across the Mediterranean Sea. Standard deviations are given below the values. Number of haplotypes, number of variable sites, haplotype diversity and nucleotide diversity were calculated using DnaSP6 (Rozas *et al.* 2017). Pairwise distance was calculated using PAUP version 4.0 (Swofford 2002).

Sampling Site	Number of Haplotypes	Number of Variable sites	Haplotype Diversity (*h*)	Nucleotide Diversity (π)	Pairwise Distance
Limmasol	4	5	0.7413 ±0.181	0.00261 ±0.00092	0.00265 ±0.00218
Kallithea	7	8	0.6947 ±0.107	0.00195 ±0.00048	0.00198 ±0.00173
Gokova	6	7	0.8211 ±0.052	0.00288 ±0.00048	0.00293 ±0.00201
Diros	6	6	0.7076 ±0.100	0.00181 ±0.00042	0.00184 ±0.00153
Agios Dimitrios	6	6	0.7619 ±0.096	0.00243 ±0.00049	0.00247 ±0.00186
Stoupa	4	3	0.6000 ±0.154	0.00126 ±0.00040	0.00127 ±0.00117
Linosa	7	7	0.8382 ±0.063	0.00293 ±0.00049	0.00306 ±0.00201
***S. luridus* total**	11	11	0.7481 ±0.037	0.00228 ±0.00021	0.00232 ±0.00187

Table 11: Genetic diversity indices for the cytochrome oxidase c subunit I marker of populations of *Siganus rivulatus* sampled from nine sites across the Mediterranean Sea. Standard deviations are given below the values. Number of haplotypes, number of variable sites, haplotype diversity and nucleotide diversity were calculated using DnaSP6 (Rozas *et al.* 2017). Pairwise distance was calculated using PAUP version 4.0 (Swofford 2002).

Sampling Site	Number of Haplotypes	Number of Variable sites	Haplotype Diversity (*h*)	Nucleotide Diversity (π)	Pairwise Distance
Limmasol	4	3	0.8000 ±0.089	0.00227 ±0.00043	0.00231 ±0.00165
Konnos Point	3	2	0.8333 ±0.222	0.00213 ±0.00067	0.00216 ±0.00140
Girne	9	9	0.8211 ±0.073	0.00242 ±0.00050	0.00221 ±0.00173
Agios Andron-ikos	4	3	0.4545 ±0.170	0.00091 ±0.00038	0.00092 ±0.00109
Kallithea	3	4	0.6000 ±0.215	0.00243 ±0.00101	0.00249 ±0.00231
Gokova	6	5	0.8485 ±0.074	0.00241 ±0.00044	0.00244 ±0.00154
Diros	2	1	0.3333 ±0.215	0.00061 ±0.00039	0.00061 ±0.00090
Trachila	5	5	0.6667 ±0.163	0. 00182 ±0.00063	0.00185 ±0.00169
Kalamata	4	4	0.8000 ±0.172	0.00243 ±0.00081	0.00247 ±0.00182
***S. rivulatus* Total**	16	18	0.7166 ±0.049	0.00203 ±0.00024	0.00195 ±0.00168

2.3.5 F-statistics: Analysis of population differentiation

All F_{ST} values obtained using Arlequin version 3.5 (Excoffier and Lischer 2010) were lower than F_{ST} = 0.387. The mean F_{ST} values for the individual species were F_{ST} = 0.102 for *S. luridus* and F_{ST} = 0.077 for *S. rivulatus*. The pairwise F_{ST} results for *S. luridus* demonstrated significant F_{ST} values in 12 of the 21 population comparisons ($p<0.05$) (Table 12). Of these significant values, moderate genetic differentiation (where $F_{ST} \geq 0.05$ and ≤ 0.15) was found between Kallithea in Rhodes and Agios Dimitrios in the Peloponnese (F_{ST} = 0.086, $p<0.05$), Gokova Bay in Turkey and Agios Dimitrios in the Peloponnese (F_{ST} = 0.104, $p<0.05$), Diros in the Peloponnese and Agios Dimitrios in the Peloponnese (F_{ST} =0.107, $p<0.05$) and also Gokova Bay in Turkey and Linosa, one of the Pelagie Islands, (F_{ST} =0.120, $p<0.05$). Significant levels of great genetic differentiation (where $F_{ST} \geq 0.15$ and ≤ 0.25) were found between Kallithea in Rhodes and Linosa in the Pelagie Islands (F_{ST} = 0.153, $p<0.05$), Diros in the Peloponnese and Linosa in the Pelagie Islands (F_{ST} =0.161, $p<0.05$), Limmasol in Cyprus and Kallithea in Rhodes (F_{ST} =0.198, $p<0.05$), Limmasol in Cyprus and Gokova Bay in Turkey (F_{ST} = 0.206, $p<0.05$), Limmasol in Cyprus and Diros in the Peloponnese (F_{ST} = 0.226, $p<0.05$), Kallithea in Rhodes and Stoupa in the Peloponnese (F_{ST} = 0.225, $p<0.05$), Gokova Bay in Turkey and Stoupa in the Peloponnese (F_{ST} = 0.216, $p<0.05$) and finally Diros in the Peloponnese and Stoupa, also in the Peloponnese (F_{ST} = 0.224, $p<0.05$). The remaining population comparisons demonstrated insignificant ($p>0.05$), low F_{ST} values below 0.05 ($F_{ST}<0.05$ signify minimal to no genetic differentiation).

Of the 36 population pairs for *S. rivulatus*, only six demonstrated F_{ST} values that significantly depart from F_{ST} = 0.00 ($p<0.05$) (Table 13). Of these six values, moderate genetic differentiation (where $F_{ST} \geq 0.05$ and ≤ 0.15) was found between Girne in Cyrus and Trachila in the Peloponnese (F_{ST} = 0.081, $p<0.05$) and Limmasol in Cyprus and Kalamata in the Peloponnese (F_{ST} = 0.146, $p<0.05$). The remaining statistically significant values demonstrated levels of great genetic differentiation (where $F_{ST} \geq 0.15$ and ≤ 0.25), as found in Limmasol in Cyprus and Agios Andronikos in Cyprus (F_{ST} = 0.154, $p<0.05$), Limmasol in Cyprus and Diros in the Peloponnese (F_{ST} = 0.196, $p<0.05$), Konnos point in

Cyprus and Agios Andronikos in Cyprus(F_{ST} = 0.199, $p<0.05$) and finally between Limmasol in Cyprus and Trachila in the Peloponnese (F_{ST} = 0.216, $p<0.05$). The remaining 30 pairwise comparisons showed insignificant F_{ST} values ($p>0.05$). Although the comparisons between Konnos Point in Cyprus and Diros in the Peloponnese (F_{ST} = 0.387, $p>0.05$) and Konnos Point in Cyprus and Trachila in the Peloponnese (F_{ST} = 0.311, $p>0.05$) demonstrated very great levels of genetic differentiation (where $F_{ST} > 0.25$) the F_{ST} values were not significant.

Table 12: F-statistics (F_{ST}) for populations of *S. luridus* collected from seven locations across the Mediterranean Sea. Each sampling site is treated as a separate population. F_{ST} were calculated using Arlequin version 3.5 (Excoffier and Lischer 2010). Significant F_{ST} values ($p<0.05$) are highlighted in bold with an asterisk.

	Limmasol	**Kallithea**	**Gokova Bay**	**Diros**	**Agios Dimitrios**	**Stoupa**	**Linosa**
	Cyprus	Rhodes	Turkey	Peloponnese	Peloponnese	Peloponnese	Pelagie Is.
Limmasol	-	-	-	-	-	-	-
Kallithea	**0.19795***	-	-	-	-	-	-
Gokova Bay	**0.20646***	0.03024	-	-	-	-	-
Diros	**0.22559***	0.00000	0.00957	-	-	-	-
Agios Dimitrios	0.00000	**0.08631***	**0.10361***	**0.10672***	-	-	-
Stoupa	0.00000	**0.22528***	**0.21603***	**0.22404***	0.04482	-	-
Linosa	0.00000	**0.15312***	**0.12020***	**0.16110***	0.00000	0.02850	-

Table 13: F-statistics (F_{ST}) for populations of *S. rivulatus* collected from nine locations across the Mediterranean Sea. Each sampling site is treated as a separate population. F_{ST} were calculated using Arlequin version 3.5. (Excoffier and Lischer 2010). Significant F_{ST} values ($p<0.05$) are highlighted in bold with an asterisk

	Limmasol	**Konnos Point**	**Girne**	**Agios Andronikos**	**Kallithea**	**Gokova Bay**	**Diros**	**Trachila**	**Kalamata**
	Cyprus	Cyprus	Cyprus	Cyprus	Rhodes	Turkey	Peloponnese	Peloponnese	Peloponnese
Limmasol	-	-	-	-	-	-	-	-	-
Konnos Point	0.00000	-	-	-	-	-	-	-	-
Girne	0.03922	0.01925	-	-	-	-	-	-	-
Agios Andronikos	**0.15355***	**0.19868***	0.06130	-	-	-	-	-	-
Kallithea	0.10423	0.12824	0.05725	0.00000	-	-	-	-	-
Gokova Bay	0.07185	0.0889	0.06855	0.00000	0.00000	-	-	-	-
Diros	**0.19559***	0.38669	0.06839	0.00000	0.00000	0.03114	-	-	-
Trachila	**0.21623***	0.31142	**0.08181***	0.00000	0.00905	0.05687	0.00000	-	-
Kalamata	**0.14595***	0.19061	0.04917	0.01645	0.00000	0.02908	0.00000	0.00000	-

2.3.6 Analysis of Evidence of Demographic Changes in *Siganus* species across the Mediterranean Sea

There were no significant departures from neutrality according to the Tajima's D results computed using Arlequin version 3.5 (Excoffier and Lischer 2010) for the *S. luridus* populations studied within the Mediterranean Sea (Table 14). The Tajima's D values were negative in all but two sites for *S. luridus*; Agios Dimitrios (the Peloponnese) and Linosa (the Pelagie Islands), despite this, all values were insignificant ($p>0.05$). The two highest Tajima's D values were found within the central and western Mediterranean in Agios Dimitrios (the Peloponnese) and Linosa (the Pelagie Islands) with respective values of $D = 0.24085$ and $D = 0.14898$, both however were insignificant with $p>0.05$.

Within the *S. rivulatus* populations studied within the Mediterranean Sea three demonstrated significant Tajima's D values (Table 15); Kallithea in Rhodes ($D = -1.43$, $p<0.05$), Trachila in the Peloponnese ($D = -1.90$, $p<0.05$) and Kalamata in the Peloponnese ($D = 1.43$, $p<0.05$), all of which are sites located within the central or east-side of the central Mediterranean. Similarly to the *S. luridus* populations, all but one population demonstrated negative Tajima's D values. The population from Konnos Point in Cyprus gave the highest and only positive D value at $D = 1.75$, however it was insignificant at $p>0.05$.

The Fu's F results were negative for all populations included in the *S. luridus* study (Table 14). Four out of the seven study sites demonstrated populations with significant Fu's F values ($p>0.05$). The significant Fu's F values found in Gokova Bay in Turkey ($D = -3.67$, $p<0.05$), Diros in the Peloponnese ($D = -2.89$, $p<0.05$), Stoupa in the Peloponnese ($D = -3.23$, $p<0.05$) and Linosa one of the Pelagie Islands ($D = -3.51$, $p<0.05$) signify these populations have an excess over the number of rare haplotypes expected under neutrality.

All but two of the Fu's F values for *S. rivulatus* populations within the Mediterranean Sea are negative (Table 15). Although the values for Konnos Point in Cyprus ($F = 1.34$, $p > 0.05$) and Kallithea in Rhodes ($F = 0.426$, $p > 0.05$) are positive neither are significant. Only two out of the nine sites gave significant Fu's F results ($p < 0.05$); these were the populations studied from Girne in Cyprus, which gave a significant, very negative results ($F = -8.58$, $p < 0.05$) and the population collected from Trachila in the Peloponnese, which gave a weaker, but still significant negative value ($F = -2.11$, $p < 0.05$).

Table 14: Results of neutrality tests for *Siganus luridus* populations collected from different sites throughout the Mediterranean Sea. Significant results ($p<0.05$) are marked in bold with an asterisk.

Site	Tajima's D	Fu's F
Limmasol	-0.45865	-1.03716
Kallithea	-1.28397	-3.38223
Gokova Bay	-0.63881	**-3.67188***
Diros	-0.55003	**-2.89639***
Agios Dimitrios	0.24085	-4.68102
Stoupa	-0.37304	**-3.22824***
Linosa	0.14898	**-3.5149***

Table 15: Results of neutrality tests for *Siganus rivulatus* populations collected from different sites throughout the Mediterranean Sea. Significant results ($p<0.05$) are marked in bold with an asterisk.

Site	Tajima's D	Fu's F
Limmasol	-0.19631	-1.61442
Konnos Point	1.75144	1.34315
Girne	-1.10216	**-8.57792***
Agios Andronikos	-1.4425	-1.66386
Kallithea	**-1.43477***	0.42629
Gokova Bay	-0.98387	-2.8688
Diros	-0.93302	-0.00275
Trachila	**-1.90129***	**-2.11488***
Kalamata	**-1.43477***	-1.08248

The historical demographic changes that occurred within the Mediterranean populations of *S. luridus* and *S. rivulatus* were analysed using a mismatch distribution test. Both *S. luridus* (Figure 12a) and *S. rivulatus* (Figure 12b) showed similar profiles for the concatenated sequences, demonstrating a bimodal distribution, not fitting the expected equilibrium distribution.

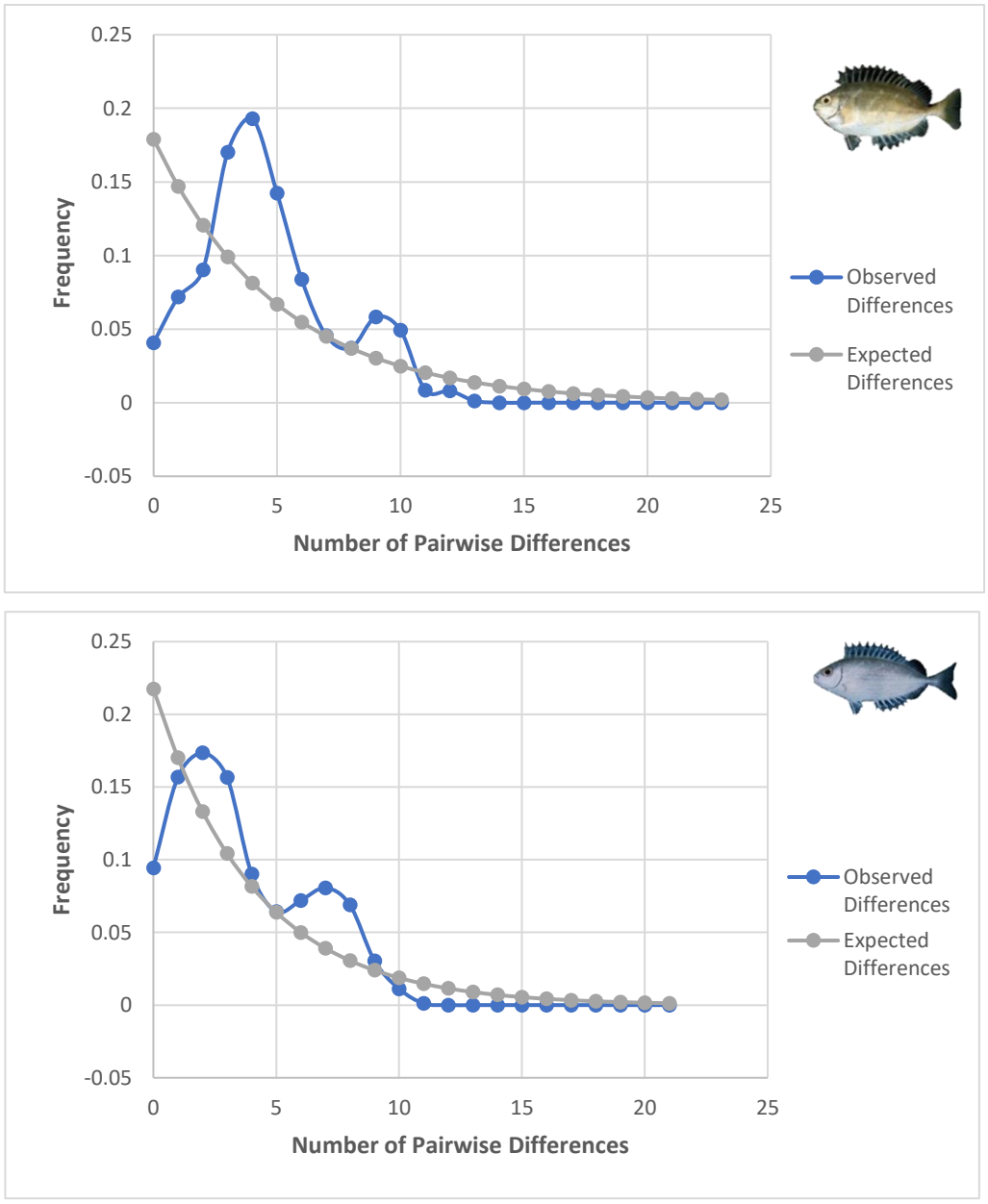

Figure 12: Results from the mismatch distribution tests run for (a) *Siganus luridus* and (b) *Siganus rivulatus*. Mismatch distribution data was calculated

using DnaSP6 (Rozas *et al.* 2017) from concatenated sequences containing data from two mitochondrial markers; cytochrome oxidase C sub-unit I and the control region.

2.4 Discussion

2.4.1 Evidence for the Presence of Two *Siganus* Species in the Mediterranean Sea

Previous literature has identified the presence of two genetically and phenotypically distinct *Siganus* species within the Mediterranean Sea (Steinitz 1927, Ben-Tuvia 1964, Bonhomme *et al.* 2003, Hassan *et al.* 2003, Azzurro *et al.* 2006). The ML trees generated in chapter 3.1.0 demonstrate the presence of two genetically distinct clades that correspond to the two species *S. luridus* and *S. rivulatus* as visually identified based on tail-shape and patterning.

The two clades are well supported with extremely high bootstrap values. Mean pairwise distances within and between these clades clearly demonstrate they are genetically distinct from one another, with very low intra-group values but a high mean inter-species distance.

2.4.2 Genetic Structure of *S. luridus* and *S. rivulatus* Populations within the Mediterranean Sea

There is minimal genetic structure present within both the *S. luridus* and *S. rivulatus* clades within the Mediterranean Sea.

The lack of genetic segregation between populations from different locations within the *S. luridus* species is clearly demonstrated on the only reliable branch (with 92% bootstrap support). This grouped individuals from sites in the eastern Mediterranean (Limmasol in Cyprus, Kallithea in Rhodes and Gokova in Turkey), the central (Agios Dimitrios in the Peloponnese) and the western Mediterranean (Linosa, one of the Pelagie Islands) together. This grouping demonstrates genetic similarity throughout the entire Mediterranean Sea, as is consistent with results published by Azzurro *et al.* (2006) wherein, even individuals from Linosa, the site with the most recently settled population, clustered with individuals from other sites throughout the Mediterranean Sea. The lack of segregation on the tree was also reflected in the haplotype networks generated for all the marker combinations, where shared haplotypes were shared

by sites throughout the Mediterranean Sea, not just individuals from one site or region.

The *S. rivulatus* group has two branches with reliable bootstrap support, consisting of two individuals each. The first, with 82.0 % bootstrap support, consists of one individual from Limmasol (Cyprus) and one from Gokova Bay (Turkey), two of the eastern-most sites. The second branch, with 87.9 % of support, groups two individuals from the central Mediterranean Sites Trachila and Kalamata, both in the Peloponnese region, together. These branches indicate there may be more segregation between populations of *S. rivulatus* within the Mediterranean Sea. However, the remaining structure of the rivulatus clade contradicts this with multiple short branches and low bootstrap support grouping large numbers of individuals from different sites together. Moreover, the haplotype network rejects the idea of genetic segregation by demonstrating that shared haplotypes are common in sites all throughout the Mediterranean, not just one region. Thus, it is clear there is no genetic segregation of haplotypes between populations of *S. rivulatus*. This observed lack of geographical genetic segregation is consistent with the results of a similar study published by Azzurro *et al.* (2006), where individuals from various eastern Mediterranean sites clustered together.

Moreover, consistent with the findings of Azzurro *et al.* (2006), the Red Sea individuals were distributed throughout the tree, indicating the genetic diversity within the Mediterranean reflects that of the Red Sea. This however, is difficult to confirm due to the small number of Red Sea samples included. To solve this, more Red Sea populations should be sampled and included within the analysis. The lack of clustering of the majority of the Mediterranean Sea samples with the Red Sea samples demonstrates that the diversity entering the Mediterranean Sea is not restricted. This is supported by the high levels of haplotype diversity within the Mediterranean Sea. To verify there is no restriction on diversity, more samples need to be collected from the Red Sea and analysed alongside the

Mediterranean Sea samples. This would also be beneficial to demonstrate relationships between populations in the novel and ancestral environments.

2.4.3 Haplotype Diversity of *Siganus* Species within the Mediterranean Sea

Haplotype diversity levels for the CR within the Mediterranean were lower than those calculated for the same species in the Red Sea by Azzurro *et al*. (2006), who utilised similar sample sizes. Despite the reduced haplotype diversity in the Mediterranean Sea compared to the Red Sea, high levels of haplotype diversity were found within both *Siganus* species throughout the entire Mediterranean Sea for the CR, COI and concatenated sequences. The CR region for *S. luridus* demonstrated a slightly higher haplotype diversity than for *S. rivulatus*, as is consistent with CR marker results published by Azzurro *et al*. (2006).

For the CR, the haplotype diversity value for *S. luridus* within the Mediterranean Sea calculated in this study (h = 0.904) was only slightly lower than the value calculated for the Red Sea (h = 0.978), however, there was a greater difference between the Red Sea haplotype diversity for the CR region of *S. rivulatus* (h = 1.000) and the value calculated in this study (h = 0.836). Similar decreases in haplotype diversity between the ancestral Red Sea populations and invasive Mediterranean populations were found in several species including *S. ghobban* and *B. pharaonis* (Terranova *et al.* 2006, Bariche and Bernardi 2009). Decreases are not unexpected when taking into account the hypothesis that invasion will result in decreased genetic variation in the invasive population compared to the ancestral populations (Azzurro *et al.* 2006).

Interestingly, when compared to the CR data from this study, over the space of 12 years, it is clear haplotype diversity has increased for *S. luridus* from 0.879 to 0.904 but has seemingly decreased for *S. rivulatus* from 0.853 to 0.836. Despite this, the total number of haplotypes identified increased for both species, from 15 to 17 for *S. luridus* and 12 to 32 for *S. rivulatus* (Azzurro *et al.* 2006). This increase in haplotype diversity for *S. luridus* may be the result of several

factors, specifically, an increased sample size and continued migration of Red Sea individuals into the Mediterranean Sea. The reduced haplotype diversity for *S. rivulatus* may be the result of the small sample size (n = 4) from Konnos Point confounding the results. Other explanations may include continued success of only a small number of the initial haplotypes present within the Mediterranean Sea. The decreased haplotype diversity identified in the *S. rivulatus* populations may also be an effect of the drastically increased sample size in this study (n = 109) compared to the original 2006 study (n = 23). This increased sample size is likely more representative of the diversity for populations throughout the entire Mediterranean. Regardless of minor fluctuations in haplotype diversity values, the consistently high levels concur with previous studies that disagree with the hypothesis that a severe genetic population bottle-neck would have occurred with the invasion of the Mediterranean Sea (Hassan *et al.* 2003, Azzurro *et al.* 2006).

The distinctly different levels of haplotype diversity found for the COI and CR markers represent the importance of incorporating multiple genetic markers into studies. This enables a more representative view of diversity through combining regions of variable diversity together. As expected, the total levels of haplotype diversity for the CR were greater than for COI; this is the result of the increased rate of evolution (accumulation of mutations) associated the hypervariable region within the CR (Lee *et al.* 1995, Sanna *et al.* 2011). Despite the differences in actual levels of haplotype diversity found between markers, the fluctuations in haplotype diversity between sites are relatively consistent between markers. For example, the *S. rivulatus* population from Diros (the Peloponnese) has consistently notably lower levels of haplotype diversity than the other *S. rivulatus* populations.

A limitation of the 2006 study is that only the mitochondrial control region marker was used for generation of haplotype data, one of the aspects this project aimed to improve. The data generated using both mitochondrial markers is more representative of the existing diversity, as it incorporates the variation in a

greater percentage of the genome into one study and presents data for regions which evolve at different rates (Zhang and Hewitt 2003). Despite this, the sole use of mitochondrial markers also has limitations; studies with microsatellites (nuclear genome markers), provide a wider scope of data as they are able to determine fine-scale differentiation within populations, as demonstrated in a study on the reef fish the blue-line snapper (*Lutjanus kasmira*) (Muths *et al.* 2012). Therefore, in the future, to improve the existing understanding of the genetic diversity, relationships, history and distribution of *Siganus* populations within the Mediterranean Sea the addition of a microsatellite marker could prove beneficial.

2.4.4 The History of Mediterranean Siganus Populations

The haplotype networks generated from the concatenated sequences for *S. luridus* and *S. rivulatus* demonstrate very different structures. The network for *S. luridus* consists of many unique haplotypes, belonging to only one individual and many haplotypes belonging to only a small number of individuals. This demonstrates a high level of haplotype diversity, as confirmed by the *h* value calculated for the concatenated sequence alignments. The *S. rivulatus* network consists of one dominant haplotype with many unique and low-frequency shared haplotypes radiating out in a star-like pattern. The fact almost 40 % of individuals share haplotype 5 within the *S. rivulatus* network agrees with the lower haplotype diversity of the *S. rivulatus* species in comparison to the *S. luridus* network, where not even 10 % of individuals have the same haplotype in common. This high-frequency haplotype (haplotype 5), which radiates out into the many unique and shared haplotypes is thought to be representative of an old allele, likely present within initial invaders from the ancestral population. The star-like structure around this ‘old’ haplotype indicates that population expansion may have occurred within the Mediterranean Sea leading to the high number of peripheral, unique and low-frequency shared haplotypes surrounding it (Ferreri *et al.* 2011).

The COI networks for both species also demonstrate the aforementioned star-like pattern of radiating haplotypes, indicative of population expansion (Ferreri *et al.* 2011). The CR networks, however, are more complex; for *S. rivulatus* there is also a subtle star-like structure. For *S. luridus* there is no clear structure with more relationships between haplotypes which are shared by fewer individuals. This increased similarity could be the result of the even more rapidly evolving CR region blurring past population history (Brown *et al.* 1979).

Although this study used mitochondrial DNA, which accumulates mutations at a more rapid rate than nuclear DNA (Zhang and Hewitt 2003), under the timescale of which the invasion has been occurring (just under 100 years) it is unlikely that all of this change has originated within the Mediterranean Sea. Instead, it is likely that haplotype 5, for example, is a common haplotype within the Red Sea and variations of this haplotype (the many radiating unique haplotypes) exist and have moved into the Mediterranean Sea alongside it.

2.4.5 The Direction of Invasion

Investigation into the number of unique versus shared haplotypes at each site throughout the Mediterranean provided the expected results. Due to their proximity to the Suez Canal, it was predicted that sites within the eastern and central Mediterranean Sea were likely to have a greater number of unique haplotypes, as they are located closest to where new invasive individuals would enter the Mediterranean Sea (Azzurro *et al.* 2006, Coll *et al.* 2010). This was the case for both species, with highest levels of unique haplotypes being recorded in Cyprus, Turkey and the Eastern-most site of the Peloponnese. The retrospective of this is that the western-most sites will have the highest number of shared haplotypes because, for a haplotype to reach Linosa (the Pelagie Islands) or the site of Kalamata (in the Peloponnese), it must have passed from the eastern to the western basin. This is feasible as such species are recorded to migrate through active swimming of adults and even drifting with currents using seaweed (Cho *et al.* 2001, Bonhomme *et al.* 2003). These results support the idea of sequential invasion and provide a direction of migration from east to west.

2.4.6 Population Genetics

It has been established that the eastern Mediterranean has high gene flow from the Red Sea (Bonhomme *et al.* 2003, Hassan *et al.* 2003). This is due to various changes within and between the environments of the Red and Mediterranean Seas. The physical barriers of width and depth of the Suez Canal, and differences in sea surface temperature and salinity between the two seas, have decreased over time allowing continued migration of a wide range of species (Goren and Galil 2005, Arndt and Schembri 2015). However, the focus of this project was to investigate the genetic structure and variability within and between the established invasive populations of the Mediterranean, as the same barriers of temperature and salinity exist on a decreasing gradient from east to west (Wuertz 2010, CEAM *et al.* 2018).

From east to west, haplotype diversity remains high in all populations of *S. luridus* and *S. rivulatus*, excluding Diros. This supports the concept of high genetic similarity between populations, as demonstrated by the lack of genetic segregation based on location in the maximum likelihood trees and the haplotype networks. Diros, a site in the Peloponnese, had a very low haplotype diversity value of 0.33 for the *S. rivulatus* population present. This seemingly anomalous value may have resulted from the small sample collected from Diros (n = 6). However, the same number of individuals were collected in Kallithea and no confounding effect is obvious. Furthermore, it is not the result of a pattern of decreased haplotype diversity, as the distance from the Suez Canal increases because the western-most site, Kalamata, also in the Peloponnese, has very high population haplotype diversity value. Further sampling from Diros would be necessary to investigate whether this site is segregated in terms of gene flow.

The invasion mechanism of *Siganus* has been described as sequential, involving dispersal (migration from the Suez Canal), establishment and then spread into near-by locations (Puth and Post 2005, Azzurro *et al.* 2006). Such sequential invasions leave genetic traces behind, such as those identifiable on the haplotype

networks. However, such traces are skewed when high genetic connectivity between populations remains, making the invasion path difficult to follow.

Despite high levels of haplotype variation, levels of true genetic variation within both *S. luridus* and *S. rivulatus* are low, as expected, because the species have not been present within the Mediterranean Sea long enough to develop mutations unique to their subsequent populations. Thus, variations observed within the species are expected to have been present since the initial invasion (Davies *et al.* 1999, Bonhomme *et al.* 2003, Azzurro *et al.* 2006).

Nucleotide diversity values (π) within *S. luridus* demonstrated minimal changes in the nucleotide sequence, both within the species as a whole, and also within and between study sites. Levels of π fluctuated when moving from east (Limmasol, Cyprus) to west (Linosa, the Pelagie Islands), however, generally levels remained consistent. The mean pairwise distance values calculated for the *S. luridus* species concurred with the low values of π, once again indicating a low level of genetic variation throughout the Mediterranean Sea. This evidence suggests there is a relatively high level of gene flow throughout the entire Mediterranean Sea, as indicated by the shared haplotypes on the haplotype networks.

For *S. rivulatus*, Diros (the Peloponnese), the site that gave a seemingly anomalous haplotype diversity unsurprisingly displayed the lowest levels of both nucleotide diversity and mean pairwise distances between sequences. These values did not fit in with the higher, but still low, values for the other sites from which *S. rivulatus* were collected. Although there are fluctuations moving from east (from Limmasol, Cyprus) to the western-most site in the central Mediterranean (Kalamata, the Peloponnese) there is a pattern suggesting levels of genetic diversity, in terms of π and mean-pairwise distance, decrease. This suggests that when moving from east to west across the Mediterranean Sea, levels of genetic diversity decline. Decreased genetic variation may be a result

of changing environmental factors moving from east to west selecting for certain phenotypes more fit to survive in lower temperatures and levels of salinity.

The F_{ST} results concur with the lower levels of haplotype and genetic diversity present within the *Siganus rivulatus* species. A significant F_{ST} value indicates that there has been a significant level of genetic differentiation between two populations.

In concurrence with the slightly higher genetic differentiation levels identified through the genetic indices tests, the F_{ST} values support that there is less genetic connectivity between populations of *S. luridus* than *S. rivulatus*. However, total values for both species fall within the "moderate genetic differentiation category" based on values between $F_{ST} > 0.05$ and $F_{ST} \leq 0.15$, demonstrating low levels of effective migration (connectivity) between populations. Reduced genetic connectivity is demonstrated within the *S. luridus* species as each population is at minimum moderately significantly differentiated from another population in the study. This is not the case with *S. rivulatus*, whereby the majority of populations do not demonstrate significant differentiation.

It is expected that eastern Mediterranean populations would be differentiated from western populations due to the continued invasion of Red Sea genotypes (Azzurro *et al.* 2006, Coll *et al.* 2010). This was not observed for *S. luridus,* where sites tended to be significantly differentiated from their neighbouring sites, not those further away. Populations of *S. rivulatus* did demonstrate the expected pattern, where sites in Cyprus were significantly differentiated from those in the Peloponnese. No populations of either species demonstrated significant levels of very great differentiation from one another, indicating that there is still a moderate to high level of gene flow between populations.

2.4.7 Demography of Mediterranean *Siganus* populations

A significant, negative value for Tajima's D indicates either expansion of the population, positive selection or a genetic bottleneck through deviation from the neutral model of evolution (Templeton 2006). Fu's F, a more powerful measure, based on the neutral model of evolution, is also able to indicate whether population expansion, selection or a bottleneck has occurred through analysis of rare haplotype presence within the population (Fu 1997). A negative value represents an excess of rare (low frequency) alleles. It was expected that due to the strong selective pressures arising from distinctly different conditions in the central and western Mediterranean Sea compared to those of the Red Sea, that western sites would demonstrate selection, thus allowing rejection of the null hypothesis that the populations fit with the neutral model of evolution (Azzurro *et al.* 2006). A limitation of these neutrality tests is their inability to distinguish whether significant results arise from true departures due to selection, or through demographic processes *i.e.* population expansion (Hahn *et al.* 2002).

No *S. luridus* populations studied demonstrated significant values for Tajima's D. The stronger statistical Fu's F test indicated that four out of the seven study sites significantly depart from the neutral model, thus, presenting an excess of rare alleles compared to what is expected. These populations are, as expected, from the western-most eastern site (Gokova Bay, Turkey), the central sites (Diros and Stoupa in the Peloponnese region) and the western-most site (Linosa, the Pelagie Islands). Although it is clear demographic change has occurred at these sites, the negative, insignificant Tajima's D values indicate this change is somewhat weak.

Two of the three *S. rivulatus* populations displaying significant departures from the neutral model (according to Tajima's D) were expected to, as they (Trachila and Kalamata, the Peloponnese) were the western-most populations studied, located in the central Mediterranean, thus any demographic changes are likely have resulted from natural selection (Azzurro *et al.* 2006). Kallithea, the third population demonstrating a significant departure from neutrality (according to

Tajima's D), was unexpected as the site lies close to the Suez Canal. Because of the population's small sample size (n = 6), more sampling will be necessary to identify any significant demographic changes, especially given the insignificant Fu's F value. The only population that can be confidently determined as significantly departed from the model of neutrality is that from Trachila in the Peloponnese, with a negative Tajima's D and Fu's F indicating an excess of rare haplotypes. This is expected due to the selective pressures that will arise from conditions of the location in the Mediterranean Sea. The highly negative Fu's F value for the *S. rivulatus* population from Girne, Cyprus was unexpected. It is possible the population may be expanding through addition of rare haplotypes, due to continued migration of individuals from the Red Sea, as this site is in close proximity with the Suez Canal (Coll *et al.* 2010). However, if this was the case other eastern sites would also be expected to demonstrate significant levels of departure from neutrality. More investigation of the haplotypes present should be conducted in combination with use of Red Sea samples to allow comparison of the ancestral haplotypes present within this site and not present within other Mediterranean Sea sites. If these haplotypes are present within the eastern Mediterranean sites only this would suggest recent invasion of these individuals.

In summary, although both species have populations with negative Tajima's D and Fu's F values, indicating deviations from the expectations of the standard model of neutrality, most results are insignificant. Thus, there is minimal evidence for selection. Furthermore, these results mean there is also little evidence for population expansion or a genetic bottleneck (Grant and Bowen 1998). Interestingly, the expectations of population expansion (low π and high *h*) are fulfilled (Rogers and Harpending 1992, Grant and Bowen 1998). However, the few departures from neutrality detected mean that for most populations, population expansion cannot be confirmed. Despite this, the haplotype networks star-like structures for both species in COI and for *S. rivulatus* in the concatenated network do suggest that rapid population expansion did occur (Ferreri *et al.* 2011). It is important to consider that such levels of demographic change are unlikely to occur in the short timeframe.

In concurrence with previous studies utilising *S. luridus* and *S. rivulatus*, the cumulative results of this study also indicate that a genetic bottleneck is unlikely to have occurred (Bonhomme *et al.* 2003, Hassan *et al.* 2003, Azzurro *et al.* 2006). This conclusion has been reached because a genetic bottleneck would be expected to leave signature low levels of both *h* and π, in addition to significant, negative Tajima's D and Fu's F values, none of which are observed (Tajima 1989, Grant and Bowen 1998).

The mismatch distribution graphs generated to evaluate the growth of the populations of invasive species in the Mediterranean did not fit with the expected unimodal curve that represents rapid demographic expansion (Rogers and Harpending 1992). Instead the bimodal curves demonstrated represent allopatric divergence followed by population growth (Sousa *et al.* 2012). This corresponds with the negative Tajima's D and Fu's F results, suggesting evidence of a demographic change, but disagrees with the levels of significance they demonstrated. It is still unclear whether significant levels of population expansion have occurred, however the star-like pattern with lots of unique haplotypes evident within the networks, especially for *S.* rivulatus, in combination with high levels of haplotype diversity and bimodal mismatch distribution suggest a signature of expansion is present within the Mediterranean Sea. Further sampling with larger sample sizes (n>20) would be useful for further analysis of these populations, as small sample size is a known limitation often leading to under-estimation of neutrality tests such as Tajima's D and Fu's F, the two aspects of the analysis which disagree with the possibility of population expansion (Subramanian 2016).

Chapter 3: Growth Rate Across the Mediterranean

3.1 Introduction

3.1.1 Movement from a Tropical, High Productivity, Coral Dominated Sea to a Temperature Sea Characterised by Rocky-Reefs and Algal Barrens

Since the *Siganus* species invasion began in 1927 (Steinitz 1927), the species have become acclimatised to a rock-reef dominated environment, changing their habitats from their ancestral environment of the Red Sea (Hassan *et al.* 2003, Brokovich *et al.* 2006, Afeworki *et al.* 2013). Within their ancestral environment of the Red Sea it is known that the species *S. luridus* occupies lagoon habitats within northern Red Sea and both *S. luridus* and *S. rivulatus* inhabit reef-flat habitats throughout the Red Sea (Brokovich *et al.* 2006, Afeworki *et al.* 2013). However since there are no coral-reef flats present within the Mediterranean Sea, the species have begun to occupy rocky-reef habitats, some characterised by an abundance of algal species (Hassan *et al.* 2003, Sala *et al.* 2011). *S. rivulatus* specifically has demonstrated high adaptability exhibiting use of multiple habitats ranging from bays, rock pools to muddy harbours and beds of sea grass (Bariche *et al.* 2004).

The difference in temperature ranges between the Red and Mediterranean Seas is one of the most noticeable factors that provokes questions regarding the ability of species to survive this dramatic change in environment. Although sea surface temperatures in the eastern Mediterranean Sea are as high as 28 °C in the summer the temperatures within the western Mediterranean sea can drop to as low as 15 °C in the winter (CEAM *et al.* 2018). These temperatures are lower and the range is also much greater than the temperature range of approximately between 29 °C and 33 °C found within the Red Sea (Chaidez *et al.* 2017).

With changes in temperature come associated changes in primary productivity (Lieth 1975). In the Red Sea, levels of chlorophyll-a vary throughout the year but still represent moderate levels of primary productivity year round, with

summer months providing the lowest values of 0.14 mg/L and winter values reaching values as high as 0.49 mg/L (Eladawy *et al.* 2017). The Mediterranean Sea, in comparison has a notably greater range of levels of chlorophyll-a signifying increased levels of primary productivity with levels ranging between 0.16 mg/L and 2.7 mg/L (European Environment Agency 2014). This range of primary productivity is reflected in the trophic gradient identified in the Mediterranean Sea, with oligotrophy increasing towards the eastern side resulting in lower levels of primary productivity where temperatures are highest (Danovaro *et al.* 1999). These increased levels of primary productivity stimulate questions about the distribution of species within the eastern Mediterranean and their access to food resources within the Mediterranean Sea, important for providing energy for growth (Dutta 1994).

Salinity is another factor that is known to decrease between the environments of the Red and Mediterranean Seas. Within the Red Sea salinity ranges from 38 ppt in the south to 42.5 ppt in the north (Talley *et al.* 2011). These values are distinctly higher than those found in the Mediterranean Sea, which has a gradient ranging between 36 % in the western basin to 39 % salinity in the eastern basin (Wuertz 2010). It is known that salinity is important for osmoregulation in fish, an energy demanding process, which when salinity is not at the optimal level (iso-osmotic) can reduce growth (Boeuf and Le Bail 1999). This change in salinity between the Red and Mediterranean Seas, and with the gradient across the Mediterranean Sea, would be predicted to induce a higher energy burden for osmoregulation in regions of lower salinity resulting in a reduction in growth.

3.1.2 How do Environmental Factors Affect Growth Rate?

As briefly discussed above, the growth rate of fish can be positively and negatively affected by various biological and abiotic factors; these include temperature, salinity and availability of food (nutrition) (Dutta 1994, Boeuf and Le Bail 1999, Rountrey *et al.* 2014). It is important to understand how the changes in these environmental factors between environments impacts growth of invasive individuals, as if growth is impacted severely, growth may be an effective predictor of invasive ability and survival success.

Temperature is a vital factor with regards to growth of fish as it regulates a number of highly important physiological processes, including metabolism and growth (Brett 1979, Jobling 1996). There are intricate links between temperature, metabolism and growth within fish (Clarke and Johnston 1999). Temperature is a determining factor for availability of oxygen and although increased temperatures can increase metabolic rate, the rate at which metabolic processes such as growth occur, they also reduce available oxygen within the water due to a decreased solubility (Clarke and Johnston 1999, Pörtner and Knust 2007). Lower temperatures reduce the metabolic rate of a fish meaning the rate of oxygen consumption is also reduced (Clark *et al.* 2013). This, combined with the increased solubility and resultant availability of oxygen within the lower temperatures of the Mediterranean Sea may mean that the aerobic scope is increased; more oxygen can be consumed, so more metabolic processes can be carried out (Clark *et al.* 2013). This theory (termed the 'allocation model') is for budgeting of energy in which physiological processes compete for energy against basal metabolic activity (Careau *et al.* 2008). However, the lower temperatures in the Mediterranean Sea may result in a trade-off; lower growth rates due to a reduced metabolic rate, but an increased availability of oxygen due to lower temperatures resulting in a greater aerobic scope, providing more availability of energy for more processes. This means metabolic processes such as growth are expected to be slower due to the temperature gradient of the Mediterranean Sea.

Fish demonstrate a response curve relationship between temperature and growth rate; initially, as temperature increases so does growth rate, eventually an optimum temperature is reached and growth peaks. Deviations from this optimal temperature, either decreases or increases in environmental temperature can reduce growth rate (Árnason *et al.* 2009). This has been demonstrated for numerous species in a variety of temperature studies, including lumpfish (*Cyclopterus lumpus L*), Atlantic salmon (*Salmo salar*), gilthead seabream (*Sparus aurata*) and turbot (*Scophthalmus maximus*) (Hernández *et al.* 2003, Handeland *et al.* 2008, Árnason *et al.* 2009, Nytrø *et al.* 2014). Understanding the relationship between temperature and growth is important in the context of

Lessepsian invasion of the Mediterranean Sea because sea surface temperatures (SSTs) within the Mediterranean Sea are dramatically reduced, compared to those of the Red Sea, depending on the region. It has been documented that the optimal temperature for growth of *S. rivulatus* is 27 °C (Saoud *et al.* 2008), thus growth should be highest in the eastern Mediterranean and a decrease in growth should be observed moving west.

Water salinity is another determining factor for growth rate, it impacts growth rate through environmental receptors which direct alteration of growth rate (Bœuf and Payan 2001). Salinity is determined by the presence of dissolved salts within the water (Riley 1965). To monitor this, fish possess prolactin cells and, on the pseudobranch of their gills, chemoreceptors (Laurent and Dunel-Erb 1984, Grau *et al.* 1994). These signal to ionic regulation mechanisms; the energetic cost of this regulation increases as salinity moves further from iso-osmotic conditions (Morgan and Godin 1985). This increased investment of energy in osmoregulation and maintaining suitable ionic conditions within the animal results in a decreased growth rate as less energy is available for growth (Árnason *et al.* 2013). This theory has been demonstrated by a number of studies, for example in Atlantic cod (*Gadus morhua*).

S. rivulatus has been documented as a highly capable osmoregulator. An experiment conducted by Saoud *et al.* (2007) demonstrated no significant changes in growth rate between individuals reared for six weeks in four different salinities (25, 30, 35 and 40 ppt). This indicates that the marbled spinefoot rabbitfish, *S. rivulatus*, may be able to resist significant changes in salinity, thus changes in growth as a result of the salinity gradient within the Mediterranean Sea are not expected.

Nutrition is a broad term incorporating multiple factors, specifically, the abundance of protein, amino acids, lipids and carbohydrates within the diet (Dutta 1994). Without the correct nutrition an animal will not be able to obtain all the basic building blocks necessary for life. As the abundance of macrophytes, the chosen food source of both rabbitfish species (Bariche 2006),

is reflected by the levels of chlorophyll-a in a region and trophic we can expect that growth will be greater in the west due to higher trophic levels. However, the reduced temperature and salinity may impact this.

3.1.3 The Importance of Understanding Growth Rate of Lessepsians

Understanding the impacts of environmental stressors on physiological processes (such as growth) may enable us to predict the extent of current invasions and the possibility of future invasions. For example, in a changing (and generally warming) climate the idea of invasion from a warmer to a cooler body of water may benefit a species, although trade-offs may exist. A decreased temperature will mean a decreased growth rate; however, it will also mean a greater concentration of dissolved oxygen is available (Clark *et al.* 2013), thus, allowing for a greater aerobic scope and higher investment in growth as resources are not sequestered to processes such as reproduction (Careau *et al.* 2008, Baudron *et al.* 2014, Neilan and Rose 2014).

3.1.4 Aims and objectives

In this study, growth was investigated using otoliths, which form bands (annuli) for each year of growth; previous studies have demonstrated a clear relationship between annulus width and somatic growth rate (Radtke *et al.* 1985, Reichert *et al.* 2000). As such, this study utilised annulus (increment) width as a proxy for somatic growth.

The locations of the study sites chosen in this study lie across a subtle latitudinal but a clear longitudinal gradient, each with different associated conditions for factors including temperature, salinity and levels of chlorophyll-a.

The aim was to investigate growth of the invasive species at different locations across the Mediterranean to allow identification of any possible candidates for factors that definitively allow or constrain invasion and establishment of a new species within an area. Through this, the impact of decreasing temperature, decreasing salinity and increasing levels of chlorophyll-a in a gradient from east

to west across the Mediterranean Sea were investigated on the growth of the two Lessepsian rabbitfish, *S. luridus* and *S. rivulatus*.

3.1.5 Predictions of Ecological Impacts due to Environmental Conditions in the Mediterranean Sea

Given that previous research has documented the optimal temperature for growth of *S. rivulatus* at 27 °C (Saoud *et al.* 2008) it was predicted that growth within the Mediterranean would be greatest within the eastern sites for individuals of *S. rivulatus*, and due to the close relationships of the species, also *S. luridus*.

Based on the research conducted by Saoud *et al.* (2007) which demonstrated that there were no significant changes in growth rate of individuals raised in various salinities, and the comparatively low differences in salinity between the Red and Mediterranean Seas no changes in growth as a result of reduced salinity were expected.

The ecology of species growth may change due to absence of normal resources. Within the Mediterranean Sea, a cooler temperate basin, the species of algae are expected to be different. For this reason, the normal food resource of the *Siganus* species may not be available and alternative resources must be sought out. The plasticity of their diets and abundance of algal species within the Mediterranean Sea indicate this should not be a problem (Bariche 2006). Thus, it was predicted that growth would be greater in regions with higher primary productivity (the western basin).

3.2 Materials and Methods

3.2.1 Otolith Collection

Samples of *S. luridus* and *S. rivulatus* (Figures 13a and 13b) were collected from fish markets and sourced through spearfishing and local fisherman from 7 sites in 5 regions throughout the Mediterranean basin; Cyprus, Turkey, Rhodes, the Peloponnese and Linosa, one of the Pelagie Islands (Figure 14), during 2016 to 2018. Care was taken to ensure all samples were caught locally to the study area. Due to the variable distribution of the fish and the methods of collection both species were not collected from all the sites. The number of samples used from each site can be seen in Table 16.

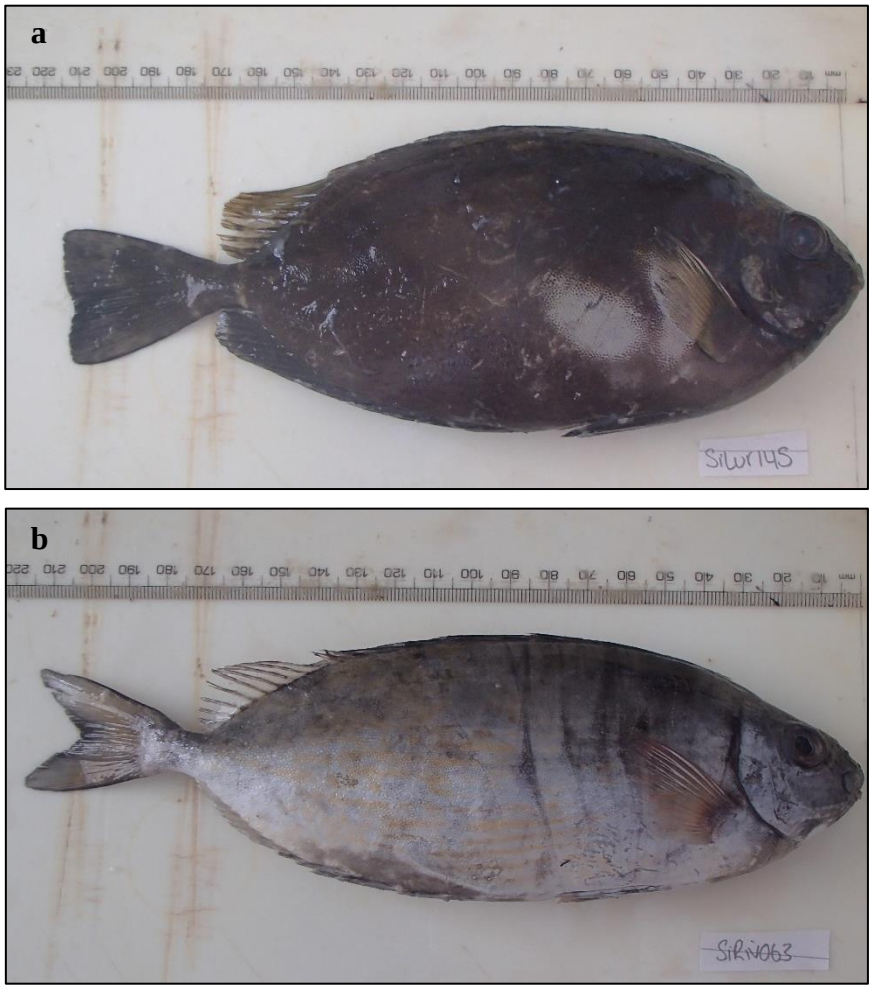

Figure 13: Photo examples of (a) *Siganus luridus* and (b) *Siganus rivulatus* individuals collected from the Mediterranean Sea. Photos were taken by Stephanie Heyworth, The University of Nottingham.

Figure 14: Map of sites across the Mediterranean Sea used for otolith collection. Purple circles show sites where both species were collected, dark blue triangles show sites where only *S. luridus* individuals were collected and light blue squares represent sites where only *S. rivulatus* samples were collected. If the site name is different to that of the study area, it is displayed next to the specific site.

Table 16: The number of individuals collected and used from each site for otolith analysis.

Population	Number of Individual Sampled	
	Siganus luridus	***Siganus rivulatus***
Limmasol, Cyprus	6	5
Kallithea, Rhodes, Greece	4	5
Gokova Bay, Turkey	6	6
Diros, Peloponnese, Greece	5	5
Trachila, Peloponnese, Greece	0	6
Stoupa, Peloponnese, Greece	5	0
Linosa, Pelagie Islands	6	0

To extract the otoliths the upper region of the brain case and brain were removed exposing the top of the otoliths. The otoliths were gently removed by breaking through the centre of the lower brain case and pulled out using tweezers. The otoliths were then washed in 99% ethanol and stored at ambient temperature.

3.2.2 Initial Otolith Preparation

Otoliths cross-sections were prepared for viewing under a reflected light microscope. Whole, ethanol-cleaned otoliths were laid flat and attached by the postrostrum end of the otolith to the top, unfrosted end of a slide using therma-bond glue which melted when exposed to the high temperatures of a heat-block; the otolith core (designated by high opacity, Figure 15) was aligned with the edge of the slide, leaving the rostral hanging over the edge of the slide (Figure 16a). 3M aluminium oxide coated sharpening film ranging from 40 µ to 12 µ was used to grind the rostral end half of the otolith until the core was reached (Figure 16b). The glue was the re-melted using a heat-block and the otolith placed in the centre of the slide, fixed with therma-bond glue, with the newly-flattened edge of the otolith attached to the slide (Figure 16c). The postrostral end was then ground away until a thin cross-section of the otolith remained, thin enough to be translucent when the slide was viewed above a light-source (Figure

16d). Extreme care had to be taken when processing the otoliths as too much pressure resulted in shattering of the bone, making it unusable in the analysis.

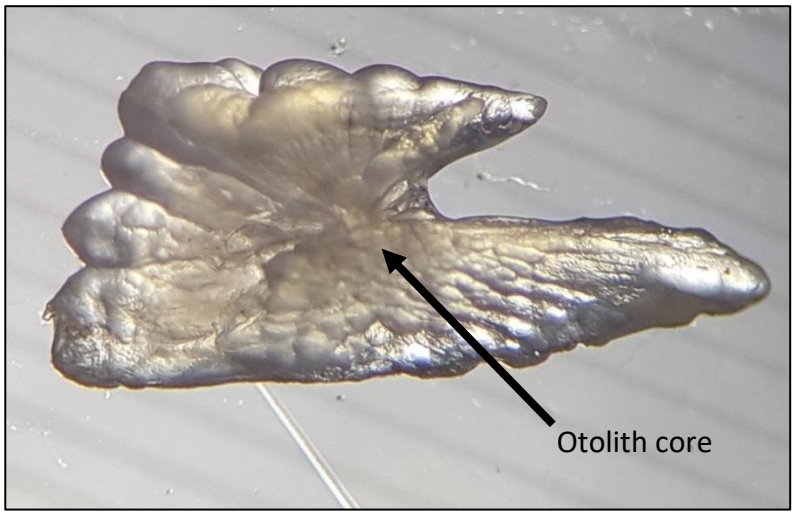

Figure 15: A photograph of a *Siganus luridus* otolith highlighting the core region. The black arrow is pointing to the core of the otolith.

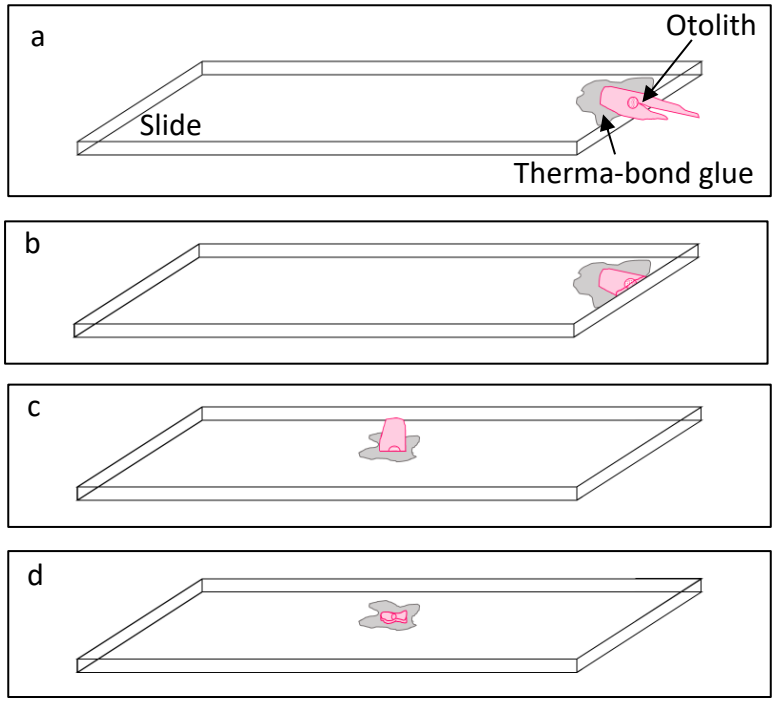

Figure 16: The consecutive stages of otolith (pink) preparation. The first stage (a) involves fixing the otolith to the slide using therma-bond glue (grey). The second stage (b) shows grinding down of the otolith to the centre-point,

wherein the growth bands start. The third stage (c) involves removing the otolith from the edge and fixing it ground-side down, now with the centre-point against the slide. The final stage (d) involves grinding of the otolith down to a thin section, translucent enough to allow light to pass through, allowing identification of the growth bands present.

3.2.3 Imaging

For investigation of differences in growth across the Mediterranean Sea, a maximum of six individuals from each population were sampled; their total length measured, and their otoliths photographed for analysis (Appendix 3 or and Table 16).

All photos of otolith sections were taken using an AxioCam MRc5 attached to a Zeiss Axio Imager.M1m microscope. The reflected light was emitted from a HAL 100 illuminator. To image the entire otolith an EC Epiplan-NEOFLUAR lens with a magnification of 5x and an aperture of 0,13 was used. Initially photos were taken using all four possible modes; bright-field, dark-field, differential interference contrast (DIC) and circular-polarised differential interference contrast (C-DIC).

3.2.4 Improving Otolith Quality

Following initial photography of the otoliths, it was clear the protocol for otolith preparation needed refinement as imaging of the otoliths using the Epiplan-NEOFLUAR lens with a magnification of 5x and an aperture of 0,13 under the brightfield setting revealed the 12 µ lapping paper from 3M left obvious scratches on the surface of the otoliths (Figure 17a and 17b). In order to rectify this, finer grades of lapping paper (3 µ and 1 µ) were used to polish the surface of the otolith prior to photography. In addition to this, instead of using a side-to-side motion, the otoliths were polished with small circular movements whilst lubricating the film with clean water.

The thickness of the otolith section was found to cause problems when identifying growth bands if it was too thick. This is because thicker sections allow for more interaction of reflected light within the otolith, making the internal structure of the otolith less defined due to this interference (Figure 18a). To fix this, otolith sections were ground further until they were as thin as possible without shattering and interference occurred in the core (Figure 18b). The mode elected to continue the photography with was dark-field (Figure 19a) as it minimised the presence of sub-annual bands, highlighting annual bands more clearly than use of bright-field, DIC or C-DIC modes (Figures 19b, 19c and 19d).

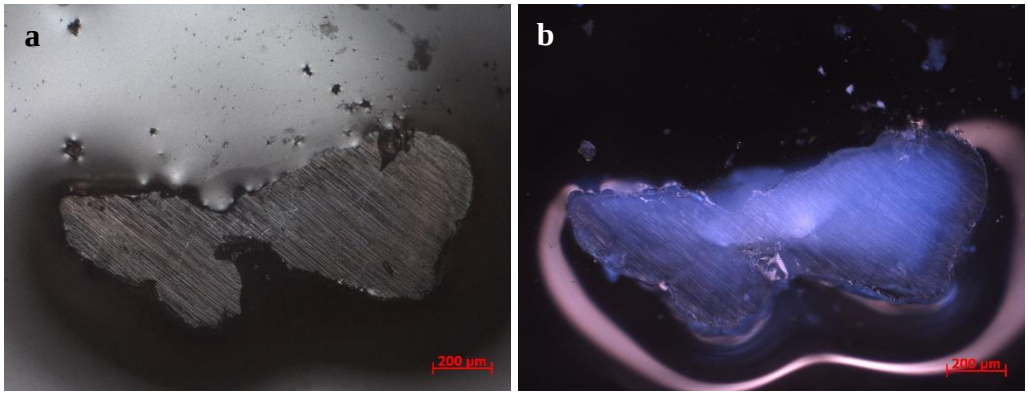

Figure 17: Otolith images showing scratches on the surface taken during the trail photography period. Photos of an otolith from a *Siganus luridus* individual from Diros, Greece in (a) bright-field and (b) dark-field modes. Images were taken on an AxioCam MRc5 attached to a Zeiss Axio Imager.M1m microscope using the Epiplan-NEOFLUAR lens with a magnification of 5x and an aperture of 0,13. Clear scratches left from preparation are visible on otoliths following preparation with 12 µ lapping film.

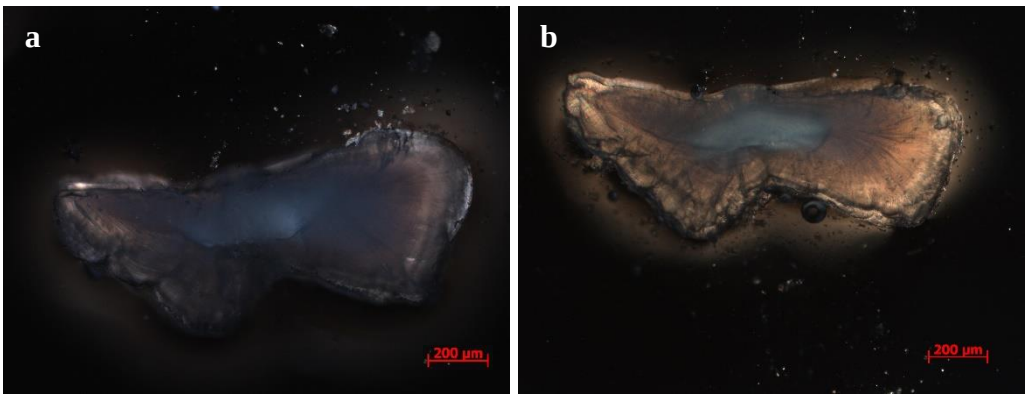

Figure 18: Otolith images showing the effect on photograph clarity of further thinning of an otolith section. Photos of an otolith from a *Siganus luridus* individual from Diros, Greece from (a) the initial photography trial section checking quality and (b) the second trial session where changes (such as thinning in this case) had been made to improve quality. Images were taken on an AxioCam MRc5 attached to a Zeiss Axio Imager.M1m microscope using the Epiplan-NEOFLUAR lens with a magnification of 5x and an aperture of 0,13 differential interference contrast mode.

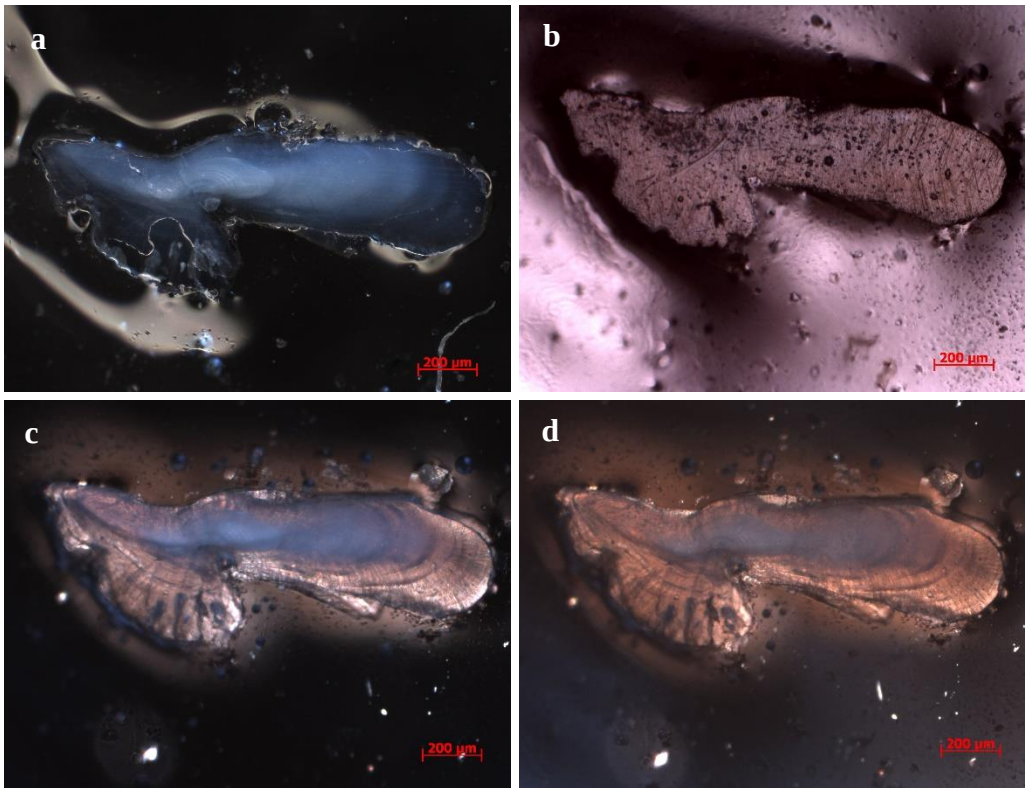

Figure 19: Photos of an otolith showing the clarity of the different modes (a) dark-field, (b) bright-field, (c) differential interference contrast (DIC) and (d) circular-polarised differential interference contrast (C-DIC). Distinct bands can be seen in the dark-field image (a), whereas the brightfield image (b) illustrates surface features only. DIC (c) and C-DIC (d) show a lot of detail, including sub-annual bands, making it difficult to identify yearly growth intervals. Images were taken on an AxioCam MRc5 attached to a Zeiss Axio Imager.M1m microscope using the Epiplan-NEOFLUAR lens with a magnification of 5x and an aperture of 0,13.

3.2.5 Calculating Fish Age and Measuring Annuli

To allow for calculation of age and measurement of annual growth otoliths from a total of 58 individual fish were used; 31 *S. luridus* and 27 *S. rivulatus* (Appendix 3). Using the dark field images otolith transects were conducted, wherein a transect line was drawn onto the otoliths and the annual bands were marked. ImageJ (Fiji (Schindelin *et al.* 2012)) was used to plot otolith transects; increments were marked by placing points on each annual band (Figure 20).

Increments were marked in approximately the same region on every otolith on the ventral side of the sulcal groove to allow for comparison between otolith width increments. Points were placed at the termination of the dark zone, starting with the first full dark zone closest to the core. The distance between the outer edge of one dark zone and the outer edge of the following dark-zone represents one year of growth in a band, or an annulus. ImageJ was used to measure the width between subsequent growth annuli in reference to the scale bar placed on the image during photography.

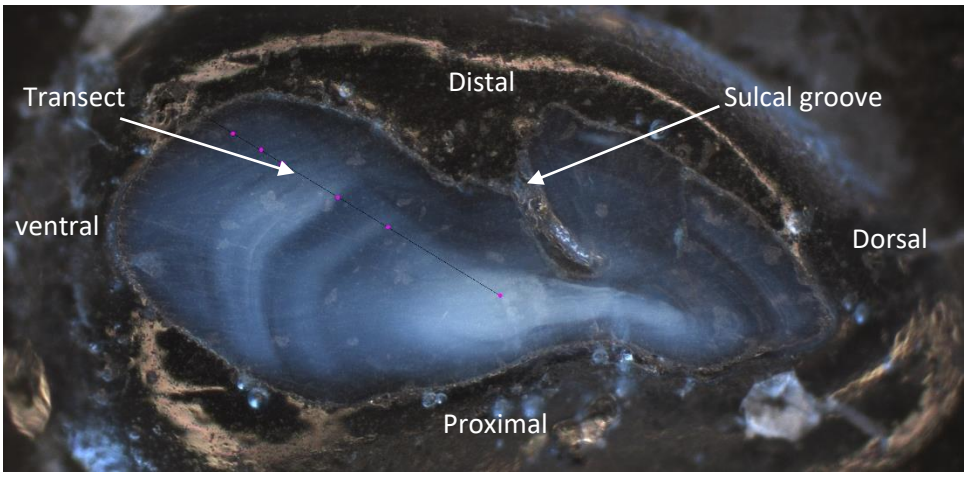

Figure 20: An example of an otolith transect used to calculate fish age and otolith growth increment width. The transect (plotted on ImageJ, Fiji (Schindelin *et al.* 2012)) was plotted along a straight line with pink, brightly visible points determining the outer edges of two dark zones. The edge from one dark zone to the other represents a year of growth. The image is of an otolith from an *S. rivulatus* individual collected from Trachila, in the Peloponnese. The photo was taken on an AxioCam MRc5 attached to a Zeiss Axio Imager.M1m microscope using the Epiplan-NEOFLUAR lens with a magnification of 5x and an aperture of 0,13.

3.2.6 Analysis of Age-Length Relationships Throughout the Mediterranean Sea

To investigate the relationship between age and body size across the Mediterranean Sea, both between populations and between the different sites, scatter graphs were generated and logarithmic curves assigned to each population (with R^2 values). To enable comparison of age-length relationships between species one graph was generated for each species. This allowed for identification of the strength of relationship between length and age across the Mediterranean Sea.

3.2.7 Does Otolith Growth Effectively Represent Somatic Growth?

To investigate if otolith size and growth effectively represent the somatic size and growth of the fish, a linear regression was plotted using the otolith transect data against the standard length. The gradient of the linear regression line was analysed and the R^2 value also taken into account.

3.2.8 Comparing Growth Increments between Sites and Species

To allow for comparison of increment width for each annulus(year) bar graphs with standard error bars were plotted for the mean increment width, of each increment at each site for each species. The same annuli from different sites and the annulus growth between species were compared.

3.2.9 Environmental Correlates to Life History Parameters

The relationship between sea surface temperature (SST), chlorophyll-a, salinity and spatially structured growth patterns were examined within both species.

Daily data for SST, chlorophyll-a and salinity were obtained from the Research Data Archive (National Centre for Academic Research Colorado 2018). For each region the mean SST (°C), chlorophyll-a level (mg/L) and salinity (ppt) were calculated. These were used to generate bar graphs (with standard error bars) for comparing the environmental factors between sites.

3.2.10 Investigating the Impact of Environmental Variables on Growth

To determine which factors (species, site or annulus (year of growth) impacted the amount of annulus growth, a general linear model was conducted in R version 3.5.1 (R Core Team 2018) using the 'aov' function. The general linear model was set to investigate the effects of annulus (year of growth), site and species on the amount of growth (mean increment width) of the otolith increments. The interactions between the three factors were also analysed.

3.3 Results

3.3.1 Age-length Relationships of *S. luridus* and *S. rivulatus* Within the Mediterranean Sea

The sites from which the populations were collected were all at different distances from the Suez Canal, ranging between 384 km in Limmasol (Cyprus) to 1873 km away in Linosa (the Pelagie Islands), the westernmost site. The remaining sites Kallithea in Rhodes, Gokova Bay in Turkey and Diros, Trachila and Stoupa in the Peloponnese were distributed at various distances away; 681 km, 750 km, 1097 km, 1107 km and 1117 km respectively (Table 17).

Table 17: Number of samples used from each population and the study sites distance from the Suez Canal.

Population / Study Site	Distance from Suez Canal (km)	Number of Individual Sampled	
		Siganus luridus	***Siganus rivulatus***
Limmasol, Cyprus	384	6	5
Kallithea, Rhodes, Greece	681	4	5
Gokova Bay, Turkey	750	6	6
Diros, Peloponnese, Greece	1097	5	5
Trachila, Peloponnese, Greece	1107	0	6
Stoupa, Peloponnese, Greece	1117	5	0
Linosa, Pelagie Islands	1873	6	0

The age range of *S. luridus* individuals encapsulated individuals from two to seven years old (Appendix 3 and Figure 21a), whereas samples of *S. rivulatus* utilised within this study showed an age range of three to nine years (Appendix 3 and Figure 21b). The largest individual recorded (*S. rivulatus* and 30 cm in total length (TL)) was also the oldest recorded at an estimated nine years of age based on observed otolith increments. *S. luridus* demonstrated a greater range of sizes for the individuals that were four years old; from approximately 14.9 cm to 22.8 cm in length, whereas individuals of *S. rivulatus* only ranged from between 16.2 cm to 17.4 cm in length. The range of sizes in the 5-year-old category was also greater in *S. luridus* than *S. rivulatus*.

All but one population of *S. luridus* (those collected from Limmasol**)** demonstrated a strong positive relationship between the fish's TL and age (Figure 21a). The relationship between TL and age for all individuals is weak, but this can be partially explained by the variation seen between sites on the graph (Figure 21a). With all populations, increasing age was closely associated with large body size (Kallithea (Rhodes), Gokova Bay (Turkey), Diros (the Peloponnese), Stoupa (the Peloponnese) and Linosa (the Pelagie Islands), with R^2 values of 0.992, 0.882, 0.689, 0.550 and 0.832 respectively), with little evidence of an asymptote in growth demonstrated (Taylor *et al.* 2017)

The graph of age of *S. luridus* individuals plotted against TL (Figure 21a), shows that with the exception of Stoupa (the Peloponnese), as the distance from the Suez Canal increases (from Limmasol, Cyprus through to Linosa, the Pelagie Islands) so does the TL of the individual, especially in later ages (between five and seven years). No such pattern is identifiable on the graph of age of *S. rivulatus* individuals plotted against the fish's TL (Figure 21b). Trachila in the Peloponnese, the furthest site from the Suez Canal from which *S. rivulatus* was collected sampled did demonstrate the lowest TL for each age on average, according to the trend-line, however the rest of the sites show no correlation with distance and reduced growth.

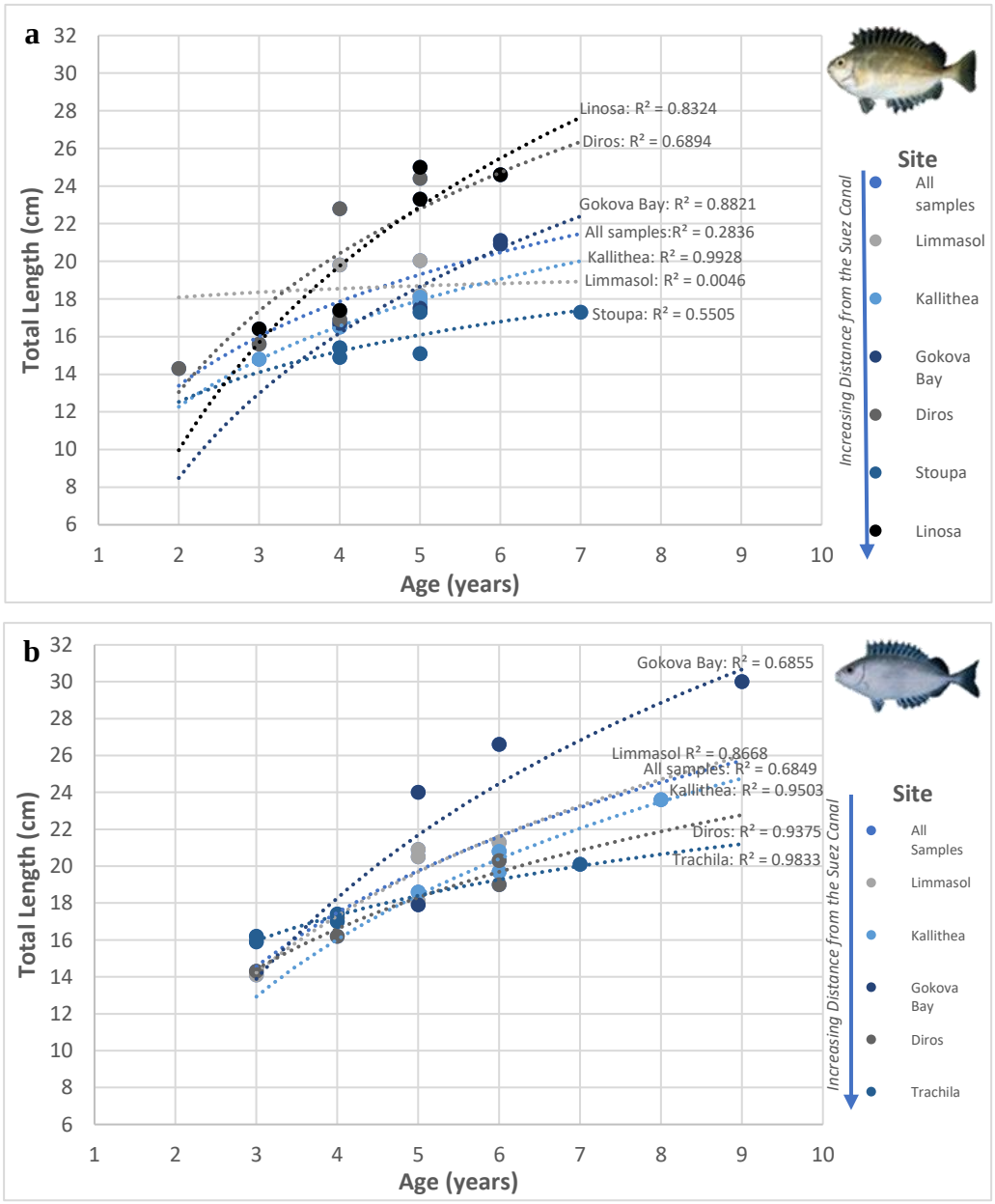

Figure 21: Age – length relationships between individuals of (a) *S. luridus* and (b) *S. rivulatus* collected from various sites across the Mediterranean with increasing distances from the Suez Canal. R^2 values describe the percentage of the variation within the dependent variable (total length) which is explained by the independent variable (age). Logarithmic curves were plotted for each site.

3.3.2 The Relationship Between Otolith Growth and Somatic Growth

To investigate the relationship between otolith growth and somatic (bodily) growth the TL of fish was plotted against the total cumulative increment width of the otolith for each individual. For all individuals of both *S. luridus* and *S. rivulatus* the relationship between total cumulative increment width and TL showed a positive, linear relationship (Figures 22a and 22b). As the width of the otolith increase, so did the body size (TL) of individuals (the somatic length). This shows that otolith increment widths recorded are representative of bodily growth.

The relationship between length and total cumulative increment width of *S. rivulatus* is steeper, but also stronger than the same relationship within *S. luridus* (Figure 22b compared with Figure 22a). The value of $R^2 = 0.54$ for *S. rivulatus*, compared to the positive, but lower value of $R^2 = 0.21$ for *S. luridus* demonstrates a stronger relationship between otolith growth and somatic size (TL) in *S. rivulatus*, because it means over 54 % of the variance in the total cumulative width is explained by total length for *S. rivulatus*, however for *S. luridus* only 21 % of the variance is explained by total length.

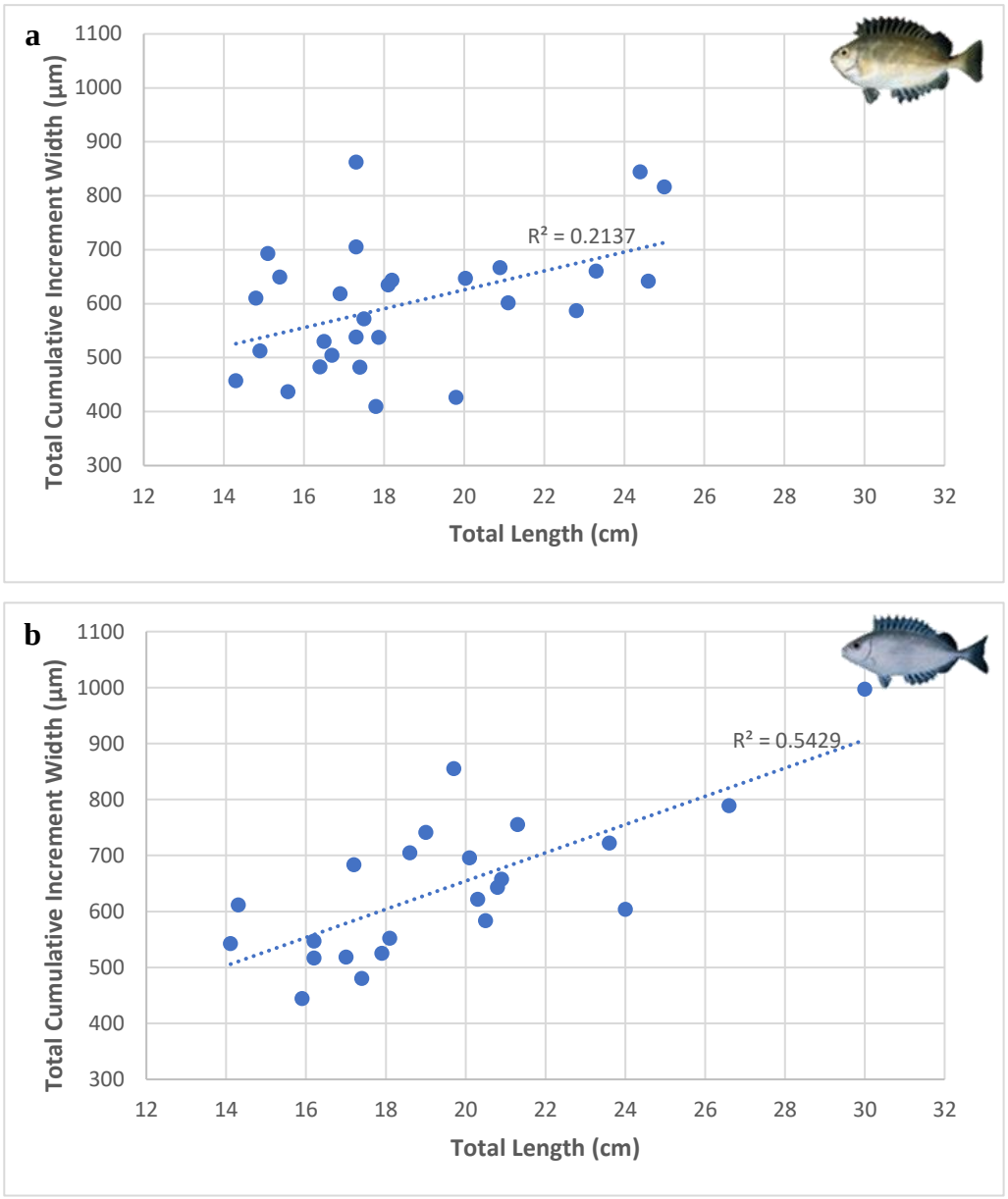

Figure 22: The relationship between otolith size (the cumulative otolith increment width) and somatic size (total length in cm) for individuals of (a) *Siganus luridus* and (b) *Siganus rivulatus* collected from various sites throughout the Mediterranean Sea. R^2 values describe the percentage of the variation within the dependent variable (total cumulative width) which is explained by the independent variable (total length).

3.3.3 Investigating Factors that Affect Otolith Growth

To identify which factors significantly affected otolith annulus increment sizes, and thus annual otolith growth, a linear model was conducted in R (R Core Team 2018). The factors that have a significant effect on the increment width of an annulus (Table 18) are the annulus number (which annulus is under study), the species, the interaction between annulus number and site at which it is found and also, the annulus number and the species it is found in. Site does not have a significant effect upon determining the width of an otolith increment/annulus.

Table 18: Results of a linear model conducted for annulus width against annulus number, site and species, with interactions between these factors considered. The species included were *Siganus luridus* and *Siganus rivulatus*. Annulus number refers to the annulus in question, i.e., annulus one would represent the annulus from the first year of growth. Interaction b/n means interaction between, and the colon between two factors represents that the interaction between those factors is being investigated. Significant values are shown in bold font; the number of asterisks represents the strength of significance: p=0 = '***', p<0.01 = '*'. DF = degrees of freedom, Sum Sq = sum of squares, mean sq = mean squared, Pr(>5) = probability value.

Factor	DF	Sum Sq	Mean Sq	F value	Pr(>F)
Annulus Number	1	998561	998561	478.510	**< 2e-16 *** **
Site	6	7761	1293	0.620	0.714357
Species	1	10006	10006	4.795	**0.029583 ***
Interaction b/n annulus: site	6	49034	8172	3.916	**0.000967 *** **
Interaction b/n annulus: species	1	26694	26694	12.792	**0.000427 *** **

Interaction b/n site: species	3	1801	600	0.288	0.834296
Interaction b/n annulus: site: species	3	1061	354	0.170	0.916870

3.3.4 The Otolith Growth of *S. luridus* and *S rivulatus* Populations within the Mediterranean Sea

Within species, the differences in values between sites were not significant, for the same increment, however the differences between annuli (the increment widths for each age) did vary significantly ($p<0.05$). The mean increment width was greatest for individuals in the first year of growth (the first annulus/increment) for all species at all sites (Figure 23).

The mean increment widths of all the populations of *S. luridus* (Figure 23a) are of similar values indicating high growth at all sites in the first year of life; Limmasol in Cyprus (273.6 µm, ±14.1), Kallithea in Rhodes (236.6 µm, ±27.5), Gokova Bay in Turkey (251.7 µm, ±12.6), Stoupa in the Peloponnese (241.2 µm, ±21.5), Linosa in the Pelagie Islands (279.7 µm, ±19.5). The majority of error bars overlap with the means other populations, showing similar values of increment width are found in all populations. The linear model confirms this lack of difference, indicating there is no clear difference between the mean values of the width of the first increment between populations collected from the different sites (Figure 23a and Table 18).

For *S. luridus* (Figure 23a) the population from Diros (the Peloponnese), showed greater growth than the other populations, with a mean value of 302.4 µm (±33.0). The lowest mean width was recorded in Kallithea (Rhodes), the second site away from the Suez Canal, with a mean width of 236.6 µm (±27.5). For all sites and both species, the mean increment width of the first annulus was

significantly greater than the other annuli, which did not appear to be sufficiently different from one another.

For populations of *S. rivulatus* (Figure 23b) the mean increment width in the first year was significantly greater ($p<0.05$) than other, subsequent years. The means from each site were even more similar than those of *S. luridus* (Figure 23b compared to Figure 23a) with no significant differences between growth at different sites for the first year of age. Similar variances are also found around each of the means showing that the values within all populations overlap. Although once again the mean increment width was greatest in Diros in the Peloponnese (260.4 µm, ±18.7), this value was only 26.1 µm greater than the smallest mean value, found once again, in Kallithea in Rhodes (234.3 µm, ±18.4), a small amount, especially once the variances are considered. Similar mean values to the highest and lowest means in addition to overlapping variances are found in all the remaining populations; Limmasol, Cyprus (258.2 µm, ±13.1), Gokova Bay, Turkey (248.2 µm, ±16.0) and Trachila, the Peloponnese (255.7 µm, ±27.5).

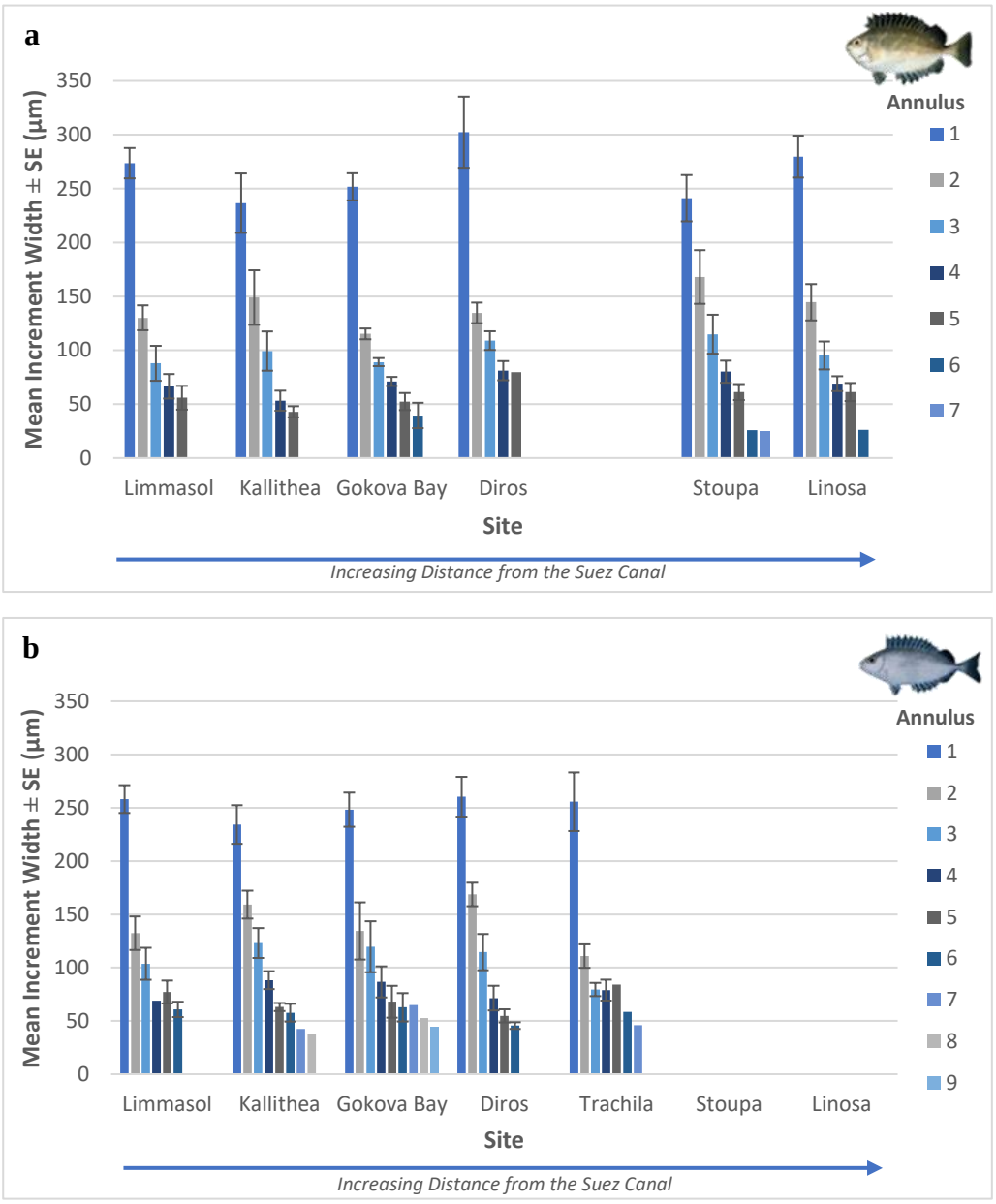

Figure 23: The mean increment widths ± standard error (SE) for annuli from (a) *Siganus luridus* and (b) *Siganus rivulatus* individuals from different sites and increasing distances from the Suez Canal within the Mediterranean Sea (distance increases from left to right). NB Increments without error bars only had one sample (n = 1). Samples of *S. luridus* from Trachila were not utilised due to the site's proximity with Diros and Stoupa. Samples of *S. rivulatus* collected from Stoupa were not utilised due to the site's proximity to Trachila. No samples of *S. luridus* were collected from Linosa.

The mean increment width of the second increment for all populations was significantly smaller than the first increment for all populations of both species, indicating reduced growth in the second year. The highest mean increment width was recorded in the region of the Peloponnese (central Mediterranean) for both species; *S. luridus* in Stoupa with a value of 168.0 µm with a variance of ±24.9 µm and a very similar value for *S. rivulatus* from Diros (168.7 µm, ±18.7). The lowest mean value for *S. luridus* was found in Gokova Bay, Turkey with a very low variance, indicating all values from this population are close to the mean value (115.2 µm, ±5.0). For *S. rivulatus* the lowest mean value was found in Trachila, the Peloponnese (110.9 µm, ±11.0). Once again, for all individuals of *S. luridus* the mean values were similar, however the variances differed greatly; Limmasol in Cyprus (130.2 µm, ±11.6), Kallithea in Rhodes (148.9 µm, ±25.3), Gokova Bay in Turkey (115.2 µm, ±5.0), Diros in the Peloponnese (134.7 µm, ±9.6), Stoupa in the Peloponnese (168.0 µm, ±24.9) and Linosa one of the Pelagie Islands (144.6 µm, ±16.9). The range in *S. rivulatus* populations was greater for the second increment than the first with greater variability between all the values in all populations; Limmasol in Cyprus (132.2 µm, ±15.7), Kallithea in Rhodes (159.1 µm, ±13.1), Gokova Bay in Turkey (134.4 µm, ±26.8) and Diros (168.7 µm, ±11.0) and Trachila (110.9, µm, ±11.0) in the Peloponnese. For both species there does not seem to be a sufficient difference between mean width across sites for the second increment.

Mean values for the third increment were generally lower for *S. luridus* across all sites (Limmasol in Cyprus (87.9 µm, ±16.2), Kallithea in Rhodes (99.3 µm, ±18.2), Gokova Bay in Turkey (89.0 µm, ±3.7), Diros (109.0 µm, ±8.7) and Stoupa (114.9 µm, ±18.1) in the Peloponnese and Linosa one of the Pelagie Islands (95.2 µm, ±13.0)) than those of *S. rivulatus* (Limmasol in Cyprus (103.6 µm, ±15.0), Kallithea in Rhodes (123.1 µm, ±14.0), Gokova Bay in Turkey (119.6 µm, ±23.9) and Diros (114.6 µm, ±17.0) and Trachila (79.5 µm, ±6.2) in the Peloponnese. The *S. rivulatus* population from Trachila is an exception, with a very low mean width of only 79.5 µm (±6.2). For *S. luridus* the greatest mean width was recorded in Stoupa, whereas for *S. rivulatus* the greatest width was

recorded in Kallithea. The lowest mean values were recorded in Limmasol and Trachila for *S. luridus* and *S. rivulatus* respectively.

The values for the fourth increment did not vary significantly between sites for populations of *S. luridus*, once again indicating no distinct difference between growth within the fourth year of life; Limmasol in Cyprus (66.6 µm, ±11.4), Kallithea in Rhodes (53.2 µm, ±9.3), Gokova Bay in Turkey (71.1 µm, ±4.2), Diros (81.1 µm, ±8.9) and Stoupa (80.1 µm, ±10.2) in the Peloponnese and Linosa one of the Pelagie Islands (69.0 µm, ±6.9). Higher mean values were once again obtained in the *S. rivulatus* population indicating greater growth at all sites, however, between populations there was no difference in growth depending on the site; Limmasol in Cyprus (69.1 µm), Kallithea in Rhodes (88.3 µm, ±8.4), Gokova Bay in Turkey (86.6 µm, ±14.6) and Diros (71.4 µm, ±11.6) and Trachila (78.9 µm, ±9.8) in the Peloponnese. The greatest widths were recorded in Diros and Kallithea for *S. luridus* and *S. rivulatus* respectively. The lowest width, and thus lowest growth was recorded in Kallithea for *S. luridus* and Limmasol for *S. rivulatus.*

Patterns in the greatest and smallest mean increment widths were consistent for the fifth increment, with greatest growth (mean widths) in Diros for *S. luridus* and in Trachila for *S. rivulatus*; both these sites are located in the central Mediterranean in the Peloponnese region. The lowest mean increment widths were recorded in Kallithea (Rhodes) and Diros (the Peloponnese) for *S. luridus* and *S. rivulatus* respectively. Once again, between populations of *S. luridus* there was no significant difference between the mean otolith increment widths at different sites; Limmasol in Cyprus (55.9 µm, ±11.0), Kallithea in Rhodes (42.9 µm, ±5.2), Gokova Bay in Turkey (52.4 µm, ±7.9), Diros (79.6 µm) and Stoupa (61.2 µm, ±7.4) in the Peloponnese and Linosa one of the Pelagie Islands (61.3 µm, ±8.4). Similarly, for *S. rivulatus* inter-population mean widths did not to vary significantly between the sites of Limmasol in Cyprus (77.1 µm, ±10.7), Kallithea in Rhodes (63.0 µm, ±3.8), Gokova Bay in Turkey (68.0 µm, ±14.9)

and Diros in the Peloponnese (54.7 µm, ±6.2) with the exception of Trachila in the Peloponnese (84.2 µm).

Three of the *S. luridus* populations did not have individuals greater than five years of age (Appendix 3 and Figure 23a). However, Gokova Bay, Stoupa and Linosa did. The population collected from Gokova Bay (Turkey) had the greatest mean increment width for the sixth increment at 39.5 µm (±11.8). This was larger than the means of the populations from Stoupa in the Peloponnese (25.8 µm) and Linosa one of the Pelagie Islands (26.0 µm), however the difference was not significant. It appears that populations of *S. rivulatus* collected from sites throughout the Mediterranean showed significantly higher mean increment widths for the sixth increment than the populations of *S. luridus*. Additionally, individuals of six years of age (with six increments) were collected from each site for *S. rivulatus*, demonstrating a greater life span. Interestingly, the Gokova Bay population also had the greatest mean increment width. The lowest mean width was recorded in Diros. Once again, however, there was no significant difference between mean increment widths from the different sites; Limmasol in Cyprus (60.8 µm, ±7.2), Kallithea in Rhodes (57.7 µm, ±8.4), Gokova Bay in Turkey (62.8 µm, ±13.3) and Diros (45.6 µm, ±3.2) and Trachila (58.6 µm) in the Pelopnnese.

Only one individual of *S. luridus* was collected which was aged at seven years; it was collected from Stoupa and had an increment width of 24.7 µm for this seventh increment. Three sites for *S. rivulatus* had individuals with an age of seven years; Kallithea (Rhodes), Gokova Bay (Turkey) and Trachila (the Peloponnese). The greatest increment width was recorded in Gokova Bay (64.9 µm) and the lowest in Kallithea (42.5 µm). The value for Gokova Bay seems distinctly larger than the other sites, however there is no apparent difference between the increment widths found in Kallithea (42.5 µm) and Trachila (45.9 µm).

Two individuals of *S. rivulatus* were collected and aged at eight years old. These were from Kallithea (Rhodes) and Gokova Bay (Turkey). The increment width measured in the individual from Gokova Bay (52.7 µm) seems distinctly larger than that measured in the individual Kallithea (38.0 µm), however because these samples are made up of one individual (n = 1) they are not necessarily representative of true population means for these increments.

Gokova Bay (Turkey) was the population that held the oldest individual, an individual of *S. rivulatus* of nine years of age. This is three years older than the oldest individuals collected from Limmasol (Cyprus) and Diros (the Peloponnese), two years older than the oldest individual collected from Trachila (the Peloponnese) and one year older than the oldest individual collected from Kallithea (Rhodes). The increment width for the ninth annulus of this individual measured 44.3 µm, as expected lower than the increment widths for the previous increments for the same population. This again reflects the idea growth decreases with age, agreeing with the age-length curves produced in Figure 21b.

3.3.5 Environmental Factors that may affect growth within the Mediterranean Sea

To determine differences in environmental variables between sites three environmental factors (sea surface temperature (SST), salinity, and the levels of chlorophyll-a) were investigated to see if there were any difference across sites, important because these factors are known to affect growth.

For SST (Figure 24a), there was a general trend of decreasing temperature the further west the site. Linosa (one of the Pelagie Islands and the westernmost site) is an exception to this trend. In Linosa warmer temperatures were recorded than for two of the central Mediterranean sites (Trachila and Stoupa). In sites where *S. luridus* were collected, with only one exception there were no drastic differences between the mean SST of each site. While the majority of sites (Limmasol, Gokova, Kallithea, Diros and Linosa) had mean recorded values

between 20.2 °C (±0.04) and 21.4 °C (±0.03), the site of Stoupa in the Peloponnese showed a distinct reduction in temperature with a recorded mean value of 17.6 °C (±0.05). In sites where *S. rivulatus* was collected, values in Limmasol, Gokova, Kallithea and Diros remained similar and between 20.9 °C (±0.04) and 21.4 °C (±0.04) showing no distinct differences. Trachila in the Peloponnese however had a slightly reduced mean of 19.7 °C (±0.04). Thus, *S. luridus* is found in a greater range of temperatures (with means between 17.6 °C (±0.05) and 21.4 °C (±0.04)) compared to *S. rivulatus* (found in sites with temperatures ranging from 19.7 °C (±0.04) to 21.4 °C (±0.04)).

Analysing the levels of salinity in each site (Figure 24b) demonstrated there was a decrease in the salinity as the distance from the Suez Canal increased. The closest sites to the Suez Canal (in the eastern Mediterranean) from Limmasol through to Kallithea had the highest levels with salinity values ranging from 39.0 ppm (±0.00) to 39.1 ppm (±0.00). Sites within the central Mediterranean, further from the Suez Canal (Diros, Trachila and Stoupa) had lower values all at 38.7 ppt (±0.00). Finally, the lowest levels were found in the western Mediterranean at the site furthest from the Suez Canal; Linosa which had a mean salinity of 37.5 ppt (±0.00). This pattern was consistent within sites where both *S. luridus* and *S. rivulatus* were collected.

There is a clear increase in levels of chlorophyll-a moving from east to west across the Mediterranean Sea (Figure 24c). Limmasol, the site closest to the Suez Canal has the lowest mean levels at approximately 0.11 mg/L (±0.00). Kallithea and Gokova, sites on the boundary between the east and central Mediterranean have higher levels of chlorophyll-a at approximately 0.15 mg/L (±0.00) in both sites. Diros, the easternmost central site has a subtly lower level of chlorophyll-a than Gokova and Kallithea (0.148 mg/L (±0.002) compared to 0.149 mg/L (±0.004)). Stoupa and Trachila, two central Mediterranean sites from which samples were collected have even higher mean values at 0.16 mg/L (±0.00) and 0.18 mg/L (±0.00) respectively. Linosa, notably, has the highest mean value of 0.21 mg/L (±0.00).

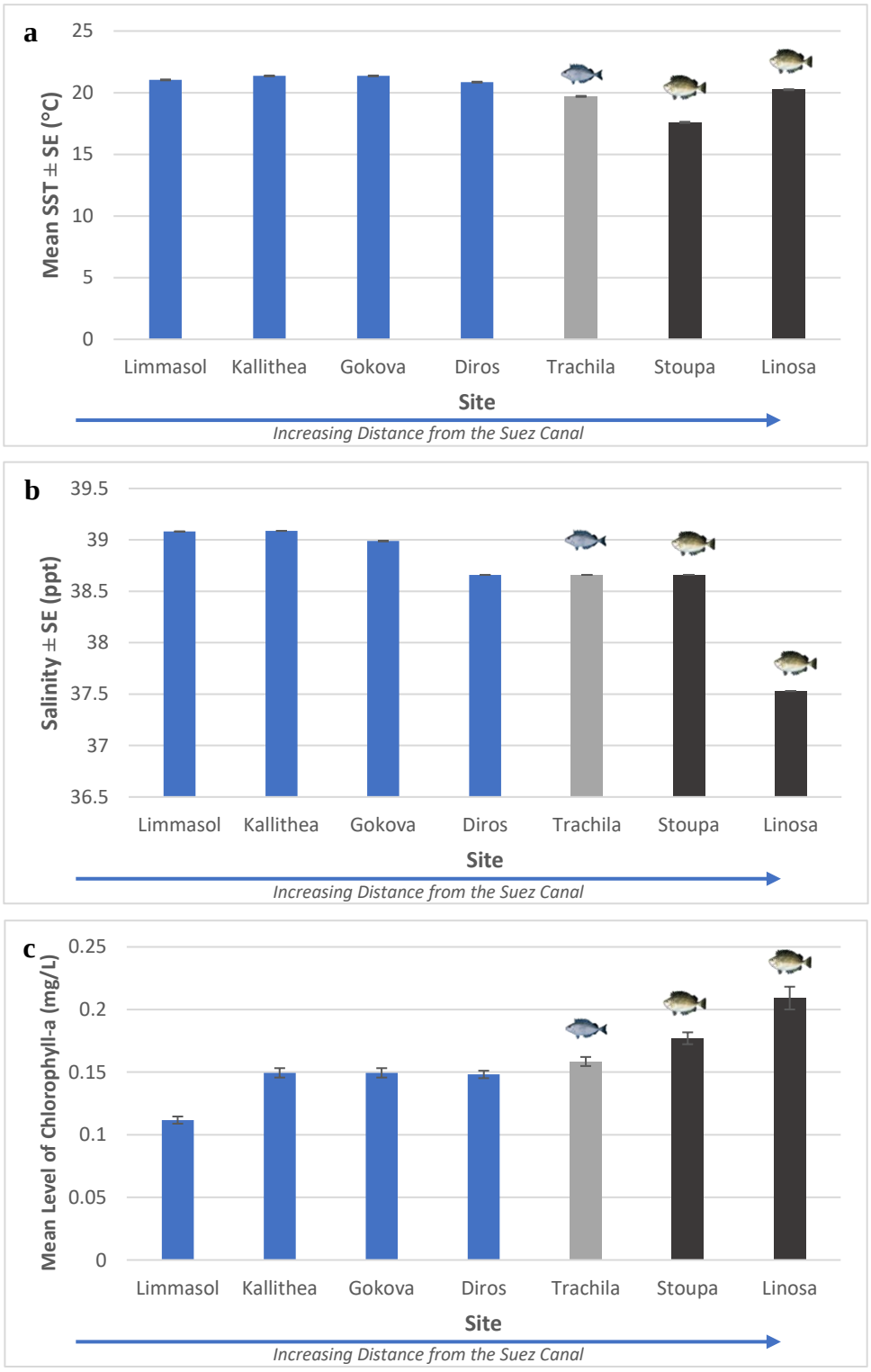

Figure 24: The (a) mean sea surface temperatures (SSTs), (b) mean salinity levels and (c) mean chlorophyll-a levels in sites where *Siganus luridus* and *Siganus rivulatus* individuals were collected. The distance from the Suez Canal increases from left to right along the X-axis. Standard error (SE) bars are displayed. Blue bars, without fish images, represent sites from which both species were collected. The light grey bars, with the images of *S. rivulatus* above,

represent the only site from where only *S. rivulatus* was collected. The dark grey bars represent sites from which only *S. luridus* were collected, as depicted by the image of *S. luridus* above the bars.

3.4 Discussion

3.4.1 Is Otolith Growth Representative of Somatic Growth?

There was a positive relationship between total length and otolith width for both species. For *S. luridus*, less of the variation within the total cumulative increment width was explained by the total length of the fish, as the total length of the fish increases, so does the size of the otolith, thus, otolith growth is representative of somatic growth. Such results are in direct alignment with the strong relationship in otolith size and somatic size found in a range of species from smelt (*Osmerus eperlanus*), fringed flounder (*Etropus crossotus*) to oyster toadfish (*Opsanus tau*) (Radtke *et al.* 1985, Reichert *et al.* 2000, Fey 2006).

Temperature can introduce variation in the relationship between total length and otolith size by significantly affecting otolith growth, even though somatic growth can remain significantly correlated with otolith growth, this is a phenomenon found in herring (*Clupea harengus*) (Fey 2006). It has also been observed that variations in environmental temperature can lead to complete uncoupling of the otolith-width somatic length relationship, as documented in the King George whiting (*Sillaginodes punctate*) (Barber and Jenkins 2001). Variation in factors, *e.g.* temperature, may explain the previously unexplained variation in total length-otolith size relationships for *S. luridus*. However, because mean temperatures remain relatively constant throughout the Mediterranean Sea, as demonstrated in the environmental factors analysis, minimal variation in otolith size should result from temperature fluctuations in the Mediterranean Sea.

3.4.2 Growth Along a Latitudinal Gradient

Individuals of both *S. luridus* and *S. rivulatus* had a longer lifespan within this study (by 1 and 3 years respectively), to those recorded 13 years ago (Bariche 2005). This increased lifespan may be due to acclimatisation of the species to the Mediterranean, or due to broader sampling, as the 2005 study was restricted to the eastern Mediterranean Sea. Interestingly, studies have demonstrated that a reduced temperature can increase lifespans of poikilotherms (Walford and Liu

1965). As the oldest individual of *S. rivulatus* was found in Gokova Bay (Turkey, eastern Mediterranean), the hypothesis of reduced temperature (through westward migration) increasing lifespan seems unlikely, as the study by Bariche (2005) also took place within the eastern Mediterranean Sea.

Despite discrepancies in the age-length relationships between sites, site does not have a significant impact on otolith (and subsequently somatic growth) of individuals of *Siganus* species within the Mediterranean Sea. This shows that growth between different sites was not significantly different, overall. These results were unexpected, especially when the gradients in temperature, salinity and chlorophyll-a are taken into account moving east to west, and previous research suggests that changes in temperature and salinity can impact growth of *Siganus* species (Collins and Nelson 1993, Saoud *et al.* 2007, Saoud *et al.* 2008). Therefore, it seems that the species are capable of compensating for these changes without reducing their growth. This suggests that growth is not a substantial indicator of invasion success as changes in key environmental factors do not affect growth as expected.

Populations of *S. luridus* did not demonstrate a decreased age-length relationship, as expected, moving from east (Limmasol, Cyprus) to west (Linosa, the Pelagie Islands). The largest sizes for each age, according to the logarithmic curves, are expected in Linosa (the westernmost site) and Diros (Peloponnese, the Central Mediterranean). This was unexpected as optimal growth was assumed to occur closest to the species' ancestral environment of the Suez Canal (Farag Abziew and Ali 2016). It is possible the increased abundance of food resources within the western Mediterranean Sea (indicated by increased chlorophyll-a levels) provide substantial energy and nutrition for growth (Dutta 1994), while the reduction in temperature is not sufficient to effectively reduce metabolic rate (Clarke and Johnston 1999). This is a trade-off, where increased temperature (thus, more effective metabolism) is exchanged for an increased access to nutrition.

This work found a significant effect of annulus number (year of growth) on the size of the annulus, with the first annulus (throughout both species, and across sites) showing the greatest levels of growth, with decreasing growth throughout the rest of the annuli. This is expected and consistent with similar studies on other species, including the blue grenadier (*Macruronus novaezelandiae*) (Sweetman *et al.* 2018).

Although for both species there was no significant effect of site on otolith growth, there was an overall trend of *S. luridus* individuals in the central and western Mediterranean Sea being predominantly larger than those in the eastern Mediterranean Sea (except in individuals collected from Stoupa). Incidentally, a significant interaction between annulus/increment number (year of life the fish is in) and site was found to affect otolith growth. We argue that the larger individuals in the western Mediterranean Sea are the result of the variation in the growth of the first annulus; in this context, the otolith increment analysis for *S. luridus* supports the findings of greatest length at age occurring in two of the more western sites (Diros and Linosa) as the greatest mean increment widths, for the first increment, where growth is greatest, are also found in the western sites, excluding Stoupa. Growth values for the first annuli in Kallithea, Linosa and Gokova were much reduced compared to those in Diros and Linosa, fitting with the reduced total size in the later years of life. The same goes for the mean increment width in Stoupa. Analysis of the remaining mean otolith increment width values does not highlight any other increments/annuli with as much variation between them.

The age-length data for populations collected from Stoupa (Peloponnese, central Mediterranean), did not follow the pattern of increased age-length relationships as distance from the Suez Canal increased. When investigating possible reasons why individuals in Stoupa did not grow as large as individuals in other Mediterranean populations, environmental analyses indicated a dramatic drop in the mean SST for that region. It is understood that if temperature is not optimal, a resultant repressed aerobic scope will reduce the growth rate of an individual

(Careau *et al.* 2008, van Rijn *et al.* 2017). Thus, it is possible that the reduced temperature in Stoupa, due to offshore fresh water springs (Tsabaris *et al.* 2011), has reduced the aerobic scope sufficiently to reduce the maximum growth rate compared to other populations in the Mediterranean Sea.

Reduced growth, leading to lower length values for each age, in the eastern Mediterranean may be the result of a decreased primary productivity in the eastern basin, previously documented by Danovaro et al. (1999) and reflected in the chlorophyll-a values obtained during the course of this study. Chlorophyll-a levels reflect the amount of primary productivity occurring within a region through representation of the amount of phytoplankton present in the water (Steele and Baird 1961, Huot *et al.* 2007). High levels of primary productivity also indicate an abundance of macrophytes present (Humerez and Umeda 2014). This is relevant as it is known that both *S. luridus* and *S. rivulatus* predominantly feed off macrophyte species (Bariche 2006, Sala *et al.* 2011). Without sufficient food resources, the individual fishes' energy reserves will be depleted and energy will be allocated to essential survival functions, reducing growth (Zahrani *et al.* 2013). An abundance of food, as may be present within the more western sites of the Mediterranean Sea, is also associated with increased levels of growth, as it has been documented that food deficit restricts growth, and, abundance allows for greater growth (Anderson 1988).

Interestingly, there was a significant effect of species on otolith growth. Thus, it can be concluded that growth of *S. rivulatus* overall is greater within the Mediterranean Sea than growth of *S. luridus*. For *S. rivulatus*, growth is expected to be greater in the eastern Mediterranean as it is known that the optimal temperature for growth of the *S. rivulatus* species is 27.0 °C (Saoud *et al.* 2008). Although differences in growth between sites overall were not significant, there was a trend of decreasing TL when looking at the regions of the central and eastern Mediterranean Sea. Central sites (Diros and Trachila) showed lower lengths for each age when compared to the eastern sites (Limmasol, Gokova Bay and Kallithea). SST and salinity differ when comparing between regions, with

SST slightly decreasing within the central Mediterranean and salinity levels decreasing considerably. Existing literature documents that *S. rivulatus* individuals can survive salinities ranging between 10 ppt and 50 ppt, and that physiological effects were only noted at 35 ppt. Subsequently, growth was only significantly impacted at very low concentrations of 10 ppt (Saoud *et al.* 2007). This means that although temperature might restrict their growth or distribution, the salinity gradient with longitude in the Mediterranean Sea should not. Therefore, the reduced growth of *S. rivulatus* in the central Mediterranean is likely the result of the decreased temperatures leading to a reduced aerobic scope, especially as the western sites have SSTs substantially lower than the optimum temperature which allows for best growth within this species (27 °C) (Saoud *et al.* 2008).

The lack of *S. rivulatus* at the most western site (Linosa) from which samples were collected, concurs with previous studies that the distribution of *S. rivulatus* is reduced compared to that of *S. luridus*, as summarised by (Azzurro *et al.* 2006). This reduced distribution of *S. rivulatus* in comparison to *S. luridus* comparable in maps made by Azzurro et al. (2016) and Galil (2008), may be explained by the temperature changes found across the Mediterranean Sea. Although the sites from which *S. rivulatus* was collected do not impact growth, the reduced distribution suggests a lesser capability of survival compared to *S. luridus* within the Mediterranean Sea. *S. luridus* is found much further west than *S. rivulatus* and existing literature could explain why. At temperatures of 14 °C it was documented that *S. rivulatus* individuals stopped feeding and multiple individuals in the study died (Saoud *et al.* 2008). Although the mean temperatures don't reach 14 °C, the reducing temperature trend indicates the conditions may not be appropriate for *S. rivulatus* survival, as although mean SSTs are still relatively high it is documented that in winter SSTs in the western Mediterranean Sea drop to as low as 15 °C (CEAM *et al.* 2018).

To further improve this study and allow further understanding of growth in the context of invasion it would be beneficial to introduce populations from the

ancestral site of the Red Sea. This would allow for analysis to identify if the change in environment (decreased salinity and temperature moving into the Mediterranean Sea from the Red Sea) impacts the growth rate. It would be interesting to compare growth rates in the ancestral site with the novel sites as it appears from this study that the gradients in abiotic factors (temperature and salinity) do not have a significant impact on growth. This lack of a significant impact on growth indicates that growth may not be a good indicator of invasion capability.

It was expected that the environmental gradients would result in a trade-off within Siganus species throughout the Mediterranean, leading to reduced growth in cooler, less saline areas to allow continued survival (Saoud *et al.* 2007). One possible reason that growth is not compromised within the invasive populations is that for many fish species, size is proportional to reproductive maturity (Udupe 1986). Once reproductive maturity has been reached, the growth rate of fish tend to decrease (Heino and Kaitala 1999, Folkvord *et al.* 2014). Within this study only adults were collected, therefore analysis of the growth of juveniles or new recruits within the Mediterranean was not possible. It would be interesting to investigate if fish reach reproductive maturity at different ages or lengths within the Red Sea compared to the Mediterranean as age or length at which reproductive maturity is reached can vary due to ecological factors (Heino and Kaitala 1999). This is demonstrated by the difference in size and age of reproductive maturity in bluefin tuna (*Thunnus thynnus*) between populations in the eastern and western Atlantic, where in the western individuals matured at a younger age and smaller size (Corriero *et al.* 2005).

Chapter 4: Conclusion

Understanding factors that allow for or constrain successful of invasion is important for future predictions and monitoring of population success, especially in context of the Mediterranean sea where over the past 140 years hundreds of species have invaded from the Red Sea and settled throughout the Mediterranean basins (Golani 2010). *Siganus luridus* and *Siganus rivulatus*, two Lessepsian rabbitfish species are among the most successful invaders established in the Mediterranean Sea to date. This project aimed to quantify the effectiveness of two factors for predicting invasion success; genetic diversity and growth.

Two genetically distinct rabbitfish species, *S. luridus* and *S. rivulatus* were identified within the Mediterranean Sea. The maximum likelihood trees and haplotype networks did not demonstrate evidence of geographic segregation of genetic types. Instead, the haplotype networks indicated high similarity between populations throughout the Mediterranean Sea due to a large number of shared haplotypes and only a small decrease in haplotype diversity, disagreeing with the hypothesis of a genetic bottleneck. Investigating the proportion of shared and unique haplotypes demonstrated that movement of invasion is from east to west with the greatest number of shared haplotypes present in the westernmost site of Linosa. With increasing distance from the Suez Canal no notable decrease in haplotype diversity was found. Haplotype diversity was high in both species but lower than previous estimates from the Red Sea indicating a slight drop in haplotype diversity with invasion (Azzurro *et al.* 2006), but this is not as significant as for other species, such as *Fistularia commersonii* demonstrating that invasion is not associated with specific genetic population characteristics. Nucleotide diversity levels (π), pairwise distances and F-statistic values revealed close genetic relationships between all populations of both species but higher levels of moderate to high differentiation were identified between populations of *S. luridus*. Tajima's D, Fu's F and mismatch distribution tests were conducted for both species. The results of the neutrality tests for *S. luridus* did not demonstrate significant deviations from the neutral models in any populations

for Tajima's D, but did indicate a demographic change (perhaps genetic bottleneck or population expansion) in populations from Turkey, the Peloponnese and the Pelagie Islands according to Fu's F, a more powerful model for detecting demographic change. For *S. rivulatus* only the population from Trachila was found to demonstrate significant values for both Tajima's D and Fu's F indicating a recent demographic change in this site. The haplotype networks indicate that if a demographic change occurred it was likely population expansion, as interpreted from the presence of star-like patterns in the haplotype networks. The slightly decreased haplotype diversity in the slightly less successful *S. rivulatus* species in accordance with high haplotype diversity levels found in other successful invasive species (Golani and Ritte 1999, Bariche and Bernardi 2009), with the exception of *F. commersonii* (Azzurro *et al.* 2013), indicates that haplotype diversity, and changes in haplotype diversity between the ancestral and novel populations, rather than genetic diversity may be an effective predictor for the success of invasive species.

Through investigation of growth, and changes in growth associated with the increased distance from the Suez Canal, the cumulative increment widths and total lengths of samples were utilised to confirm the positive relationship between otolith and somatic growth. Somatic growth is efficiently represented by otolith growth in the species studied. Age length relationships were used to investigate overall growth and different sites with increasing distance from the Suez Canal. In *S. rivulatus* sites within the eastern Mediterranean Sea demonstrated higher levels of growth than sites in the central Mediterranean Sea, this pattern did not exist for populations of *S. luridus,* where sites in the western Mediterranean held the largest individuals for their ages. The linear model revealed the effect of annulus (year of growth) was significant on the amount of growth that occurred within the otolith (and thus the body size of the fish), with growth in the first year being significantly greater than subsequent years. The model also demonstrated that site did not have a significant effect on otolith growth indicating that the environmental factors associated with increasing distance from the Suez Canal did not have a significant impact on growth between sites. Species did have a significant effect on growth, confirming greater

growth in *S. rivulatus* than *S. luridus.* Interestingly, although site alone did not have an impact on otolith growth, the interaction between annulus number at site did; for example, the first increment for *S. luridus* was significantly greater in Diros than in Kallithea. The interaction between annulus and species was also significant; in the first year of growth *S. luridus* demonstrates greater growth than *S. rivulatus*. Unfortunately, the lack of a significant reduction in growth between sites indicates that growth is not a good predictor of invasion success.

References

Afeworki, Y., Videler, J.J., and Bruggemann, J.H., 2013. Seasonally changing habitat use patterns among roving herbivorous fishes in the southern Red Sea: the role of temperature and algal community structure. *Coral Reefs*, 32 (2), 475–485.

Almeida, M., Frutos, I., Tecchio, S., Lampadariou, N., Company, J.B., Ramirez-Llodra, E., and Cunha, M.R., 2017. Biodiversity patterns of crustacean suprabenthic assemblages along an oligotrophic gradient in the bathyal Mediterranean Sea. *Deep-Sea Research Part I: Oceanographic Research Papers*, 121, 224–236.

Anderson, J.T., 1988. A Review of Size Dependant Survival During Pre-recruit Stages of Fishes in Relation to Recruitment. *Journal of Northwest Atlantic Fishery Science*, 8, 55–66.

Árnason, T., Björnsson, B., Steinarsson, A., and Oddgeirsson, M., 2009. Effects of temperature and body weight on growth rate and feed conversion ratio in turbot (*Scophthalmus maximus*). *Aquaculture*, 295 (3–4), 218–225.

Árnason, T., Magnadóttir, B., Björnsson, B., Steinarsson, A., and Björnsson, B.T., 2013. Effects of salinity and temperature on growth, plasma ions, cortisol and immune parameters of juvenile Atlantic cod (*Gadus morhua*). *Aquaculture*, 380–383, 70–79.

Arndt, E. and Schembri, P.J., 2015. Common traits associated with establishment and spread of Lessepsian fishes in the Mediterranean Sea. *Marine Biology*, 162 (10), 2141–2153.

Ashton, G. V., Stevens, M.I., Hart, M.C., Green, D.H., Burrows, M.T., Cook, E.J., and Willis, K.J., 2008. Mitochondrial DNA reveals multiple Northern Hemisphere introductions of *Caprella mutica* (Crustacea, Amphipoda). *Molecular Ecology*, 17 (5), 1293–1303.

Ashton, G. V., Willis, K.J., Cook, E.J., and Burrows, M., 2007. Distribution of the introduced amphipod, *Caprella mutica* Schurin, 1935 (Amphipoda:

Caprellida: Caprellidae) on the west coast of Scotland and a review of its global distribution. *In*: *Hydrobiologia*. Springer Netherlands, 31–41.

Azzurro, E. and Andaloro, F., 2004. A new settled population of the lessepsian migrant *Siganus luridus* (Pisces: Siganidae) in Linosa Island—Sicily Strait. *Journal of the Marine Biological Association of the UK*, 84 (4), 819–821.

Azzurro, E., Franzitta, G., Milazzo, M., Bariche, M., and Fanelli, E., 2016. Abundance patterns at the invasion front: The case of *Siganus luridus* in Linosa (Strait of Sicily, Central Mediterranean Sea). *Marine and Freshwater Research*, 68 (4), 697–702.

Azzurro, E., Golani, D., Bucciarelli, G., and Bernardi, G., 2006. Genetics of the early stages of invasion of the Lessepsian rabbitfish *Siganus luridus*. *Journal of Experimental Marine Biology and Ecology*, 333 (2), 190–201.

Azzurro, E., Soto, S., Garofalo, G., and Maynou, F., 2013. *Fistularia commersonii* in the Mediterranean Sea: Invasion history and distribution modeling based on presence-only records. *Biological Invasions*, 15 (5), 977–990.

Bandelt, H.J., Forster, P., and Röhl, A., 1999. Median-joining networks for inferring intraspecific phylogenies. *Molecular Biology and Evolution*, 16 (1), 37–48.

Barber, M.C. and Jenkins, G.P., 2001. Differential effects of food and temperature lead to decoupling of short-term otolith and somatic growth rates in juvenile King George whiting. *Journal of Fish Biology*, 58 (5), 1320–1330.

Bardamaskos, G., Tsiamis, K., Panayotidis, P., and Megalofonou, P., 2009. New records and range expansion of alien fish and macroalgae in Greek waters (south-east Ionian Sea). *Marine Biodiversity Records*, 2 (e124), 1–9.

Bariche, M., 2005. Age and growth of Lessepsian rabbitfish from the eastern Mediterranean. *Journal of Applied Ichthyology*, 21 (2), 141–145.

Bariche, M., 2006. Diet of the Lessepsian fishes, *Siganus rivulatus* and *S. luridus* (Siganidae) in the eastern Mediterranean: A bibliographic analysis. *Cybium*, 30 (1), 41–49.

Bariche, M. and Bernardi, G., 2009. Lack of a genetic bottleneck in a recent Lessepsian bioinvader, the blue-barred parrotfish, *Scarus ghobban*. *Molecular Phylogenetics and Evolution*, 53 (2), 592–595.

Bariche, M., Letourneur, Y., and Harmelin-Vivien, M., 2004. Temporal Fluctuations and Settlement Patterns of Native and Lessepsian Herbivorous Fishes on the Lebanese Coast (Eastern Mediterranean). *Environmental Biology of Fishes*, 70 (1), 81–90.

Bariche, M., Sadek, R., and Azzurro, E., 2009. Fecundity and condition of successful invaders: *Siganus rivulatus* and *S. luridus* (Actinopterygii: Perciformes: Siganidae) in the eastern Mediterranean Sea. *Acta Ichthyologica et piscatoria*, 39 (1), 11–18.

Baudron, A.R., Needle, C.L., Rijnsdorp, A.D., and Tara Marshall, C., 2014. Warming temperatures and smaller body sizes: Synchronous changes in growth of North Sea fishes. *Global Change Biology*, 20 (4), 1023–1031.

Ben-Tuvia, A., 1964. Two siganid fishes of Red Sea origin in the Eastern Mediterranean. *Bulletin. Sea Fisheries Research Station (Haifa)*, 37, 3–9.

Bernardi, G., Golani, D., and Azzurro, E., 2010. *The genetics of Lessepsian bioinvasions*. Sofia-Moscow: Pensoft Publishers.

Bianchi, C.N. and Morri, C., 2000. Marine biodiversity of the Mediterranean Sea: Situation, problems and prospects for future research. *Marine Pollution Bulletin*, 40 (5), 367–376.

Bingpeng, X., Heshan, L., Zhilan, Z., Chunguang, W., Yanguo, W., and Jianjun, W., 2018. DNA barcoding for identification of fish species in the Taiwan Strait. *PLoS ONE*, 13 (6), e0198109.

Bivand, R., Keitt, T., and Rowlingson, B., 2018. Rgdal: Bindings for the 'Geospatial' Data Abstraction Library.

Bock, W.J., 1980. The definition and recognition of biological adaptation.

Integrative and Comparative Biology, 20 (1), 217–227.

Boeuf, G. and Le Bail, P.Y., 1999. Does light have an influence on fish growth? *Aquaculture*, 177 (1–4), 129–152.

Bœuf, G. and Payan, P., 2001. How should salinity influence fish growth? *In*: *Comparative Biochemistry and Physiology - C Toxicology and Pharmacology*. Elsevier, 411–423.

Bonfield, J.K., Beal, K.F., Betts, M.J., and Staden, R., 2002. Trev: A DNA trace editor and viewer. *Bioinformatics*, 18 (1), 194–195.

Bonhomme, F., Baranes, A., Golani, D., and Harmelin-Vivien, M., 2003. Lack of mitochondrial differentiation between Red Sea and Mediterranean populations of the Lessepsian rabbitfish, *Siganus rivulatus* (Perciformes : Siganidae). *Scientia Marina*, 67 (2), 215–217.

Boris, D., Piro, S., Charbonnel, E., Francour, P., and Letourneur, Y., 2009. Lessepsian rabbitfish *Siganus luridus* reached the French Mediterranean coasts. *Cybium*, 33, 163–164.

Borsa, P., Lemer, S., and Aurelle, D., 2007. Patterns of lineage diversification in rabbitfishes. *Molecular Phylogenetics and Evolution*, 44 (1), 427–435.

Brett, J.R., 1979. Environmental factors and growth. *In*: W. Hoar, D. Randall, and J. Brett, eds. *Fish Physiology: Bioenergetics and Growth, Vol. 8*. New York, USA: Academic Press, 599–675.

Brokovich, E., Baranes, A., and Goren, M., 2006. Habitat structure determines coral reef fish assemblages at the northern tip of the Red Sea. *Ecological Indicators*, 6 (3), 494–507.

Brown, W.M., George, M., and Wilson, A.C., 1979. Rapid evolution of animal mitochondrial DNA. *Proceedings of the National Academy of Sciences of the United States of America*, 76 (4), 1967–1971.

Careau, V., Thomas, D., Humphries, M.M., and Réale, D., 2008. Energy metabolism and animal personality. *Oikos*, 117 (5), 641–653.

Carpentieri, P., Lelli, S., Colloca, F., Mohanna, C., Bartolino, V., Moubayed,

S., and Ardizzone, G.D., 2009. Incidence of lessepsian migrants on landings of the artisanal fishery of south Lebanon. *Marine Biodiversity Records*, 2, e71.

CEAM, NCEI, and NOAA, 2018. Mediterranean Sea Surface Temperature Climatology: Monthly Averaged SST Climatology [online]. Available from: http://www.ceam.es/ceamet/SST/SST-climatology.html [Accessed 17 Sep 2018].

Çeviker, D. and Albayrak, S., 2006. Three alien molluscs from Iskenderun Bay (SE Turkey). *Aquatic Invasions*, 1 (2), 76–79.

Chaidez, V., Dreano, D., Agusti, S., Duarte, C.M., and Hoteit, I., 2017. Decadal trends in Red Sea maximum surface temperature. *Scientific Reports*, 7 (1), 8144.

Cheminée, A., Sala, E., Pastor, J., Bodilis, P., Thiriet, P., Mangialajo, L., Cottalorda, J.-M., and Francour, P., 2013. Nursery value of Cystoseira forests for Mediterranean rocky reef fishes. *Journal of Experimental Marine Biology and Ecology*, 442, 70–79.

Cho, S.-H., Myoung, J.-G., Kim, J.-M., and Hwan Lee, J., 2001. Fish Fauna Associated with Drifting Seaweed in the Coastal Area of Tongyeong, Korea. *Transactions of the American Fisheries Society*, 130 (6), 1190–1202.

Clark, T.D., Sandblom, E., and Jutfelt, F., 2013. Aerobic scope measurements of fishes in an era of climate change: respirometry, relevance and recommendations. *Journal of Experimental Biology*, 216 (15), 2771–2782.

Clarke, A. and Johnston, N.M., 1999. Scaling of metabolic rate with body mass and temperature in teleost fish. *Journal of Animal Ecology*, 68 (5), 893–905.

Coll, M., Piroddi, C., Steenbeek, J., Kaschner, K., Lasram, F.B.R., Aguzzi, J., Ballesteros, E., Bianchi, C.N., Corbera, J., Dailianis, T., Danovaro, R., Estrada, M., Froglia, C., Galil, B.S., Gasol, J.M., Gertwage, R., Gil, J., Guilhaumon, F., Kesner-Reyes, K., Kitsos, M.S., Koukouras, A.,

Lampadariou, N., Laxamana, E., de la Cuadra, C.M.L.F., Lotze, H.K., Martin, D., Mouillot, D., Oro, D., Raicevich, S., Rius-Barile, J., Saiz-Salinas, J.I., Vicente, C.S., Somot, S., Templado, J., Turon, X., Vafidis, D., Villanueva, R., and Voultsiadou, E., 2010. The biodiversity of the Mediterranean Sea: Estimates, patterns, and threats. *PLoS ONE*, 5 (8), e11842

Collins, L.A. and Nelson, S.G., 1993. Effects of temperature on oxygen consumption, growth, and development of embryos and yolk-sac larvae of *Siganus randalli* (Pisces: Siganidae). *Marine Biology*, 117 (2), 195–204.

Coro, G., Vilas, L.G., Magliozzi, C., Ellenbroek, A., Scarponi, P., and Pagano, P., 2018. Forecasting the ongoing invasion of *Lagocephalus sceleratus* in the Mediterranean Sea. *Ecological Modelling*, 371, 37–49.

Corriero, A., Karakulak, S., Santamaria, N., Deflorio, M., Spedicato, D., Addis, P., Desantis, S., Cirillo, F., Fenech-Farrugia, A., Vassallo-Agius, R., de la Serna, J.M., Oray, Y., Cau, A., Megalofonou, P., and De Metrio, G., 2005. Size and age at sexual maturity of female bluefin tuna (*Thunnus thynnus L*. 1758) from the Mediterranean Sea. *Journal of Applied Ichthyology*, 21 (6), 483–486.

Corsini-Foka, M., Mastis, S., Kondylatos, G., and Batjakas, I.E., 2017. Alien and native fish in gill nets at Rhodes, eastern Mediterranean (2014–2015). *Journal of the Marine Biological Association of the United Kingdom*, 97 (3), 635–642.

Danovaro, R., Dinet, A., Duineveld, G., and Tselepides, A., 1999. Benthic response to particulate fluxes in different trophic environments: A comparison between the Gulf of Lions-Catalan Sea (western-Mediterranean) and the Cretan Sea (eastern-Mediterranean). *In*: *Progress in Oceanography*. Pergamon, 287–312.

Davies, N., Villablanca, F.X., and Roderick, G.K., 1999. Determining the source of individuals: Multilocus genotyping in nonequilibrium population genetics. *Trends in Ecology and Evolution*.

Deagle, B.E., Jarman, S.N., Coissac, E., Pompanon, F., and Taberlet, P., 2014.

DNA metabarcoding and the cytochrome c oxidase subunit I marker: Not a perfect match. *Biology Letters*, 10 (9), 20140562.

Dulĉić, J. and Pallaoro, A., 2004. First record of the marbled spinefoot *Siganus rivulatus* (Pisces: Siganidae) in the Adriatic Sea. *Journal of the Marine Biological Association of the UK*, 84 (5), 1087–1088.

Dupont, L. and Viard, F., 2003. Isolation and characterization of highly polymorphic microsatellite markers from the marine invasive species *Crepidula fornicata* (Gastropoda: Calyptraeidae). *Molecular Ecology Notes*, 3 (4), 498–500.

Dutta, H., 1994. Growth in Fishes. *Gerontology*, 40 (2), 97–112.

Eladawy, A., Nadaoka, K., Negm, A., Abdel-Fattah, S., Hanafy, M., and Shaltout, M., 2017. Characterization of the northern Red Sea's oceanic features with remote sensing data and outputs from a global circulation model. *Oceanologia*, 59 (3), 213–237.

Emig, C. and Geistdoerfer, P., 2004. The Mediterranean deep-sea fauna: historical evolution, bathymetric variations and geografical changes. *Carnets de Géologie / Notebooks on Geology*, 1, 1–10.

European Environment Agency, 2014. *Indicator Assessment: Chlorophyll in transitional, coastal and marine waters*.

Excoffier, L. and Lischer, H.E.L., 2010. Arlequin suite ver 3.5: A new series of programs to perform population genetics analyses under Linux and Windows. *Molecular Ecology Resources*, 10 (3), 564–567.

Farag Abziew, E.A. and Ali, S.M., 2016. Historical records of the Lessepsian migrants, the Dusky Spinefoot Fish *Siganus luridus* (Ruppell, 1829) and the Marbled Spinefoot *S. rivulatus* (Rorsskal, 1775), in the eastern coast of Libya Mediterranean sea. *International Journal of Fisheries and Aquaculture Research*, 2 (3), 13–33.

Ferreri, M., Qu, W., and Bo, H., 2011. Phylogenetic networks: A tool to display character conflict and demographic history. *African Journal of Biotechnology*, 10 (60), 12799–12803.

Fey, D.P., 2006. The effect of temperature and somatic growth on otolith growth: The discrepancy between two clupeid species from a similar environment. *Journal of Fish Biology*, 69 (3), 794–806.

Folkvord, A., Jørgensen, C., Korsbrekke, K., Nash, R.D.M., Nilsen, T., Skjæraasen, J.E., and Marshall, C.T., 2014. Trade-offs between growth and reproduction in wild Atlantic cod. *Canadian Journal of Fisheries and Aquatic Sciences*, 71 (7), 1106–1112.

Fricke, R., Golani, D., and Appelbaum-Golani, B., 2015. First record of the Indian anchovy *Stolephorus indicus* (van Hasselt, 1823) (Clupeiformes: Engraulidae) in the Mediterranean Sea. *BioInvasions Records*, 4 (4), 293–297.

Froese, R. and Pauly, D., 2018. FishBase (Version 06/2016) [online]. Available from: http://www.fishbase.org/. [Accessed 23 Sep 2018].

Fu, Y.X., 1997. Statistical tests of neutrality of mutations against population growth, hitchhiking and background selection. *Genetics*, 147 (2), 915–925.

Galil, B., 2008. *Siganus rivulatus*: Map (European distribution) [online]. Available from: http://www.europe-aliens.org/pdf/Siganus_rivulatus.pdf [Accessed 17 Sep 2018].

Galil, B., Marchini, A., Occhipinti-Ambrogi, A., and Ojaveer, H., 2017. The enlargement of the Suez Canal – Erythraean introductions and management challenges. *Management of Biological Invasions*, 8 (2), 141–152.

Galtier, N., Nabholz, B., Glémin, S., and HURST, G.D.D., 2009. Mitochondrial DNA as a marker of molecular diversity: a reappraisal. *Molecular Ecology*, 18 (22), 4541–4550.

Golani, D., 2002. Lessepsian fish migration-characterization and impact on the eastern Mediterranean. *In*: B. Öztürk, N. Başusta, and Türk Deniz Araştırmaları Vakfı, eds. *Workshop on Lessepsian Migration proceedings*. Istanbul : Turkish Marine Research Foundation, 1–9.

Golani, D., 2010. Colonization of the Mediterranean by Red Sea fishes via the Suez Canal - Lessepsian migration. *In*: *Fish invasions of the Mediterranean Sea: Change and Renewal*. Pensoft, Sofia, 145–188.

Golani, D., Azzurro, E., Corsini-Foka, M., Falautano, M., Andaloro, F., and Bernardi, G., 2007. Genetic bottlenecks and successful biological invasions: The case of a recent Lessepsian migrant. *Biology Letters*, 3 (5), 541–545.

Golani, D. and Ritte, U., 1999. Genetic relationship in goatfishes (Mullidae: Perciformes) of the Red Sea and the Mediterranean, with remarks on Suez Canal migrants. *Scientia Marina*, 63 (2), 129–135.

Goodacre, S.L. and Wade, C.M., 2001. Molecular evolutionary relationships between partulid land snails of the Pacific. *Proceedings. Biological sciences*, 268 (1462), 1–7.

Goren, M. and Galil, B.S., 2005. A review of changes in the fish assemblages of Levantine inland and marine ecosystems following the introduction of non-native fishes. *In*: *Journal of Applied Ichthyology*, 21 (4), 364–370.

Grant, W.S., 2015. Problems and cautions with sequence mismatch analysis and Bayesian skyline plots to infer historical demography. *Journal of Heredity*, 106 (4), 333–346.

Grant, W.S. and Bowen, B.W., 1998. Shallow population histories in deep evolutionary lineages of marine fishes: Insights from sardines and anchovies and lessons for conservation. *Journal of Heredity*, 89 (5), 415–426.

Grau, E.., Richman, N.I., and Borski, R.., 1994. Osmoreception and a simple endocrine reflex of the prolactin cell of the tilapia *Oreochromis mossambicus*. *In*: K.. Davey, R.. Peter, and S.. Tobe, eds. *Perspectives in Comparative Endocrinology*. Ottawa: National Research Council, 251–256.

Greenwood, P.H., Rosen, D.E., Weitzman, S.H., and Myers, G.S., 1966. Phyletic Studies of Teleostean Fishes , With a Provisional Classification of Living Forms. *Bulletin of th American Museum of Natural History*,

133, 339–456.

Guindon, S., Dufayard, J.-F., Lefort, V., Anisimova, M., Hordijk, W., and Gascuel, O., 2010. New Algorithms and Methods to Estimate Maximum-Likelihood Phylogenies: Assessing the Performance of PhyML 3.0. *Systematic Biology*, 59 (3), 307–321.

Hahn, M.W., Rausher, M.D., and Cunningham, C.W., 2002. Distinguishing between selection and population expansion in an experimental lineage of bacteriophage T7. *Genetics*, 161 (1), 11–20.

Handeland, S.O., Imsland, A.K., and Stefansson, S.O., 2008. The effect of temperature and fish size on growth, feed intake, food conversion efficiency and stomach evacuation rate of Atlantic salmon post-smolts. *Aquaculture*, 283 (1–4), 36–42.

Hassan, M., Harmelin-Vivien, M., and Bonhomme, F., 2003. Lessepsian invasion without bottleneck: Example of two rabbitfish species (*Siganus rivulatus* and *Siganus luridus*). *Journal of Experimental Marine Biology and Ecology*, 291 (2), 219–232.

Hedrick, P.W., 2011. *Genetics of populations*. Sudbury, Massachusetts: Jones and Bartlett Publishers.

Heino, M. and Kaitala, V., 1999. Evolution of resource allocation between growth and reproduction in animals with indeterminate growth. *Journal of Evolutionary Biology*, 12 (3), 423–429.

Hernández, J.M., Gasca-Leyva, E., León, C.J., and Vergara, J.., 2003. A growth model for gilthead seabream (*Sparus aurata*). *Ecological Modelling*, 165 (2–3), 265–283.

Humerez, E. and Umeda, M., 2014. Macrophyte biomass, nutrients and primary productivity of a tropical glacial river in the Andes. *Journal of Japan Society of Civil Engineers, Ser. G (Environmental Research)*, 70 (5), 227–233.

Huot, Y., Babin, M., Bruyant, F., Grob, C., Twardowski, M.S., and Claustre, H., 2007. Does chlorophyll *a* provide the best index of phytoplankton

biomass for primary productivity studies? *Biogeosciences Discussions*, 4 (2), 707–745.

Ivanova, N. V., Zemlak, T.S., Hanner, R.H., and Hebert, P.D.N., 2007. Universal primer cocktails for fish DNA barcoding. *Molecular Ecology Notes*, 7 (4), 544–548.

Jackson, A.M., Tenggardjaja, K., Perez, G., Azzurro, E., Golani, D., and Bernardi, G., 2015. Phylogeography of the bluespotted cornetfish, *Fistularia commersonii*: A predictor of bioinvasion success? *Marine Ecology*, 36 (4), 887–896.

Jobling, M., 1996. Temperature and growth: modulation of growth rate via temperature change. *In*: C. Wood and D. McDonlad, eds. *Global warming: implications for freshwater and marine fish*. Cambridge, UK: Cambridge University Press, 225–253.

Kahle, D. and Wickham, H., 2013. Ggmap: Spatial Visualization with ggplot2. *The R Journal*, 5 (1), 144–161.

Kasapidis, P., Peristeraki, P., Tserpes, G., and Magoulas, A., 2007. A new record of the Lessepsian invasive fish *Etrumeus teres* (Osteichthyes: Clupeidae) in the Mediterranean Sea (Aegean, Greece). *Aquatic Invasions*, 2 (2), 152–154.

Kiparissis, S., Peristeraki, P., Tampakakis, K., Kosoglou, I., Doudoumis, V., and Batargias, C., 2018. Range expansion of a restricted lessepsian: westbound expansion breakthrough of *Lagocephalus spadiceus* (Richardson, 1844) (Actinopterygii: Tetraodontidae). *BioInvasions Records*, 7 (2), 197–203.

Kuriiwa, K., Hanzawa, N., Yoshino, T., Kimura, S., and Nishida, M., 2007. Phylogenetic relationships and natural hybridization in rabbitfishes (Teleostei: Siganidae) inferred from mitochondrial and nuclear DNA analyses. *Molecular Phylogenetics and Evolution*, 45 (1), 69–80.

Lasram, F.B.R. and Mouillot, D., 2009. Increasing southern invasion enhances congruence between endemic and exotic Mediterranean fish fauna. *Biological Invasions*, 11 (3), 697–711.

Laurent, P. and Dunel-Erb, S., 1984. The pseudobranch: morphology and function. *In*: W.. Hoar, ed. *Fish Physiology, Vol. 10B*. New York, USA: Academic Press, 285–320.

Lee, C.E., 2002. Evolutionary genetics of invasive species. *Trends in Ecology & Evolution*, 17 (8), 386–391.

Lee, W.-J., Conroy, J., Howell, W.H., and Kocher, T.D., 1995. Structure and evolution of teleost mitochondrial control regions. *Journal of Molecular Evolution*, 41 (1), 54–66.

Leigh, J.W. and Bryant, D., 2015. POPART: Full-feature software for haplotype network construction. *Methods in Ecology and Evolution*, 6 (9), 1110–1116.

Lejeusne, C., Saunier, A., Petit, N., Béguer, M., Otani, M., Carlton, J.T., Rico, C., and Green, A.J., 2014. High genetic diversity and absence of founder effects in a worldwide aquatic invader. *Scientific Reports*, 4 (1), 5808.

Lieth, H., 1975. Modeling the Primary Productivity of the World. *In*: L. H and R.. Whittaker, eds. *Primary Productivity of the Biosphere. Ecological Studies (Analysis and Synthesis), Vol 14*. Springer, Berlin, Heidelberg, 237–263.

Mavruk, S., Bengil, F., Yeldan, H., Manasirli, M., and Avsar, D., 2017. The trend of lessepsian fish populations with an emphasis on temperature variations in Iskenderun Bay, the Northeastern Mediterranean. *Fisheries Oceanography*, 26 (5), 542–554.

Morgan, M.J. and Godin, J.-G.J., 1985. Antipredator Benefits of Schooling Behaviour in a Cyprinodontid Fish, the Banded Killifish (Fundulus diaphanus). *Zeitschrift für Tierpsychologie*, 70 (3), 236–246.

Moritz, C., Dowling, T.E., and Brown, W.M., 1987. Evolution of animal mitochondrial DNA: Relevance for population biology and systematics. *Annual Review of Ecology and Systematics*, 18, 269–292.

Murakami, M., Matsuba, C., and Fujitani, H., 2001. The maternal origins of the triploid ginbuna (*Carassius auratus langsdorfi*): Phylogenetic

relationships within the *C. auratus* taxa by partial mitochondrial D-loop sequencing. *Genes & Genetic Systems*, 76 (1), 25–32.

Muths, D., Gouws, G., Mwale, M., Tessier, E., and Bourjea, J., 2012. Genetic connectivity of the reef fish *Lutjanus kasmira* at the scale of the western Indian Ocean. *Canadian Journal of Fisheries and Aquatic Sciences*, 69 (5), 842–853.

National Centre for Academic Research Colorado, 2018. NCAR UCAR Research Data Archive [online]. Available from: https://rda.ucar.edu/ [Accessed 20 Sep 2018].

Nei, M., 1978. Estimation of average heterozygosity and genetic distance from a small number of individuals. *Genetics*, 89 (3), 583–590.

Nei, M., 1987. *Molecular evolutionary genetics*. Columbia University Press.

Neilan, R.. and Rose, K., 2014. Simulating the effects of fluctuating dissolved oxygen on growth, reproduction, and survival of fish and shrimp. *Journal of Theoretical Biology*, 343, 54–68.

Nytrø, A. V., Vikingstad, E., Foss, A., Hangstad, T.A., Reynolds, P., Eliassen, G., Elvegård, T.A., Falk-Petersen, I.-B., and Imsland, A.K., 2014. The effect of temperature and fish size on growth of juvenile lumpfish (*Cyclopterus lumpus L.*). *Aquaculture*, 434, 296–302.

Papanicolopulu, I., 2015. The Mediterranean Sea. *In*: R. Donald R, E. Alex G Oude, S. Karen N, and S. Tim, eds. *The Oxford Handbook of the Law of the Sea*. Oxford University Press, 604–625.

Por, F.D., 1971. One Hundred Years of Suez Canal - A Century of Lessepsian Migration: Retrospect and Viewpoints. *Systematic Zoology*, 20 (2), 138.

Por, F.D., 1978. *Lessepsian migration. The influx of Red Sea biota into the Mediterranean by way of the Suez Canal*. Springer Verlag publ., Berlin. Berlin: Springer Berlin Heidelberg.

Pörtner, H.O. and Knust, R., 2007. Climate change affects marine fishes through the oxygen limitation of thermal tolerance. *Science*, 315 (5808), 95–97.

Puth, L.M. and Post, D.M., 2005. Studying invasion: Have we missed the boat? *Ecology Letters*, 8 (7), 715–721.

R Core Team, 2018. R: A Language and Environment for Statistical Computing.

Radtke, R.L., Fine, M.L., and Bell, J., 1985. Somatic and otolith growth in the oyster toadfish (*Opsanus tau L.*). *Journal of Experimental Marine Biology and Ecology*, 90 (3), 259–275.

Rambaut, A., 2016. FigTree.

Ramírez-Soriano, A., Ramos-Onsins, S.E., Rozas, J., Calafell, F., and Navarro, A., 2008. Statistical power analysis of neutrality tests under demographic expansions, contractions and bottlenecks with recombination. *Genetics*, 179 (1), 555–567.

Randall, J.E., 1997. Randall's tank photos. Collection of 10,000 large-format photos (slides) of dead fishes. Unpublished.

Randall, J.E. and Kulbicki, M., 2005. Siganus woodlandi, new species of rabbitfish (Siganidae) from New Caledonia by. *Cybium*, 29 (1), 185–189.

Ratnasingham, S. and Hebert, P.D.N., 2007. BOLD: The Barcode of Life Data System: Barcoding. *Molecular Ecology Notes*, 7 (3), 355–364.

Reichert, M.J.., Dean, J.M., Feller, R.J., and Grego, J.M., 2000. Somatic growth and otolith growth in juveniles of a small subtropical flatfish, the fringed flounder, *Etropus crossotus*. *Journal of Experimental Marine Biology and Ecology*, 254 (2), 169–188.

van Rijn, I., Buba, Y., DeLong, J., Kiflawi, M., and Belmaker, J., 2017. Large but uneven reduction in fish size across species in relation to changing sea temperatures. *Global Change Biology*, 23 (9), 3667–3674.

Riley, J.., 1965. Analytical chemistry of sea water. *In*: J.. Riley and G. Skirrow, eds. *Chemical Oceanography*. London, UK: Academic Press, 295–424.

Rogers, A.R. and Harpending, H., 1992. Population growth makes waves in the distribution of pairwise genetic differences. *Molecular Biology and*

Evolution, 9 (3), 552–69.

Roman, J. and Darling, J.A., 2007. Paradox lost: genetic diversity and the success of aquatic invasions. *Trends in Ecology and Evolution*.

Rountrey, A.N., Coulson, P.G., Meeuwig, J.J., and Meekan, M., 2014. Water temperature and fish growth: Otoliths predict growth patterns of a marine fish in a changing climate. *Global Change Biology*, 20 (8), 2450–2458.

Rozas, J., Ferrer-Mata, A., Sánchez-DelBarrio, J.C., Guirao-Rico, S., Librado, P., Ramos-Onsins, S.E., and Sánchez-Gracia, A., 2017. DnaSP 6: DNA Sequence Polymorphism Analysis of Large Data Sets. *Molecular biology and evolution*, 34 (12), 3299–3302.

Sala, E., Kizilkaya, Z., Yildirim, D., and Ballesteros, E., 2011. Alien Marine Fishes Deplete Algal Biomass in the Eastern Mediterranean. *PLoS ONE*, 6 (2), e17356.

Sanna, D., Merella, P., Lai, T., Farjallah, S., Francalacci, P., Curini-Galletti, M., Pais, A., and Casu, M., 2011. Combined analysis of four mitochondrial regions allowed the detection of several matrilineal lineages of the lessepsian fish *Fistularia commersonii* in the Mediterranean Sea. *Journal of the Marine Biological Association of the United Kingdom*, 91 (6), 1289–1293.

Saoud, I.P., Kreydiyyeh, S., Chalfoun, A., and Fakih, M., 2007. Influence of salinity on survival, growth, plasma osmolality and gill Na+–K+–ATPase activity in the rabbitfish *Siganus rivulatus*. *Journal of Experimental Marine Biology and Ecology*, 348 (1–2), 183–190.

Saoud, I.P., Mohanna, C., and Ghanawi, J., 2008. Effects of temperature on survival and growth of juvenile spinefoot rabbitfish (*Siganus rivulatus*). *Aquaculture Research*, 39 (5), 491–497.

Sará, G., Romano, C., and Mazzola, A., 2008. A new lessepsian species in the western Mediterranean (*Brachidontes pharaonis* Bivalvia: Mytilidae): density, resource allocation and biomass. *Marine Biodiversity Records*, 1, e8.

Schembri, P.J., Deidun, A., and Falzon, M.A., 2012. One Siganus or two? On the occurrence of *Siganus luridus* and *Siganus rivulatus* in the Maltese Islands. *Marine Biodiversity Records*, 5, e71.

Schindelin, J., Arganda-Carreras, I., Frise, E., Kaynig, V., Longair, M., Pietzsch, T., Preibisch, S., Rueden, C., Saalfeld, S., Schmid, B., Tinevez, J.Y., White, D.J., Hartenstein, V., Eliceiri, K., Tomancak, P., and Cardona, A., 2012. Fiji: An open-source platform for biological-image analysis. *Nature Methods*, 9 (7), 676–682.

Smith, S.W., Overbeek, R., Woese, C.R., Gilbert, W., and Gillevet, P.M., 1994. The genetic data environment an expandable GUI for multiple sequence analysis. *Bioinformatics*, 10 (6), 671–675.

Sousa, L.C.C., Gontijo, C.M.F., Botelho, H.A., and Fonseca, C.G., 2012. Mitochondrial genetic variability of *Didelphis albiventris* (Didelphimorphia, Didelphidae) in Brazilian localities. *Genetics and Molecular Biology*, 35 (2), 522–529.

Steele, J.H. and Baird, I.E., 1961. Relations between primary production, chlorophyll and particulate carbon. *Limnology and Oceanography*, 6 (1), 68–78.

Steinitz, W., 1927. *Beiträge zur Kenntnis der Küstenfauna Palästinas*. Giannini, printer.

Subramanian, S., 2016. The effects of sample size on population genomic analyses - implications for the tests of neutrality. *BMC Genomics*, 17 (1), 123.

Sweetman, P.C., Haddy, J.A., and Robertson, S.G., 2018. Multi-decadal variation in cohort specific sex ratios and otolith increment growth characteristics of juvenile blue grenadier (*Macruronus novaezelandiae*). *Fisheries Research*, 201, 79–87.

Swofford, D.L., 2002. *PAUP*. Phylogenetic Analysis Using Parsimony (*and Other Methods).* Sunderland, Massachusetts: Sinauer Associates.

Tajima, F., 1989. Statistical method for testing the neutral mutation hypothesis

by DNA polymorphism. *Genetics*, 123 (3), 585–595.

Talley, L.D., Pickard, G.L., Emery, W.J., and Swift, J.H., 2011. Gravity Waves, Tides, and Coastal Oceanography. *In*: *Descriptive Physical Oceanography*. Academic Press, 1–31.

Taylor, B.M., Gourley, J., and Trianni, M.S., 2017. Age, growth, reproductive biology and spawning periodicity of the forktail rabbitfish (*Siganus argenteus*) from the Mariana Islands. *Marine and Freshwater Research*, 68 (6), 1088–1097.

Templeton, A.R., 2006. *Population Genetics and Microevolutionary Theory*. Population Genetics and Microevolutionary Theory. Hoboken, NJ, USA: John Wiley & Sons, Inc.

Tenggardjaja, K., Jackson, A., Leon, F., Azzurro, E., Golani, D., and Bernardi, G., 2013. Genetics of a Lessepsian sprinter: The bluespotted cornetfish, *Fistularia commersonii*. *Israel Journal of Ecology and Evolution*, 59 (4), 181–185.

Terranova, M.S., Lo Brutto, S., Arculeo, M., and Mitton, J.B., 2006. Population structure of *Brachidontes pharaonis* (P. Fisher, 1870) (Bivalvia, Mytilidae) in the Mediterranean Sea, and evolution of a novel mtDNA polymorphism. *Marine Biology*, 150 (1), 89–101.

Tsabaris, C., Anagnostou, M.N., Patiris, D.L., Nystuen, J.A., Eleftheriou, G., Dakladas, T., Papadopoulos, V., Prospathopoulos, A., Papadopoulos, A., and Anagnostou, E.N., 2011. A marine groundwater spring in Stoupa, Greece: Shallow water instrumentation comparing radon and ambient sound with discharge rate. *In*: *Procedia Earth and Planetary Science*. Elsevier, 3–9.

Turan, C., 2010. Status and Trend of Lessepsian Species in Marine Waters of Turkey. *FAO-EastMed Technical Document*, 4, 109–118.

Udupe, K.S., 1986. *Statistical Method of Estimating the Size At First Maturity in Fishes*. Fishbyte.

Vergés, A., Tomas, F., Cebrian, E., Ballesteros, E., Kizilkaya, Z., Dendrinos,

P., Karamanlidis, A.A., Spiegel, D., and Sala, E., 2014. Tropical rabbitfish and the deforestation of a warming temperate sea. *Journal of Ecology*, 102 (6), 1518–1527.

Viard, F., Ellien, C., and Dupont, L., 2006. Dispersal ability and invasion success of *Crepidula fornicata* in a single gulf: Insights from genetic markers and larval-dispersal model. *Helgoland Marine Research*, 60 (2), 144–152.

Vieira, M.L.C., Santini, L., Diniz, A.L., and Munhoz, C. de F., 2016. Microsatellite markers: What they mean and why they are so useful. *Genetics and Molecular Biology*, 39 (3), 312–328.

Walford, R.L. and Liu, R.K., 1965. Husbandry, life span, and growth rate of the annual fish, *Cynolebias adloffi* E. Ahl. *Experimental Gerontology*, 1 (2), 161–168.

Ward, R.D., Zemlak, T.S., Innes, B.H., Last, P.R., and Hebert, P.D.N., 2005. DNA barcoding Australia's fish species. *Philosophical Transactions of the Royal Society B: Biological Sciences*, 360 (1462), 1847–1857.

Wickham, H., 2016. Ggplot2: Elegant Graphics for Data Analysis.

Wilson, A.C., Cann, R.L., Carr, S.M., George, M., Gyllensten, U.B., Helm-Bychowski, K.M., Higuchi, R.G., Palumbi, S.R., Prager, E.M., Sage, R.D., and Stoneking, M., 1985. Mitochondrial DNA and two perspectives on evolutionary genetics. *Biological Journal of the Linnean Society*, 26 (4), 375–400.

Woodland, D.J., 1990. Revision of the fish family Siganidae with descriptions of two new species and comments on distribution and biology. *In*: *Indo-Pacific Fishes*. Honolulu, Hawaii : Bernice Pauahi Bishop Museum, 1–136.

Wuertz, M., 2010. *Mediterranean pelagic habitat: oceanographic and biological processes, an overview*. Mediterranean pelagic habitat: oceanographic and biological processes, an overview. Gland, Switzerland and Malaga, Spain: IUCN.

Xin, Z. and Chen, J., 2012. A high throughput DNA extraction method with high yield and quality. *Plant Methods*, 8, 26.

Zahrani, A.W. Al, Mohamed, A.H., Serrano Jr, A.E., and Traifalgar, M., 2013. Effects of feeding rate and frequency on growth and feed utilization efficiency in the camouflage grouper (*Epinephelus polyphekadion*) fingerlings fed a commercial diet. *European Journal of Experimental Biology*, 3 (1), 596–601.

Zhang, D.X. and Hewitt, G.M., 2003. Nuclear DNA analyses in genetic studies of populations: Practice, problems and prospects. *Molecular Ecology*, 12 (3), 563–584.

Appendices

Appendix 1: R Code used to Generate Mediterranean Sites Map

```
###Load packages
library("ggmap")
library("gdata")
library("gridExtra")
library("rgdal")
library("maptools")
library("RColorBrewer")
library("rgeos")
library("raster")
library("plyr")
library('readxl')
library('ggspatial')

### Set working directory.
setwd("/Users/steph/OneDrive/Documents/Masters/R/Maps/")
### Make Mediterranean map
### Load, crop & fortify world shapefile
Med_map <-
fortify(crop(readOGR("/Users/steph/OneDrive/Documents/Masters/R/Maps/world_countries.geojson", verbose = F), extent(10, 38, 30, 40)))
### Set up my data
StephSiteMapData<-read_xlsx("MapDataMediterranean.xlsx")
### Set up map
library(ggsn)
Medmap<-ggplot()+geom_polygon(data=Med_map,
                              aes(x=long,y=lat,group=group),
```

```
                color='gray',

                fill='lightgray')+coord_map()+theme(legend.position =
'none') +  ggsn::scalebar(Med_map, dist = 200, st.size=3, height=0.01, dd2km
= TRUE, model = 'WGS84')

###Check map outline

Medmap


### Put my data onto the map

Med_map1<-
Medmap+geom_point(data=StephSiteMapData,aes(x=Lon,y=Lat),size=2,shap
e=22,fill='Red')

Med_map1

Med_map1<-Med_map1+annotate("text",x=13, y=35.5,label='Linosa', size=4)

Med_map1<-Med_map1+annotate("text",x=22.1, y=36,label='The
Peloponnese', size=4)

Med_map1<-Med_map1+annotate("text",x=28, y=36,label='Rhodes', size=4)

Med_map1<-Med_map1+annotate("text",x=33.2, y=34.3,label='Cyprus',
size=4)

Med_map1<-Med_map1+annotate("text",x=27.7, y=37.5,label='Turkey',
size=4)

#Save map from this file

Med_map1
```

Appendix 2: Assigning Traits (sites) to Haplotypes

The following text was added to the NEXUS haplotype data file generated in DnaSP6 (Rozas *et al.* 2017) and was then opened in POPART

BEGIN TRAITS;

Dimensions NTRAITS=7;

Format labels=yes missing=? separator=Comma;

TraitLabels Limmasol Kallithea Gokova_Bay Diros Agios_Dimitrios Stoupa Linosa;

Matrix

Hap_1 1,0,0,0,0,0,0

Hap_2 1,1,2,1,0,0,1

Hap_3 4,11,6,10,7,7,6

Hap_4 1,1,2,0,3,0,3

Hap_5 0,0,2,1,1,0,3

Hap_6 0,2,6,2,1,1,2

Hap_7 0,0,0,0,0,0,1

Hap_8 0,2,2,3,2,2,1

Hap_9 0,0,0,0,0,1,0

Hap_10 0,1,0,0,1,0,0

Hap_11 0,2,0,2,0,0,0;

END;

Appendix 3: Age and Length data

ID	Species	Site	Age	TL (cm)
SILUR001	*S. luridus*	Limmasol	4	19.80
SILUR002	*S. luridus*	Limmasol	4	17.30
SILUR003	*S. luridus*	Limmasol	5	20.03
SILUR005	*S. luridus*	Limmasol	5	17.87
SILUR006	*S. luridus*	Limmasol	5	18.20
SILUR008	*S. luridus*	Linosa	5	25.00
SILUR009	*S. luridus*	Linosa	5	23.30
SILUR012	*S. luridus*	Linosa	6	24.60
SILUR015	*S. luridus*	Linosa	3	16.40
SILUR018	*S. luridus*	Linosa	4	17.40
SILUR022	*S. luridus*	Stoupa	7	17.30
SILUR024	*S. luridus*	Stoupa	5	17.30
SILUR027	*S. luridus*	Stoupa	5	15.10
SILUR029	*S. luridus*	Stoupa	4	14.90
SILUR031	*S. luridus*	Stoupa	4	15.40
SILUR053	*S. luridus*	Diros	5	24.40
SILUR063	*S. luridus*	Diros	2	14.30
SILUR064	*S. luridus*	Diros	4	22.80
SILUR077	*S. luridus*	Diros	4	16.90
SILUR080	*S. luridus*	Diros	3	15.60
SILUR094	*S. luridus*	Kallithea	4	16.50
SILUR105	*S. luridus*	Kallithea	3	14.80
SILUR113	*S. luridus*	Kallithea	5	17.80
SILUR115	*S. luridus*	Kallithea	5	18.10
SILUR123	*S. luridus*	Gokova Bay	6	21.10
SILUR124	*S. luridus*	Gokova Bay	6	20.90
SILUR129	*S. luridus*	Gokova Bay	5	17.50
SILUR136	*S. luridus*	Gokova Bay	4	16.70
SIRIV004	*S. rivulatus*	Limmasol	3	14.11
SIRIV006	*S. rivulatus*	Limmasol	5	20.50
SIRIV007	*S. rivulatus*	Limmasol	5	20.90
SIRIV008	*S. rivulatus*	Limmasol	6	21.30
SIRIV011	*S. rivulatus*	Limmasol	5	18.10

SIRIV026	*S. rivulatus*	Trachila	4	17.40
SIRIV027	*S. rivulatus*	Trachila	7	20.10
SIRIV031	*S. rivulatus*	Trachila	4	17.00
SIRIV033	*S. rivulatus*	Trachila	3	16.20
SIRIV034	*S. rivulatus*	Trachila	3	15.90
SIRIV047	*S. rivulatus*	Diros	6	20.30
SIRIV048	*S. rivulatus*	Diros	3	14.30
SIRIV053	*S. rivulatus*	Diros	6	19.00
SIRIV055	*S. rivulatus*	Diros	4	16.20
SIRIV056	*S. rivulatus*	Diros	4	17.20
SIRIV058	*S. rivulatus*	Kallithea	5	18.60
SIRIV061	*S. rivulatus*	Kallithea	8	23.60
SIRIV064	*S. rivulatus*	Kallithea	6	19.70
SIRIV074	*S. rivulatus*	Kallithea	6	20.80
SIRIV077	*S. rivulatus*	Gokova Bay	5	17.90
SIRIV085	*S. rivulatus*	Gokova Bay	9	30.00
SIRIV090	*S. rivulatus*	Gokova Bay	5	24.00
SIRIV092	*S. rivulatus*	Gokova Bay	6	26.60